Energy & Environmental Science

ROYAL SOCIETY OF CHEMISTRY

REVIEW

View Article Online
View Journal | View Issue

Cite this: *Energy Environ. Sci.*, 2024, **17**, 925

Electrification of gasification-based biomass-to-X processes – a critical review and in-depth assessment†

Marcel Dossow,*[a] Daniel Klüh,*[b] Kentaro Umeki,[ac] Matthias Gaderer,[b] Hartmut Spliethoff[a] and Sebastian Fendt[a]

To address the impacts of climate change, it is imperative to significantly decrease anthropogenic greenhouse gas emissions. Biomass-based chemicals and fuels will play a crucial role in substituting fossil-based feedstocks and reducing emissions. Gasification-based biomass conversion processes with catalytic synthesis producing chemicals and fuels (Biomass-to-X, BtX) are an innovative and well-proven process route. Since biomass is a scarce resource, its efficient utilization by maximizing product yield is key. In this review, the electrification of BtX processes is presented and discussed as a technological option to enhance chemical and fuel production from biomass. Electrified processes show many advantages compared to BtX and electricity-based processes (Power-to-X, PtX). Electrification options are classified into direct and indirect processes. While indirect electrification comprises mostly the addition of H_2 from water electrolysis (Power-and-Biomass-to-X, PBtX), direct electrification refers to power integration into specific processing steps by converting electricity into the required form of energy such as heat, electrochemical energy or plasma used (eBtX). After the in-depth review of state-of-the-art technologies, all technologies are discussed in terms of process performance, maturity, feasibility, plant location, land requirement, and dynamic operation. H_2 addition in PBtX processes has been widely investigated in the literature with process simulations showing significantly increased carbon efficiency and product yield. Similar studies on direct electrification (eBtX) are limited in the literature due to low technological maturity. Further research is required on both, equipment level technology development, as well as process and system level, to compare process options and evaluate performance, economics, environmental impact and future legislation.

Received 29th August 2023,
Accepted 19th December 2023

DOI: 10.1039/d3ee02876c

rsc.li/ees

Broader context

To reduce GHG emissions and thus mitigate the consequences of climate change, all sectors need to be defossilized and decarbonized. Sustainable biomass and residues are key renewable alternatives to substitute fossil resources, especially for sectors like transportation or the chemical industry, which still heavily rely on fossil resources. The conversion of lignocellulosic biomass *via* gasification to syngas and further to fuels or chemicals like methane, methanol, dimethyl ether, or Fischer–Tropsch syncrude is a promising technology option (Biomass-to-X, BtX). To exploit the biomass resources to their fullest potential while reducing greenhouse gas emissions, the direct or indirect electrification of BtX processes using renewable electricity is discussed in this paper. Electricity can be used, for example, to supply energy to individual process steps (direct electrification) or to produce green hydrogen to drive chemical reactions (indirect electrification). These processes can show significantly higher economic, energetic, and environmental performances than conventional biomass-based (BtX) or electricity-based (Power-to-X) processes. Therefore, the electrified BtX processes show great potential to accelerate the defossilization and decarbonization of the chemical industry and transport sector.

1. Introduction

The climate crisis is an imminent threat to life on Earth, necessitating significant greenhouse gas (GHG) reductions by 2030. Fossil resources, excluding nuclear power, accounted for more than 80% of the global primary energy supply in 2021 and contributed significantly to anthropogenic GHG emissions.[1]

[a] *Technical University of Munich, Chair of Energy Systems, Boltzmannstr. 15, 85748, Garching b. München, Germany*
[b] *Technical University of Munich, Campus Straubing for Biotechnology and Sustainability, Professorship of Regenerative Energy Systems, Schulgasse 16, 93415 Straubing, Germany. E-mail: daniel.klueh@tum.de*
[c] *Luleå University of Technology, Division of Energy Science, 97187 Luleå, Sweden*
† Electronic supplementary information (ESI) available. See DOI: https://doi.org/10.1039/d3ee02876c

Besides reducing energy consumption by energy efficiency measures or avoiding consumption, replacing fossil resources with renewable alternatives is required. For defossilization, renewable and sustainable carbon sources are needed to produce high-density fuels, materials, and chemicals. Biomass and CO_2 are the main feedstock options. The hydrogenation of CO_2, so-called Power-to-X (PtX), is an emerging process route towards renewable fuels and chemicals that requires H_2 and CO_2 as educts. Biomass can be converted to sustainable products *via* various process routes. The annual growth rate, however, limits the availability of sustainable biomass. Therefore, biomass must be utilized as efficiently as possible.

Electrification of industrial processes has been identified as a key technology by the IPCC (Intergovernmental Panel on Climate Change) to meet climate targets.[2] Van Kranenburg *et al.* developed a roadmap for the electrification of the chemical industry.[3] They identified economic benefits, improved sustainability, and the development of new products as primary drivers for electrification. Moreover, the electrification of industrial processes can provide a flexible load in an energy system dominated by fluctuating renewable energy sources,[3] and offers economic benefits during times of low electricity prices.[4] Electrification can also reduce GHG emissions if low-carbon electricity is used. However, current regulatory ambiguity between biogenic and non-biogenic

Marcel Dossow

Marcel Dossow is a research associate and PhD candidate at the Chair of Energy Systems at the Technical University of Munich (TUM). He graduated from RWTH Aachen University in 2018 with a BSc in Mechanical Engineering. In 2020 he completed his MSc in Energy and Process Engineering at TUM. His research in the research-group of Dr-Ing. Sebastian Fendt is focused on Biomass-to-Liquid and Power-to-Liquid processes, as well as combinations of both (Power-and-Biomass-to-Liquid). This involves the simulative investigation of entrained-flow gasification in combination with the integration of renewable electricity and hydrogen and the subsequent Fischer–Tropsch synthesis into sustainable aviation fuel (SAF).

Daniel Klüh

Daniel Klüh works as a research assistant at the Professorship for Regenerative Energy Systems at the Technical University of Munich. His primary research revolves around the development and assessment of processes aimed at producing sustainable fuels or chemicals. The raw materials involved in these processes include biomass, CO_2, H_2, and/or electricity. The focus of his doctoral research is on incorporating hydrogen-based power-to-X technologies into pulp mills. Daniel holds a BSc in Mechanical Engineering from the Technical University of Darmstadt and Virginia Tech (USA), along with an MSc in Energy Science and Engineering from the Technical University of Darmstadt.

Kentaro Umeki

Kentaro Umeki is a full Professor in Energy Engineering at Luleå University of Technology (LTU) since 2019 and a guest professor at the Chair of Energy Systems at the Technical University of Munich (TUM) during 2023 and 2024. Umeki studied Mechanical Engineering (BEng) and Environmental Science and Technology (MEng and PhD) at Tokyo Institute of Technology. His research group is developing gasification-based biofuel production technologies as well as pyrolysis technologies for high-quality biocarbon and liquid production. Umeki has co-authored more than 70 scientific articles in renowned international journals.

Hartmut Spliethoff

Hartmut Spliethoff studied mechanical engineering at the universities of Kaiserslautern and Stuttgart. In 1991 he was appointed head of the Boiler Technology department at the IVD, University of Stuttgart. In 1999 he finished his postdoctoral thesis and in 2000 he was appointed as full-time professor at the Chair of Energy Conversion at TU Delft. Since 2004 he has been a full-time professor at the TUM Chair of Energy Systems. Prof. Spliethoff has over 30 years of research experience and co-authored more than 350 scientific articles. Furthermore, he has been coordinator of both national and international multidisciplinary centers and consortia.

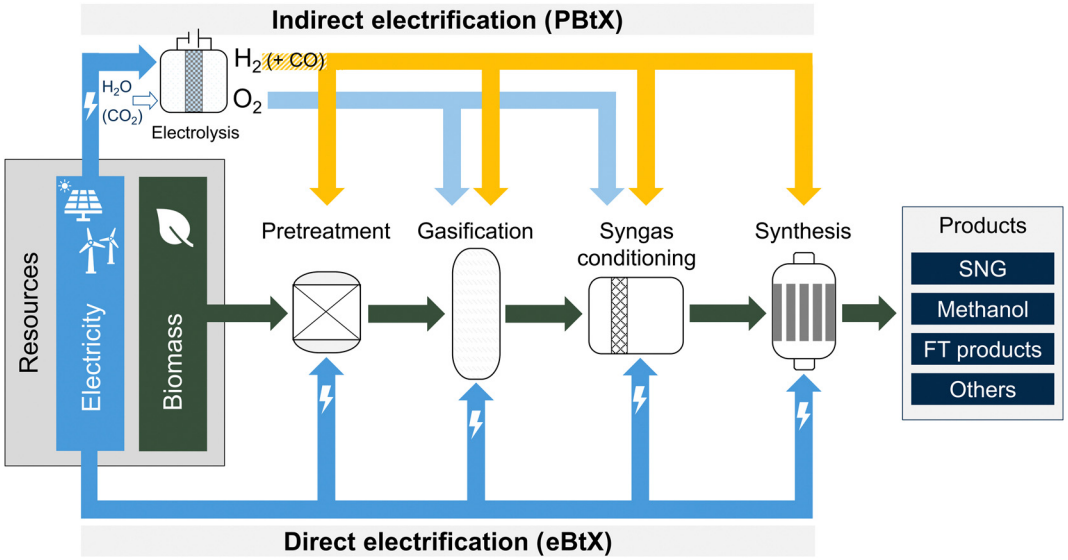

Fig. 1 Direct and indirect electrification options for BtX processes, including biomass pretreatment, gasification, syngas conditioning, and synthesis to synthetic natural gas (SNG), methanol, Fischer–Tropsch (FT) products, and others.

alternative fuels hinders the potential contributions of electrified process options to achieve ambitious goals.

Given the limited biomass availability, the maximized utilization of carbon from biomass should be one of the main priorities for developing new pathways toward sustainable products. One promising approach is the electrification of the thermochemical Biomass-to-X (BtX) process, which involves the gasification of solid or liquid biomass and the conversion of synthesis gas, also known as syngas, to products. Agrawal and Sing reasoned that biomass is not only a source of energy but primarily a carbon source.[5] Since a stand-alone BtX process generally could transfer less than 50% of the carbon from biomass to final products, additional energy in as heat, H_2, or electricity is required to improve carbon utilization.[5]

Sebastian Fendt

Sebastian Fendt studied Chemical Engineering at Technical University of Munich (TUM) and University of California, Berkeley. After finishing his studies, he started his PhD at the Chair of Energy Systems at TUM. Since 2015, he heads a research group with the focus on energetic utilization of biomass, renewable fuels and Power-to-X systems. Besides acting as project manager and coordinator of various research projects like the international future lab REDEFINE Hydrogen Economy, he acts as coordinator for the TUM.Hydrogen and PtX network and holds lectures and seminars. Sebastian Fendt authored and co-authored more than 50 publications in various renowned scientific journals.

Electrification of BtX processes aims at increasing product yield per biomass input, reducing carbon loss as CO_2, possibly enabling flexible electricity use, and supplying low carbon products.[6] Thus, it will be essential in reaching net zero emissions, especially in the industrial sector.[7]

1.1 Scope

This review paper focuses on converting solid lignocellulosic biomass to 2nd generation fuels or chemicals *via* the gasification-based BtX pathway. The term "biomass" is used consistently to refer to non-edible, sustainable lignocellulosic biomass and its residues, such as crop residues, grasses, sawdust, wood chips, solid waste, *etc.* Furthermore, the BtX pathway *via* thermochemical conversion of biomass means the process in Fig. 1, including biomass pretreatment, gasification, syngas conditioning, and catalytic synthesis. Without any electrification option, the central part (dark green arrows) from biomass to products represents the BtX route. Final products are primarily in liquid form, such as Fischer–Tropsch (FT) products, methanol (MeOH), ethanol, and dimethyl ether (DME). The only gaseous product considered is synthetic natural gas (SNG).

Electrification refers to using electricity as feedstock to produce fuels and chemicals or as a significant utility for such a process. When electricity is used as conventional utility for equipment operation such as compressors or pumps, it is not considered electrification. In the following, the term electricity refers to renewable and low-carbon electricity.

This paper differentiates between indirect and direct electrification. Fig. 1 shows the directly (lower part) or indirectly (upper part) electrified BtX process. We use the term, Power-and-Biomass-to-X (PBtX), for indirect electrification (mostly H_2 addition), and directly electrified BtX (eBtX), for directly electrified process steps. In indirect electrification, electricity is

used to produce H_2 *via* water electrolysis which can be fed to different locations along the process chain. Direct electrification means using electricity to provide energy to the process directly, for example, in form of heat, electromagnetic waves or plasma This work does not consider using H_2 as a substitute for natural gas in fired heaters. Additionally, the electrification of product purification and upgrading is excluded.

1.2 Outline

This work reviews possible electrification options for the gasification-based BtX process. The paper starts with an introduction followed by a technological background on conventional BtX processes in Section 2 including biomass pretreatment, gasification technologies, syngas conditioning and cleaning, and synthesis. The technologies and concepts for indirect and direct electrification are presented in Sections 3 and 4. Indirect electrification technologies comprise the addition of H_2 produced *via* water electrolysis and the addition of syngas from parallel co-electrolysis of CO_2 and H_2O. Indirect electrification is presented along the process steps of the PBtX process chain at points where H_2 can be added. Direct electrification includes a variety of technologies and is grouped into electrically-heated processes (Section 4.1), plasma-assisted processes (Section 4.2), and co-electrolysis (Section 4.3). Among all available technologies for electrifying BtX processes, those that do not show relevance to this review are summarized in the ESI.†

In Section 5, the discussed technologies are assessed concerning feasibility for the integration into BtX processes and maturity. Section 6 deals with the meta-analysis of literature data focusing on indirect electrification. Furthermore, available data from process simulations of direct and indirect electrification options are compared. More general topics of electrified BtX processes are discussed in Section 7 regarding the feedstock supply, production potentials, land use, GHG emissions, economics, and dynamic operation.

1.3 Novelty

Poluzzi *et al.* recently published a review on PBtX processes featuring an overview of selected indirectly electrified processes.[8] Their review mainly considers the comparison between conventional and indirectly electrified BtX with H_2 addition before synthesis based on a limited number of literature sources. In contrast, our literature review covers multiple process design options for direct and indirect electrification. Additionally, our discussion quantitatively compares key performance indicators between different electrification routes and products. The goal is to holistically summarize and evaluate the work as well as provide suggestions for the most promising routes.

Reviews for direct electrification are already established for microwave-based or electrically-heated process steps[9–13] and plasma-based process steps.[14–17] However, these reviews do not discuss the applicability and impact of the electrified subprocesses in the BtX process chain. Therefore, this review puts the direct electrification options in perspective to the whole BtX process. It merges and consolidates all possible technologies to assess the most promising technologies for direct electrification.

Considering both direct and indirect electrification of BtX processes, we give an overarching picture of all available technologies for electrification of the gasification-based BtX process. This paper aims to provide a guideline on which electrification options are most promising and beneficial in terms of efficiency, technological readiness, flexibility, and benefits of electrification.

1.4 Key performance indicators

Key performance indicators (KPI) evaluate and compare PtX, BtX, eBtX, and PBtX process routes. Due to the different definitions of efficiencies in literature, the direct comparison of the literature values is misleading and should be treated cautiously. For this reason, we unified the assumptions for the KPI calculations to make the processes comparable.

The carbon efficiency η_C is defined as the ratio between the carbon mass flow rate in the product $\dot{m}_{C,product}$ and in the input biomass $\dot{m}_{C,biomass}$ as the sole carbon source:

$$\eta_C = \frac{\dot{m}_{C,product}}{\dot{m}_{C,biomass}} \quad (1)$$

The gravimetric product yield (PY) compares the product mass flow rate $\dot{m}_{product}$ to the mass flow rate of initial dry biomass $\dot{m}_{biomass,dry}$. It is linked to η_C when the carbon content (w_C) of product and biomass are known:

$$PY = \frac{\dot{m}_{product}}{\dot{m}_{biomass,dry}} = \frac{\frac{\dot{m}_{C,product}}{w_{C,product}}}{\frac{\dot{m}_{C,biomass,dry}}{w_{C,biomass,dry}}} = \eta_C \cdot \frac{w_{C,biomass,dry}}{w_{C,product}} \quad (2)$$

Gross energy yield (EY) considers the output of the process as the chemical energy flow of the product based on the lower heating value (LHV) ($\dot{E}_{prod} = \dot{m}_{product} \cdot LHV_{product}$). The inputs are either the energy flow of biomass ($\dot{E}_{feed,BtX} = \dot{m}_{biomass} \cdot LHV_{biomass}$), the electrical power requirement for electrolysis ($\dot{E}_{feed,PtX} = P_{electrolysis}$), or the sum of the energy flow of biomass and the electric power requirement for electrolysis ($\dot{E}_{feed,PBtX} = \dot{m}_{biomass} \cdot LHV_{biomass} + P_{electrolysis}$), or direct electrification ($\dot{E}_{feed,eBtX} = \dot{m}_{biomass} \cdot LHV_{biomass} + P_{el.direct}$) as shown in eqn (3). In all cases, the electrical power demand of auxiliaries like pumping or compression is neglected and only the electrical energy to the electrolysis $P_{electrolysis}$ and direct electrification processes $P_{el.direct}$ are considered.

$$EY = \frac{\dot{E}_{prod}}{\dot{E}_{feed}} = \begin{cases} \frac{\dot{m}_{product} \cdot LHV_{product}}{\dot{m}_{biomass} \cdot LHV_{biomass}} & (BtX) \\ \frac{\dot{m}_{product} \cdot LHV_{product}}{P_{electrolysis}} & (PtX) \\ \frac{\dot{m}_{product} \cdot LHV_{product}}{\dot{m}_{biomass} \cdot LHV_{biomass} + P_{electrolysis}} & (PBtX) \\ \frac{\dot{m}_{product} \cdot LHV_{product}}{\dot{m}_{biomass} \cdot LHV_{biomass} + P_{el.direct}} & (eBtX) \end{cases} \quad (3)$$

To compare the degree of electrification of BtX processes, the electrification ratio (ER) is introduced in eqn (4). It quantifies the ratio between electricity and biomass input:

$$\mathrm{ER} = \frac{P_{\mathrm{el}}}{\dot{E}_{\mathrm{biomass}}} = \begin{cases} \dfrac{P_{\mathrm{electrolysis}}}{\dot{m}_{\mathrm{biomass}} \cdot \mathrm{LHV}_{\mathrm{biomass}}} & (\mathrm{PBtX}) \\ \dfrac{P_{\mathrm{el.direct}}}{\dot{m}_{\mathrm{biomass}} \cdot \mathrm{LHV}_{\mathrm{biomass}}} & (\mathrm{eBtX}) \end{cases} \quad (4)$$

2. Conventional gasification-based biomass-to-X processes

The conventional thermochemical BtX process comprises biomass pretreatment, gasification, syngas conditioning, and synthesis. Compared to fossil feedstock, biomass faces feedstock-inherent challenges mainly related to its low energy density, high moisture content, hydrophilicity, and low heating value. To overcome these challenges, pretreatment technologies can be either located off-site or integrated into a BtX plant.[18] The choice of biomass pretreatment depends on the feedstock, gasifier technology, operating parameters, and syngas quality requirements.[19]

Pretreatment technologies aim to increase energy density, reduce moisture content, and increase the C/O ratio. Furthermore, pretreatment improves grindability and conveyability. Usually, pretreatment processes operate between 50 °C and 300 °C, needing a heat source to supply the required low-temperature thermal energy.[20] Examples of pretreatment technologies are thermal drying, hydrothermal carbonization (HTC), and torrefaction.[21,22] If the pretreatment temperature is further increased to 300–800 °C in the absence of an oxidation agent, direct thermal decomposition of biomass occurs.[23] This so-called pyrolysis yields gaseous, liquid, and solid products.[24] After the thermochemical pretreatment process, the obtained solid fuel might need to be ground or milled, depending on the gasifier technology.

In the subsequent gasification, the biomass is converted *via* endothermic reactions into syngas which contains primarily H_2, CH_4, CO, CO_2, and H_2O with smaller quantities of tar, char, soot, and ash.[25] A minimum temperature of 800–900 °C is required for biomass gasification.[26] Besides biomass as feedstock, the gasifier needs a gasification agent like air, O_2, steam, or CO_2. O_2 is typically produced by a cryogenic air separation.[27] Required heat for gasification can be supplied autothermally (heat is generated within the gasifier from the exothermic combustion reaction of the fuel and the gasification agent) or allothermally (heat is externally provided to the gasifier).

The most characteristic feature of the gasification process is the type of reactor (fixed bed, fluidized bed, or entrained flow), which has the most substantial influence on product gas composition and gasification efficiency.[27] For the gasification of biomass, available technologies include fluidized bed (bubbling (BFB) and circulating (CFB)) and fixed bed (FB) gasifiers (co-current, counter-current).[25,27] The entrained flow gasification (EFG) of biomass is currently at the demonstration scale.[28] Table 1 provides an overview of gasifier technologies.

After the gasification, the syngas must be conditioned to suit the synthesis. Depending on the gasification technology, typical syngas conditioning processes for EFG include syngas quenching with a downstream scrubber, which already removes most of the HCl and NH_3. Next steps include raw gas reforming for tar removal, a (sour) water–gas shift (WGS) reactor to adjust the stoichiometric number (SN), and the removal of sour gases in the acid gas removal (AGR) followed by a purification for the removal of other contaminants.[22,26] A typical syngas conditioning train for thermochemical BtX processes is shown in Fig. 2. In addition to removing impurities from the raw synthesis gas, the aim is to adjust the synthesis-specific SN.[30]

$$\mathrm{SN} = \frac{\dot{n}_{\mathrm{H_2}} - \dot{n}_{\mathrm{CO_2}}}{\dot{n}_{\mathrm{CO}} + \dot{n}_{\mathrm{CO_2}}} \quad (5)$$

Critical contaminants in the raw syngas after biomass gasification leading to erosion, corrosion, and deposits on process components, include inorganic particles, tars, halide compounds, N-species, and S-species.[26] In addition, contaminants can lead to catalyst poisoning in downstream processes like the synthesis. Multiple options for separating impurities are available (for more detail, readers are referred to[22,26]). The focus is removing hydrocarbons and adjusting SN since these processes are the most relevant for electrification.

Hydrocarbons, such as tar, methane, and ethylene, present in the syngas, must be either removed or converted to CO and H_2 before the catalytic fuel synthesis.[31] Reforming the hydrocarbons has, in comparison to scrubbing, the advantage of

Table 1 Comparison of gasification technologies based on[22,29]

	Unit	Fixed bed (FB)	Fluidized bed (BFB, CFB)	Entrained flow (EFG)
Particle size	mm	5–100	1–20	<0.1
Outlet temperature	°C	150–250 (600–800[a])	800–950	1300–1700
Residence time	min	10–30	1–10	<0.1
Carbon conversion	%	>95 (80–90[a])	88–95	≫95
Cold gas efficiency		Very high (medium[a])	High	Medium
Capacity		Low	Medium	High
Oxidizer requirement		Low	Medium	High
Gas velocity		Low	High	Very high
Tar content		Very high (low[a])	High	Very low
Typical operation mode		Autothermal	Allo-/autothermal	Autothermal

[a] Co-current.

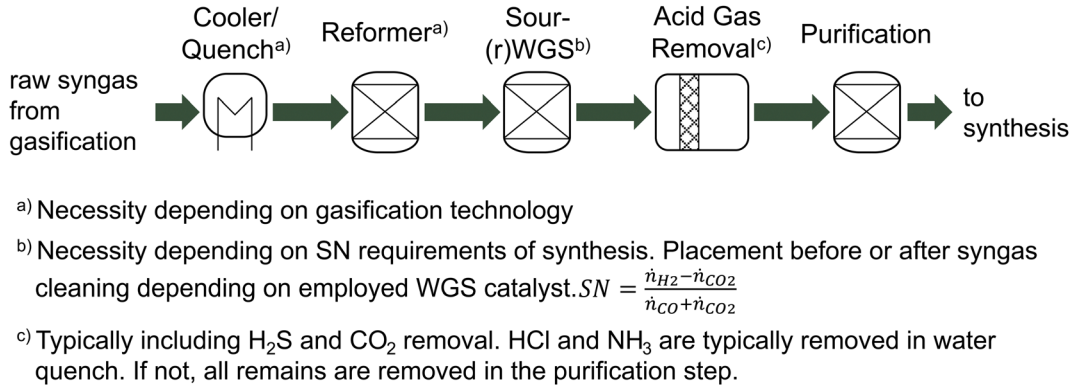

Fig. 2 Simplified flowsheet of syngas conditioning train for gasification-based BtX processes.

increasing the syngas yield.[31] To remove tars, physical processes like scrubbers or wet electrostatic precipitators, catalytic reforming, or thermal reforming are available.[22] Different thermal reforming methods such as steam reforming, dry reforming, partial oxidation reforming (POX), autothermal reforming (ATR) exist.[32] Catalytic reforming uses a catalyst to lower the reforming temperature. Catalytic reforming is particularly suitable for syngas applications because it also handles the non-condensable hydrocarbons and converts organic sulfur species to H_2S, a more readily removable form of sulfur in the AGR.[33] In all cases, a reforming agent like O_2 or H_2O is used to oxidize hydrocarbons to CO and H_2.[34]

Since the syngas produced *via* biomass gasification often has a H_2/CO ratio below 1, a WGS reactor can be employed to increase the ratio as required by the synthesis.[35] The WGS reaction takes place according to reaction (6). Depending on the reaction temperature and catalyst, the concentration of H_2 (forward WGS at 250–400 °C) or CO (reverse WGS at 400–500 °C) can be increased.[26,36] Excess CO_2 in the syngas is usually separated in the AGR using a chemical or physical scrubber which is also used to remove H_2S.[26]

$$H_2O_{(g)} + CO_{(g)} \rightleftharpoons H_{2(g)} + CO_{2(g)} \quad \Delta H_R^0 = -41.2 \text{ kJ mol}^{-1} \tag{6}$$

The cleaned and conditioned syngas is converted in a catalytic synthesis to products like SNG (reaction (7)), MeOH (reaction (8)), or FT hydrocarbons (reaction (9)).

The reaction equations below are generally coupled *via* the WGS reaction (reaction (6)). The SN for FT and MeOH is at roughly 2, while SNG requires an SN of 3.

$$CO_{(g)} + 3H_{2(g)} \rightleftharpoons CH_{4(g)} + H_2O_{(g)} \quad \Delta H_R^0 = -206.2 \text{ kJ mol}^{-1} \tag{7}$$

$$CO_{(g)} + 2H_{2(g)} \rightleftharpoons CH_3OH_{(g)} \quad \Delta H_R^0 = -90.6 \text{ kJ mol}^{-1} \tag{8}$$

The formation of hydrocarbons in the FT process is depicted as exemplary in producing alkanes in reaction (9).[37] The process yields a mixture of hydrocarbons of different chain lengths, mainly alkanes, alkenes, and alcohols. The chain length distribution is described by the chain growth probability α, which depends on factors like catalyst, temperature, pressure, and syngas composition.

$$nCO_{(g)} + 2nH_{2(g)} \rightarrow -(CH_2)_{n(g)} + nH_2O_{(g)}$$
$$\Delta H_R\ (250\ ^\circ\text{C}) = n(-158.5) \text{ kJ mol}^{-1} \tag{9}$$

Most raw products, including SNG, MeOH, and FT products, require further processing before they can be used as fuel or chemicals. After the conversion in the synthesis, the separation of unwanted by-products and unconverted reactants from the final product is needed. Especially in the case of FT, the hydrocarbons produced must be upgraded in a refinery. More information on catalytic synthesis and raw product upgrading can be found in literature.[30,38]

The three main products identified in this paper are typically produced from fossil feedstock. The products are mainly used in the chemical industry as feedstock and as transportation fuel. The MeOH production is based on the catalytic, low-pressure conversion of syngas derived from different feedstock.[39] The majority of MeOH is used in the chemical industry as feedstock (for example: formaldehyde, methyl *tert*-butyl ether, acetic acid, dimethyl ether, propene or methyl methacrylate) or as solvent.[39] The utilization in the fuel and energy sector is increasing.[39] MeOH can be either used directly as fuel or for blending. Additionally, it can be further converted to methyl *tert*-butyl ether, DME or gasoline *via* the methanol-to-gasoline route.

The FT process was discovered in 1923 and first commercial plants were up running in 1936 in Germany.[40,41] Today, the technology is used in several plants in mostly South Africa and Qatar based on natural gas and coal.[42] The type and utilization of the products depend on the process and operating conditions. Typical applications are feedstock for the chemical industry (for example olefins or naphtha) and transportation fuels. SNG can have the same applications as natural gas which is used as feedstock in the chemical industry, as transportation fuel and for electricity or heat generation. However, SNG is not widely produced today. In the oil crisis in the 1970s, SNG was produced from syngas derived from coal gasification.[43] FT hydrocarbons and SNG will have the highest market potential as these products replace crude oil and natural gas which account for 31% and 24% of the worldwide primary energy

consumption.[1] The methanol market showed a demand of 47 Mt in 2011.[39]

3. Indirect electrification of BtX processes (PBtX)

This section deals with the indirect electrification of the BtX processes *via* H_2 addition from water electrolysis or parallel integration of co-electrolysis. As shown in Fig. 3, H_2 can be added at various locations along the process chain. The parallel integration of co-electrolysis allows the addition of H_2 and CO. The PBtX concept of adding H_2 from water electrolysis to BtX processes is reviewed in Section 3.1. Parallel integration of co-electrolysis is reviewed in Section 3.2, while the in-line co-electrolysis integration is reviewed in Section 4.3.

3.1 H_2 addition

In this section, only the production of H_2 *via* water electrolysis (eqn (10)) powered by renewable electricity is considered.

$$2H_2O_{(l)} \rightleftharpoons 2H_{2(g)} + O_{2(g)} \quad \Delta H_R^0 = 285.83 \text{ kJ mol}_{H_2O(l)}^{-1} \tag{10}$$

Water electrolysis technologies are grouped into high and low-temperature processes. The already commercialized low-temperature options are the alkaline (AEL) and the proton exchange membrane electrolysis (PEMEL), both running below 100 °C.[44,45] Low-temperature electrolyzers reach system efficiencies of up to 67% based on the LHV of H_2.[44] SOEL can achieve efficiencies of 74%.[44]

Solid oxide electrolysis (SOEL) operates between 700 °C and 900 °C.[45] Operating with steam instead of water as the reactant, SOEL can offer thermodynamic and kinetic advantages. For higher temperatures, the equilibrium voltage of the cell decreases, leading to lower electricity demand, consequently increasing the electrolysis efficiency.[45] However, the pressurized operation of SOEL remains challenging since the absolute pressure difference between the half-cells should stay below 20 mbar.[46] Compared to the extensive long-term degradation investigations performed at atmospheric conditions,[47] the current state of research is insufficient to make statements about the long-term effects of operating pressure on degradation behavior.

As a sweep gas on the O_2 side, air is typically used in SOEL. The system can also be operated with O_2 as sweep gas. This way, pure O_2 can be generated and potentially used in other process steps, such as oxygen-blown gasification or reforming. While this offers advantages in terms of overall process efficiency, it is crucial to be aware of the significant technical challenges associated with handling high-temperature pure O_2.[48] Another challenge on the O_2 electrode in SOEL is the oxidation of the metallic components. Therefore, all metals used have to form a stable oxidation layer to avoid complete destruction of the material by oxidation. It can be assumed that future SOEL cells can operate on an industrial scale producing pure O_2.[49] For low-temperature electrolyzers, pure O_2 production is state of the art.

PBtX processes have gained much attention in literature recently. The first publications on the concept date back to the 90s.[50,51] In general, the SN of biomass-based syngas needs to be increased by either adding H_2 or removing carbon-containing compounds for subsequent synthesis. If CO_2 is removed from the syngas stream, it is vented and not contained in the product. Thus, H_2 addition increases the product yield and carbon utilization.

H_2 addition to the pretreatment step is not an option since drying, torrefaction, and other thermochemical pretreatment technologies use thermal effects rather than chemical

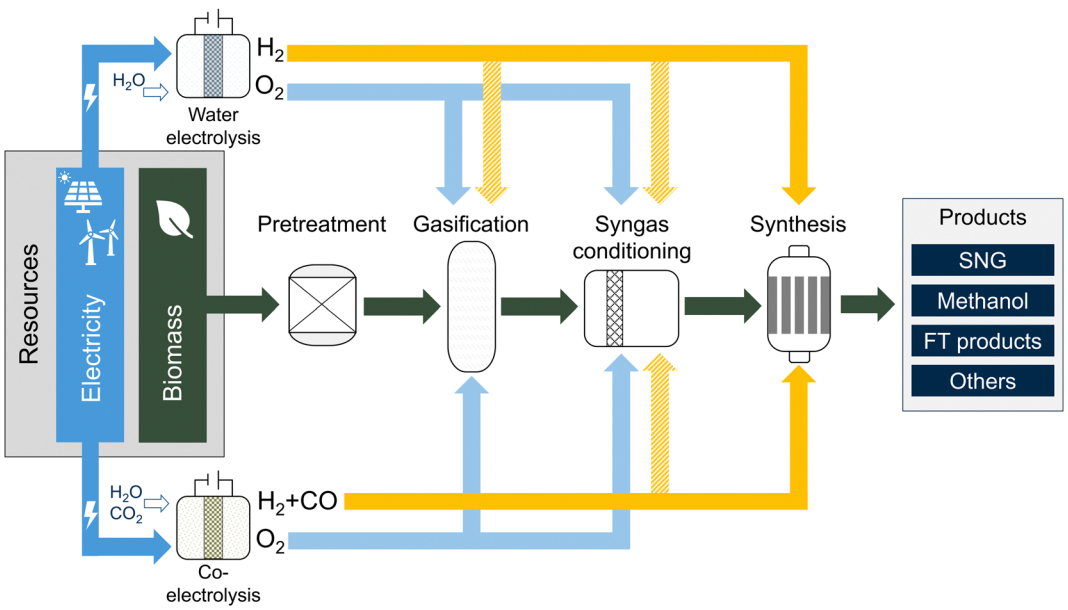

Fig. 3 Water and co-electrolysis integration options along the process chain for indirect BtX electrification (PBtX).

conversion. Only H_2-enhanced pyrolysis (hydropyrolysis) is discussed in literature.[52,53] In hydropyrolysis, biomass pyrolysis occurs under an H_2 atmosphere producing a stable bio-oil with low O_2 content and high heating value. The process substitutes the pathway *via* pyrolysis and bio-oil hydrogenation in a single conversion step to yield bio-oils comparable to fossil fuels.[54] Hydropyrolysis is outside the scope of a pretreatment step for gasification in this review as it aims to produce a higher-value liquid bio-oil for direct utilization as fuels.

H_2 addition to gasification and syngas conditioning like gas quenching, H_2 enhanced reforming, and WGS is relevant for PBtX applications and is presented below. Due to the availability of process modeling studies, we extensively elaborate on the H_2 addition to the synthesis step in Section 3.1.3.

3.1.1 H_2 addition to gasification. Two major concepts for utilizing H_2 directly in the gasifier are shown in Fig. 4(b) and (c). H_2 combustion inside the gasification chamber can generate the required heat for biomass gasification.[55] The combustion of H_2 instead of biomass inside the gasifier (Fig. 4b) is an option to operate the gasifier closer to allothermal mode and to improve the product gas heating value. Water generated from H_2 combustion is not only easily separated from the syngas but highly reactive with biomass and char reversely producing H_2. Consequently, steam addition to the process to enhance the H_2 content in the syngas can be reduced. Calculations show that H_2-reactivity with O_2 is higher than that of CO, preventing the conversion of CO to CO_2.[55] Since H_2 is selectively oxidized, it reduces the formation of CO_2. The technology is probably most suited for EFG. In fluidized bed gasifiers, high-temperature steam generated by H_2 combustion can likely cause bed agglomeration. In 2007, Agrawal *et al.* proposed the H_2 addition to a not further specified biomass gasifier with a subsequent FT synthesis step to produce liquid transportation fuels.[56]

As an alternative, gasification can occur in an H_2-enriched atmosphere to produce a methane-rich product gas (Fig. 4c).[57] This concept is called hydrogasification. The process was developed in the 1930s for the hydrogasification of coal and follows the exothermic reaction of solid carbon and H_2, as shown in (Fig. 4c).[57] Several simulative studies suggest a higher energy yield for the production of SNG by hydrogasification compared to conventional gasification with subsequent SNG synthesis (see ESI†).[57,58] Such a PBtX process using biomass hydrogasification would require H_2 addition of 95 MW_{LHV} for a 100 MW_{th} biomass input and outputs 154 MW_{LHV} SNG.[58] According to Barbuzza *et al.*, a methane fraction in the product gas from hydrogasification of up to 90 mol% on a dry basis can be expected.[57] With CH_4 as the main product of hydrogasification, the production of SNG *via* such a PBtX process is most reasonable. However, the gasification reaction rate in H_2 atmosphere is significantly lower than that when gasifying in CO_2 or H_2O atmosphere.[59] Consequently, higher temperatures and pressures are needed for hydrogasification than for conventional gasification. Furthermore, some studies on hydrogasification[57,60] assume that hydrogen supply alone is sufficient to reach the gasification temperatures and assume that reaction temperatures are unreasonably low. However, the slightly exothermic hydrogasification reaction itself does not supply enough energy to the reactor to drive the gasification of the solid biomass. Thus, an additional heat source is required to reach gasification temperatures. Such an external heat source allows for a combination of direct electrification of the gasification reactor and H_2 addition. At very high temperatures reached, especially in EFG, the thermodynamic equilibrium of the exothermic reaction prevents hydrogasification from playing a major role.

3.1.2 H_2 addition to syngas conditioning. Fig. 5 shows possible points for indirect electrification along the syngas conditioning train, including H_2 addition to syngas cooling or quenching, to syngas reforming or to sour (r)WGS. When adding the H_2 before an optional rWGS reactor, CO_2 can be converted into CO according to the reverse WGS reaction (see reaction (6)). This is particularly necessary when aiming at maximizing carbon efficiency when CO_2 cannot be converted in the synthesis, *e.g.*, in the FT synthesis. Since studies often add H_2 to both the rWGS and the synthesis itself, the respective

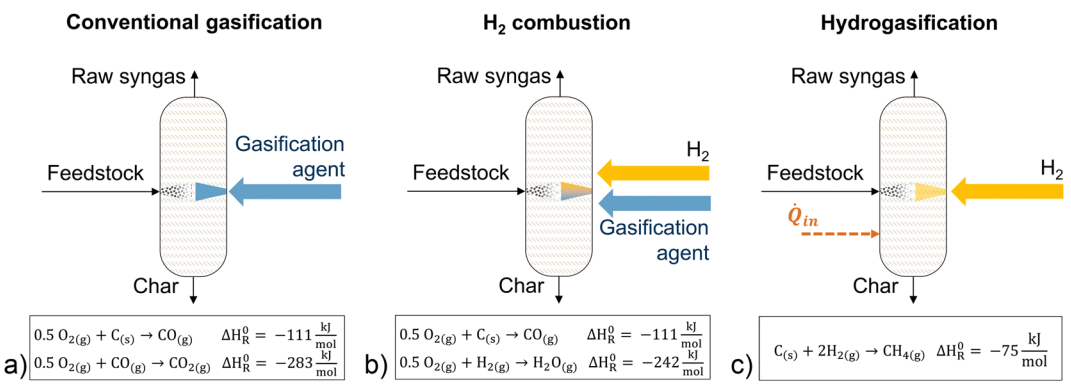

Fig. 4 Simplified representation of the concepts for H_2 addition to gasification: (a) conventional allothermal gasification using gasification agent to generate heat through (partial) combustion; (b) H_2 combustion to generate heat for gasification; (c) hydrogasification of solid feedstock with H_2 and external heat source.

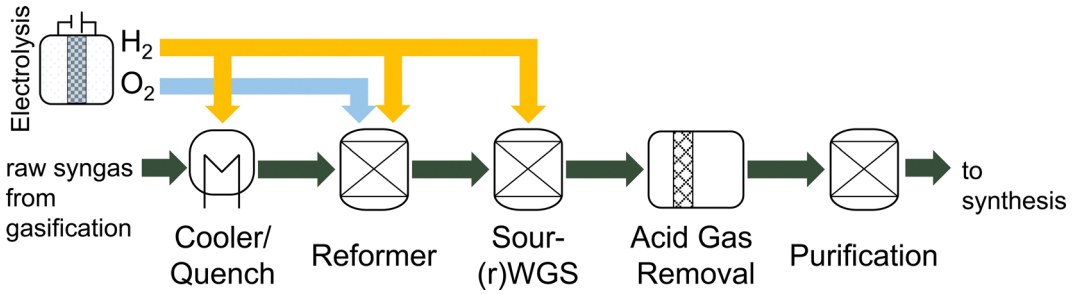

Fig. 5 H_2 addition options along the syngas conditioning train for indirect BtX electrification (PBtX).

literature considering H_2 addition before the (r)WGS reactor is included in Section 3.1.3.

There are multiple options to cool down the hot syngas after gasification, including radiant cooling, convective cooling, or direct quenching.[26] Especially in EFG, the hot syngas must be directly quenched after the gasifier, using either water, gas, or chemical quenching. Instead of using recycled syngas for gas quenching, H_2 can be mixed with hot syngas to lower the temperature. Adding H_2 can be seen as a combined gas and chemical quench. The effect of chemical quenching is the conversion of CO_2 to CO *via* the endothermic rWGS reaction proceeding at high temperatures, which further lowers the temperature of the raw syngas. A disadvantage of H_2 addition as gas quenching is that impurities are diluted, resulting in a less efficient separation in the syngas cleaning steps. Furthermore, the mass flow of the gas stream is increased, requiring larger downstream equipment starting from the gas quench. A techno-economic evaluation and a practical demonstration of such a process are still pending.

Clausen proposed a MeOH-producing PBtX process using H_2 addition for quenching after EFG.[61] Clausen showed that using H_2 in a chemical quench can increase carbon efficiency to up to 97% and energy yield to 58% for an ER of 1.[61] Alternatively, he proposed using the volatiles from torrefaction for the chemical quenching while feeding the electrolytic H_2 to the synthesis unit.[62] The comparison suggests that the latter would be beneficial since the torrefaction can be integrated into the process and the volatiles from torrefaction can be used within the process.[62] Butera *et al.* further investigated the proposed concept, achieving energy yields above 70% using gas and chemical quench *via* H_2 injection to cool the produced gas before the high-temperature syngas cooler.[63]

After gasification and quenching, hydrocarbons produced during gasification, especially tars, must be either removed or converted to CO and H_2 before the catalytic fuel synthesis. The H_2 content in the syngas influences the conversion of tars in the reforming step, as shown by experimental and simulative work. Houben *et al.* showed with naphthalene as a model compound that the tar content can be decreased *via* partial oxidation.[64] With higher H_2 content, almost all naphthalene is converted to benzene and syngas. Van der Hoeven *et al.* both experimentally and simulatively confirmed the assumption that H_2 is beneficial for converting tars in partial oxidation reactors.[65] Higher tar conversion due to higher H_2 content was experimentally confirmed by Ahmad *et al.*[66] Additionally, H_2 suppresses soot formation in POX.[64] Yet, models must be improved to capture this effect in simulation.[67]

3.1.3 H_2 addition to synthesis processes. To adjust SN for any catalytic synthesis, generally two options are available: removing carbon from the syngas before synthesis (BtX) or adding H_2 to the syngas before synthesis (PBtX). In BtX processes, removing carbon from the syngas prevents the biomass potential from being fully utilized, limiting the maximum possible carbon efficiency and thus the product yield. In this section, adding H_2 before the synthesis step is presented as the straightforward option to adjust SN for catalytic synthesis without the need for carbon removal.

Tables 2–4 show the available publications for SNG, MeOH, and FT products. Most literature targets SNG, MeOH, and FT products. Reviewed studies often add H_2 to the rWGS, the synthesis itself or both at the same time. Therefore, the relevant literature is reviewed in this section considering the H_2 addition to the following points: before the (r)WGS reactor, before the chemical synthesis or between reactors of the chemical synthesis in the case of cascading reactors. The determined KPIs are based on eqn (1) to (4) using the data presented in the publications to make the indicators comparable.‡

As mentioned above, one of the main advantages of H_2 addition is the increase in carbon efficiency. As shown in Tables 3–5, the carbon efficiency of the processes vary from 34 to 100% and are potentially higher than in the BtX processes of 32 to 40%.[68] However, a carbon efficiency of 100% cannot be reached due to losses in purge streams and limitations of carbon conversion in the gasifier. PY in Tables 3–5 ranges from 0.31 to 0.79 kg_{SNG} per $kg_{biomass,dry}$ for SNG, from 0.70 to 1.28 kg_{MeOH} per $kg_{biomass,dry}$ for MeOH and from 0.20 to 0.57 kg_{FT} per $kg_{biomass,dry}$ for FT. These values compare to 0.23 kg_{SNG} per $kg_{biomass,dry}$, 0.53 kg_{MeOH} per $kg_{biomass,dry}$ and 0.21 kg_{FT} per $kg_{biomass,dry}$ for conventional BtX processes.[68] The ER shows that a considerable amount of energy input can come from H_2 addition. More than twice the amount of biomass thermal energy input can be added as electricity for PBtX processes.

‡ In case of inaccessibility or lack of data in the publications, a LHV of biomass of 18 MJ kg_{dry}^{-1} and an energy requirement for the electrolysis of 50 kW h_{el} $kg_{H_2}^{-1}$, corresponding to a 65% system efficiency (based on LHV) is used.

Table 2 Literature overview for Power-and-Biomass-to-SNG studies including the scope and the used gasification and electrolysis technologies. KPI values derived from the data in the respective literature

Ref.	Scope[a]	Gasifier[b]	Electrolyzer[c]	ER MW_{el} per MW_{th}	PY kg_{SNG} per $kg_{biomass,dry}$	η_C %	EY %
Gassner and Maréchal (2008)[69]	P	CFB	Not specified	1.37	0.75	100%	75%
Ridjan *et al.* (2013)[70]	E	Not specified	SOEL	1.26	0.64	95%	75%
Hannula (2015)[71]	P	CFB	AEL	0.66	0.39	56%	60%
Hannula (2016)[72]	P	CFB	AEL	2.52	0.79	98%	58%
Trop and Goricanec (2016)[73]	P	EFG	Not specified	2.26	0.64	96%	54%
Clausen (2017)[74]	P	TSG	SOEL	1.24	0.31	100%	74%
Sigurjonsson and Clausen (2018)[75]	P	TSG	SOEL	1.52	0.64	100%	75%
Anghilante *et al.* (2019)[76]	P	FB	SOEL/SOEL/PEMEL	1.35/1.38/1.96	0.72/0.74/0.74	98%/98%/98%	64%/65%/52%
Zhang *et al.* (2020)[77]	P	EFG	SOEL	1.3	0.557	89%	63%
Poluzzi *et al.* (2020)[78]	P	CFB/DFB/SEG[d]	not specified	0.39 (3)	0.37/0.37/0.33	55%/55%/50%	78%/78%/71%
Kofler and Clausen (2021)[79]	P	CFB	AEL	0.78	0.61	68%	53%
Giglio *et al.* (2021)[80]	P	CFB	SOEL	1.53	0.67	100%	75%

[a] Scope: P: process simulation, E: estimation-based calculation approach. [b] EFG: entrained flow gasification, CFB: circulating fluidized bed, FB: fixed bed, TSG: two-stage gasifier (by Technical University of Denmark (DTU)). [c] AEL: alkaline electrolysis, SOEL: solid oxide electrolysis, PEMEL: proton exchange membrane electrolysis. [d] DFB: dual fluidized bed indirect gasifier, SEG: dual fluidized bed sorption-enhanced gasifier.

Table 3 Literature overview for Power-and-Biomass-to-MeOH studies including the scope and the used gasification and electrolysis technologies. KPI values derived from the data in the respective literature

Ref.	Scope[a]	Gasifier[b]	Electrolyzer[c]	ER MW_{el} per MW_{th}	PY kg_{MeOH} per $kg_{biomass,dry}$	η_C %	EY %
Oulette and Scott (1995)[50]	E	FB	Not specified	1.29	1.21	100%	57%
Specht *et al.* (1999)[51]	E	Not specified	Not specified	1.47	1.22	81%	51%
Mignard and Pritchard (2008)[81]	E	FB	PME[d]	1.39	1.27	87%	54%
Hertwich and Zhang (2009)[82]	E	Not specified	Not specified	1.19	1.21	90%	58%
Clausen *et al.* (2010)[83]	P	CFB	AEL	0.64	1.10	88%	72%
Clausen (2011)[61]	P	EFG	AEL	1.10	1.27	97%	61%
Ridjan *et al.* (2013)[70]	E	Not specified	SOEL	0.63	1.08	81%	74%
Hannula (2015)[71]	P	CFB	AEL	0.35	0.76	55%	58%
Clausen (2015)[62]	P	EFG	AEL	1.19	1.21	96%	62%
Hannula (2016)[72]	P	CFB	AEL	1.70	1.31	92%	58%
Trop and Goricanec (2016)[73]	P	EFG	Not specified	1.48	1.17	88%	52%
Firmansyah *et al.* (2018)[84]	E	FB	AEL	1.19	1.14	85%	57%
Zhang *et al.* (2019)[85]	P	EFG	SOEL	0.61	0.89	67%	60%
Butera *et al.* (2020)[86]	P	CFB	SOEL	0.42	0.70	58%	58%
Zhang *et al.* (2020)[87]	P	EFG	SOEL	0.61	0.89	66%	60%
Zhang *et al.* (2020)[77]	P	EFG	SOEL	0.85	1.12	99%	63%
Poluzzi *et al.* (2020)[78]	P	CFB, DFB, SEG[e]	Not specified	0.39/0.39/0.39	0.73/0.73/0.67	55%/55%/50%	62%/62%/56%
Henning and Haase (2021)[88]	P	EFG (slurry)	AEL	1.00	0.97	78%	55%
Butera *et al.* (2021)[89]	P	TSG	SOEL	0.40	0.95	74%	74%
Kofler and Clausen (2021)[79]	P	CFB	AEL	0.24	[f]	[f]	[f]
Poluzzi *et al.* (2022)[90]	P	CFB	Not specified	1.29/0.67/0.63	1.24/0.93/0.88	90%/68%/64%	61%/62%/61%
Melin *et al.* (2022)[91]	P	CFB	AEL	1.56	[g]	[g]	[g]
Fournas and Wei (2022)[92]	P	EFG	PEMEL	1.12	1.24	92%	62%
Ostadi *et al.* (2023)[93]	P	EFG	SOEL	0.86	1.30	94%	73%
Anetjärvi *et al.* (2023)[94]	P	CFB	AEL	1.11/0.41	1.28/0.88	90%/62%	64%/66%

[a] Scope: P: process simulation, E: estimation-based calculation approach. [b] EFG: entrained flow gasification, CFB: circulating fluidized bed, FB: fixed bed, TSG: two-stage gasifier (by DTU). [c] AEL: alkaline electrolysis, SOEL: solid oxide electrolysis, PEMEL: proton exchange membrane electrolysis. [d] Pressure module electrolyzer. [e] DFB: dual fluidized bed indirect gasifier, SEG: dual fluidized bed sorption-enhanced gasifier. [f] DME as main product with MeOH as intermediate. PY: 0.33 kg_{DME} per $kg_{biomass,dry}$, DME-based η_C: 27%, DME-based EY: 32%. [g] Ethanol as main product with MeOH as intermediate. PY: 0.952 kg_{EtOH} per $kg_{biomass,dry}$, Ethanol-based η_C: 91%, ethanol-based EY: 53%.

Due to the extent of the literature, a comprehensive description of all studies is omitted here. Such a narrative review paired with an extensive comparative study table is available in the ESI.† Here, developments in the field are briefly discussed and the limitations of this review are identified. A detailed discussion and meta-analytical comparison of the KPIs can be found in Section 6.1.

In the 1990's, early literature investigated the improvement of BtX processes by H_2 addition. Oulette and Scott proposed

Table 4 Literature overview for Power-and-Biomass-to-FT studies including the scope and the used gasification and electrolysis technologies. KPI values derived from the data in the respective literature

				ER	PY	η_C	EY
Ref.	Scope[a]	Gasifier[b]	Electrolyzer[c]	MW_{el} per MW_{th}	kg_{FT} per $kg_{biomass,dry}$	%	%
Seiler *et al.* (2010)[55]	E	EFG	Not specified	1.07	0.50	100%	56%
Baliban *et al.* (2010)[95]	P	CFB	Not specified	0.51	0.48	100%	79%
Bernical *et al.* (2012)[96]	P	EFG	SOEL	0.84	0.36	61%	46%
Bernical *et al.* (2013)[97]	P	EFG	SOEL	0.87	0.37	62%	46%
Albrecht *et al.* (2017)[98]	P	EFG (slurry)	PEMEL	1.57	0.50	98%	47%
Hillestad *et al.* (2018)[99]	P	EFG	SOEL	0.95	0.50	91%	65%
Kurkela[a] (2019)[100]	E	FB	Not specified	1.17	0.49	85%	54%
Zhang *et al.* (2020)[77]	P	EFG	SOEL	0.49	0.34	62%	50%
Habermeyer *et al.* (2021)[101]	P	CFB	AEL	0.94	0.38	61%	50%
Dossow *et al.* (2021)[102]	P	EFG	PEMEL SOEL	1.6/1.1/0.75 1.3/0.9/0.6	0.57/0.47/0.40 0.57/0.47/0.40	97%/79%/67% 97%/79%/67%	47%/47%/47% 53%/53%/53%
Pandey *et al.* (2022)[103]	P	EFG	SOEL	1.04/0.71/1.02/0.8	0.56/0.53/0.55/0.50	96%/91%/96%/86%	62%/70%/62%/62%
Habermeyer *et al.* (2023)[104]	P	FB	AEL SOEL	0.84/0.63/1.17/1.09	0.35/0.20/0.40/0.35	60%/34%/69%/57%	53%/34%/51%/46%
				0.63	0.35	60%	59%

[a] Scope: P: process simulation, E: estimation-based calculation approach. [b] EFG: entrained flow gasification, CFB: circulating fluidized bed, FB: fixed bed. [c] AEL: alkaline electrolysis, SOEL: solid oxide electrolysis, PEMEL: proton exchange membrane electrolysis.

Table 5 Literature overview for process simulation studies of parallel integration of co-electrolysis into BtX processes (PBtX) KPI values derived from the data in the respective literature, all using entrained flow gasification and SOEL

	ER	PY	η_C	EY
Ref.	MW_{el} per MW_{th}		%	%
Zhang *et al.* (2020)[77]	1.33	0.51 kg_{SNG} per $kg_{biomass,dry}$	75%	63%
	0.87	1.00 kg_{MeOH} per $kg_{biomass,dry}$	75%	61%
	0.69	0.35 kg_{FT} per $kg_{biomass,dry}$	60%	50%
Steinrücken *et al.* (2023)[124]	0.59	0.50 kg_{FT} per $kg_{biomass,dry}$	84%	64%
	0.69	0.53 kg_{FT} per $kg_{biomass,dry}$	89%	65%
	0.74	0.54 kg_{FT} per $kg_{biomass,dry}$	92%	64%
	0.83	0.56 kg_{FT} per $kg_{biomass,dry}$	94%	63%

adding H_2 before the catalytic synthesis step in 1995.[50] The authors argue that syngas from biomass gasification contains excess carbon to produce MeOH. In 1999, Specht *et al.* also investigated MeOH production through allothermal steam gasification and the addition of H_2 before the synthesis unit.[51] The authors argued that CO_2 separation or H_2 addition are the options to adjust the SN of the syngas, with the latter enabling almost complete utilization of the carbon atoms of the biomass while simultaneously using the O_2 from electrolysis as a gasification agent in the gasifier.[50,51] The increasing number of publications since 2010 demonstrates a strong interest in the PBtX process for all three final products.

Although most available literature on PBtX investigates the improvement of process efficiency *via* process simulations, a few experimental works have attempted to demonstrate the feasibility of the concept at laboratory and pilot scales. In 2018, Müller *et al.* performed a FT synthesis in a laboratory-scale reactor using a side stream of real syngas produced from the Güssing gasification plant with the addition of H_2.[105] They showed the system's feasibility and that adding H_2 can increase the product output Pilot-scale experimental work on a 5 kW_{th} bubbling fluidized bed gasifier under allothermal conditions demonstrated the general feasibility and plausibility of H_2 addition to methanation increasing the CH_4 yield.[106]

Most studies applied gasifier types with high potential to scale up (*i.e.*, CFB and EFG), but some studies have investigated small-scale applications and utilized fixed bed gasifiers or two-stage pyrolysis and gasification reactor (so-called "Viking" gasifier). In general, high-temperature gasifiers, as they have a higher oxygen demand, tend to produce syngas with lower SN. Therefore, PBtX based on EFG is expected to show a more significant gain in carbon efficiency.

As for the electrolyzers, the literature can be divided into the use of more established, low-temperature electrolyzers (PEMEL and AEL) and more efficient, high-temperature electrolyzers (SOEL). It is essential to acknowledge that most studies have

assumed, albeit questionable, that SOEL can be operated pressurized and O_2 from electrolysis is available as a pure stream for gasification and reforming. As discussed above, these assumptions are currently not technically viable.

In addition to the experiment-oriented studies and analyses of process flexibility,[107] a few studies of PBtX processes are excluded in Tables 2–4 due to incompatibility between the scope of the work and the KPI analyses. A study by Ali *et al.* on MeOH production using a low-temperature CFB gasifier and SOEL is excluded since their work is focused on comparing different reformer technologies rather than the overall system performance.[32] A study by Larose *et al.* does not include the analyses of the entire system and ends after syngas production without a synthesis.[108] Bareschino *et al.*[109] investigated the performance of a 3-stage methanation processes with the syngas composition from the experiments using catalytic BFB[110] and PEM using a 1-D kinetic model. Melin *et al.* investigated ethanol production performance using syngas from a fluidized bed gasifier and AEL.[91] However, the overall process performance was assessed focusing on ethanol production *via* a multi-step synthesis process of MeOH-to-acetic acid-to-EtOH, which makes it difficult to compare with other studies. Likewise, the evaluation of KPIs for the study by Putta *et al.* was not possible because it shows only economic indicators of the plant despite carrying out process simulations for the PBtX system with an entrained flow gasifier and SOEL.[111] Nielsen *et al.* integrated a SOEL into a BtX process with FT synthesis, using external steam and the volatile products from the FT reactor as the anode inlet stream. Compared with process variants in which H_2 from water electrolysis is added to the syngas, this fuel-assisted scenario where tail gas is delivered to the SOEL anode reduces the process's power requirement and increases energy efficiency.[112] Due to the challenges related to fuel assistance, like thermal gradients and stresses within the cell, the study is excluded. In 2020, Wang *et al.* proposed a polygeneration concept based on biomass gasification and rSOC allowing for power generation, power storage, or power neutrality.[107] The research is focused on the optimal conceptual plant design employing multi-time heat and mass integration platform and multiple objective functions.

3.2 Parallel integration of co-electrolysis

There are three competing technologies for electrochemical CO_2 reduction to CO, *i.e.* co-electrolysis, including low-temperature electrolysis, molten carbonate electrolysis,[113] and solid oxide electrolysis (SOEL).[114] Considering the respective technological maturity, achievable conversion, and energy efficiencies of the three options, SOEL proves to be a particularly applicable technology for electrifying BtX processes.[114–116] It should be mentioned here, that low-temperature electrolysis cells can potentially directly produce other chemicals from CO_2 such as formic acid, ethanol, or ethylene, which cannot be synthesized directly in other electrolysis systems.[114]

In high-temperature co-electrolysis using SOEL, H_2O, and CO_2 are supplied to the co-electrolysis yielding CO and H_2 on the cathode. CO_2 is split electrochemically into O_2 and CO according to reaction (11).[116,117] CO_2 electrolysis plays a minor role in CO generation and occurs exclusively due to diffusion limitations when the limiting current density is reached.[118] The majority of CO produced in co-electrolysis is due to the rWGS reaction inside the cell. Simultaneously, O_2 evolves at the electrode. Whether a high O_2 purity can be received on the anode side depends on the used purge gas (discussed in Section 3.1).

$$CO_{2(g)} \rightleftharpoons CO_{(g)} + 0.5O_{2(g)} \quad \Delta H_R^0 = 283.2 \text{ kJ mol}^{-1} \tag{11}$$

The energetic efficiency of CO_2 electrolysis in SOEL is above 70% even at current densities of 700–800 mA cm^{-2}.[114] The pressurized operation also remains challenging using SOEL. In addition to the presence of catalyst poisons, the deposition of elemental carbon can also lead to irreversible damage to the cell. Whether carbon deposition takes place depends on the inlet composition, pressure, and temperature.

The integration of a co-electrolysis unit into BtX processes can generally be achieved by two options (parallel or in-line), as shown in Fig. 6. Placing the co-electrolysis in parallel to the BtX process chain means that the CO_2 stream separated from the syngas can be further converted into CO and consequently into products in the subsequent synthesis step. This approach is within the scope of indirect electrification (PBtX). The in-line integration of co-electrolysis is an indirect electrification approach (eBtX) and is further discussed in Section 4.3.

Several authors investigated the electricity-based PtX path employing co-electrolysis,[119–122] while there is limited research on the combination of BtX and PtX in a parallel PBtX approach. When integrating co-electrolysis in parallel to a BtX process, the inlet gas composition to the electrolysis mainly determines the product composition.[119] Since, the partial pressure of the reactants in this configuration is very high, and the total volume flow through the electrolysis is limited to a minimum, the PBtX approach can lead to economic savings compared to the in-line configuration. Table 5 shows the few available publications for SNG, MeOH, and FT products.

In 2018, Samavati *et al.* investigated a process using EFG coupled with co-electrolysis (800 °C and 1 bar) and a subsequent FT synthesis.[123] The co-electrolysis setup uses external water and water produced by the FT synthesis and CO_2 separated from the syngas by a Selexol® wash after gasification. It was scaled only to use excess electricity from renewable power when available. The SOEL is thus more of an alternative pathway to the continuously operated BtX route. Consequently, the investigated process still requires external O_2 input to the EFG and a WGS step to adjust the H_2/CO ratio and is excluded in Table 5.

Zhang *et al.* compared a process using the SOEL in co-electrolysis mode at 750 °C and 1 bar to a process with H_2 addition from SOEL producing either SNG, MeOH, DME, or SAF *via* FT.[77] In co-electrolysis mode, the process uses the CO_2 stream separated in AGR after gasification. When renewable

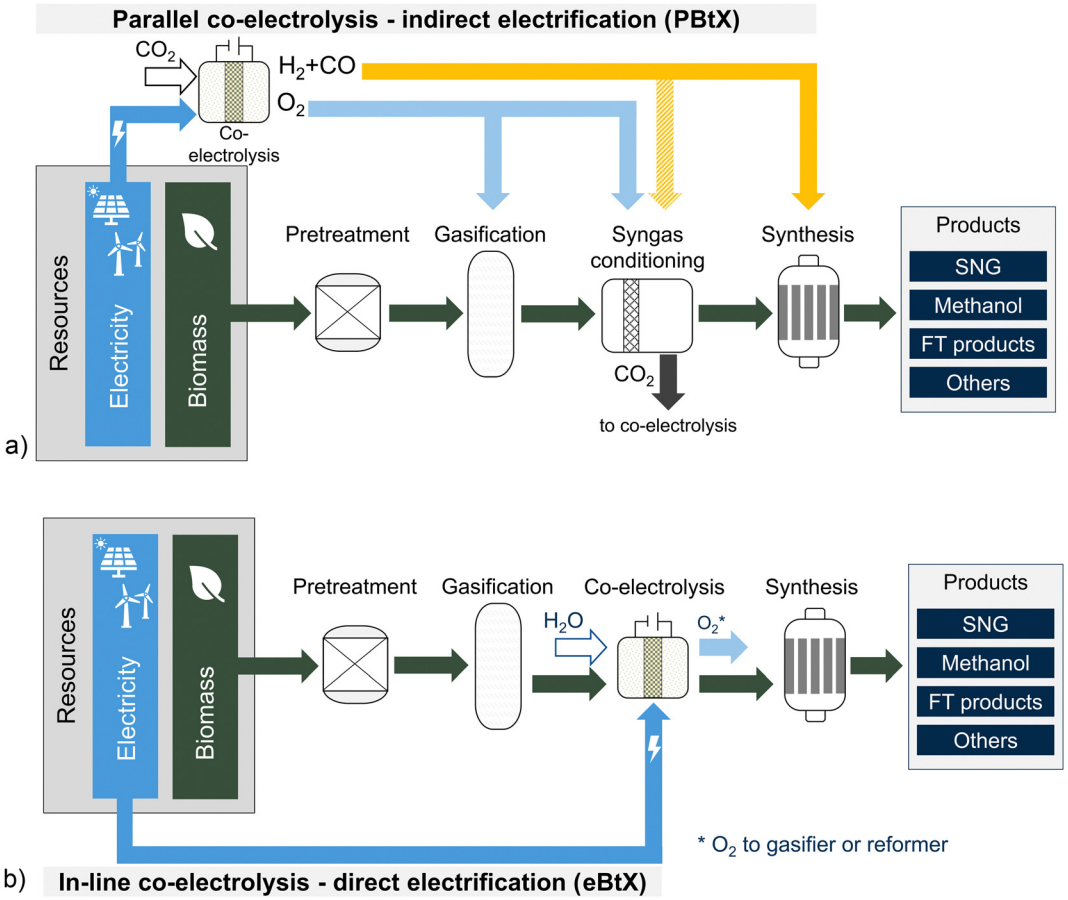

Fig. 6 Integration of co-electrolysis into BtX processes for: (a) parallel integration, *i.e.*, indirect electrification (PBtX) or (b) in-line integration, *i.e.* with the remaining syngas processing omitted for simplicity.

electricity is unavailable, the process runs in BtX mode with CO_2 stored for the period with available renewable electricity.[77]

Using a detailed 0D model, Steinrücken *et al.* simulated an electrified BtX process using co-electrolysis for both parallel and an in-line process design.[124] The developed process model employing a SOEL at atmospheric pressure and 800 °C is based on their process model using H_2 addition before synthesis[102] as presented in Section 3.1.3. In co-electrolysis mode, the parallel process option uses a mixture of the light ends from FT and the CO_2 stream separated in AGR after gasification. Comparing the process options with co-electrolysis to the H_2 addition processes and the conventional BtX and PtX reference models, they show that process efficiency and energy yield can be significantly increased by integrating co-electrolysis for an identical product yield and carbon efficiency.

4. Direct electrification of BtX processes (eBtX)

Direct electrification of BtX processes mean the direct use of electricity for individual process steps. One main advantage of eBtX is replacing partial oxidation in gasification or reforming, reducing the need for O_2 supply and potentially increasing carbon efficiency (reducing CO_2 production). Additionally, eBtX technologies can lead to smaller reactor sizes, which reduces investment costs and makes the process more cost-effective.

As shown in Fig. 7, the directly electrified eBtX process options are grouped by the type of electricity integration (electrically-heated, plasma, and electrochemical), contrary to indirect electrification processes, which are grouped by process steps. Electrically-heated processes (microwave, induction and resistance heating) are discussed in Section 4.1. Plasma-assisted processes are discussed in Section 4.2. In-line co-electrolysis processes are discussed in Section 4.3.

4.1 Electrically-heated processes

Electricity in the form of heat can be directly supplied to any process step along the BtX process chain. However, the electric heating option is not applicable for exothermic processes, including the forward WGS and catalytic syntheses. Several electric heating technologies exist, with electric resistance heating and microwave heating being the most relevant for eBtX processes. Other processes are infrared and induction heating. Other technologies, such as heat pumps, only apply to low-temperature applications. Therefore, they are unsuitable for the electrification of high-temperature applications in the BtX pathway and play a minor role. The review focuses on

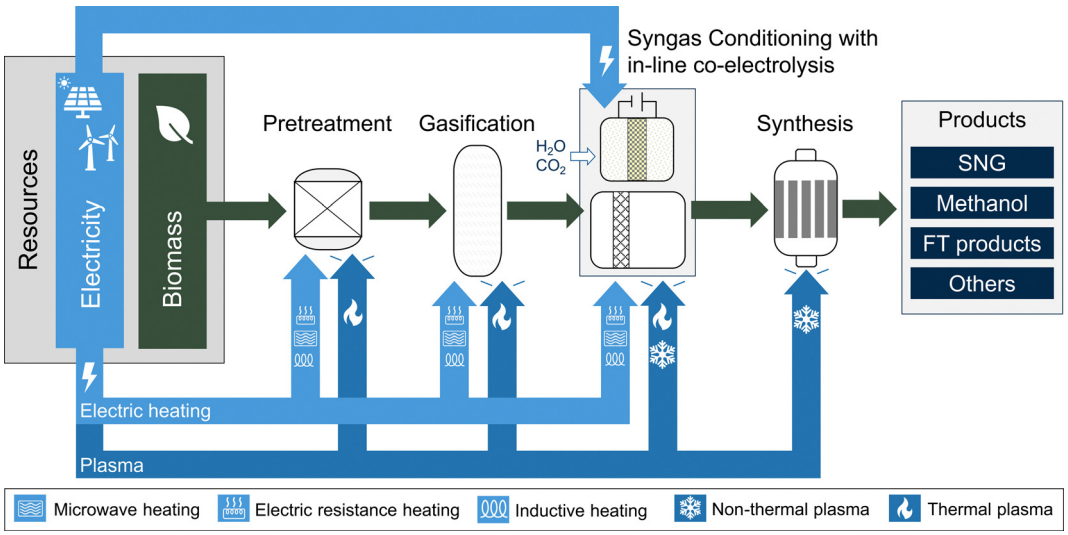

Fig. 7 Electrification options *via* electric heating, plasma, and in-line co-electrolysis integration along the process chain for direct BtX electrification (eBtX).

experimental work since the technologies are not yet widely investigated in process simulations.

In this review, the term electric resistance heating refers to an electric heating method that uses the Joule effect inside a heating element, in which the passage of an electric current through a conductor generates heat reaching efficiencies of >90%.[125] Heat is transferred to the target material or process *via* conduction, convection, and/or radiation.[125] Electric resistance heating is categorized as direct heating since it relies on heat transfer from the heating element to the medium that is supposed to have a temperature increase (*e.g.*, biomass or catalyst). It can also be used for indirect heating if air, steam or thermal oil are used as heat transfer medium. Heating elements are established technologies that are widely used in various industries.[125] The choice of heating element material depends on the heat transfer process, and the physical and chemical properties of the process environment, with the target temperature usually being the key factor.[125] Heating elements can supply heat at temperatures of up to 1200 °C for Nickel-based alloys, 1400 °C for Iron-based alloys, 2500 °C for exotic metals such as Tantalum, and up to 3000 °C for graphite, with the latter two not to be used in corrosive or oxidative atmospheres.[125]

In addition to convective or conductive heat transfer, the heat generated in indirect electric resistance heating can be also transferred to the desired material *via* radiation. Specific heating devices can be designed to increase the radiative heat transfer The electromagnetic waves emitted by a hot object are absorbed by molecules when changing rotational-vibrational movements.[125–128] Therefore, the spectral output of the emitter must be matched to the reflection and absorption characteristics of the product to use radiation efficiently.[125] Infrared radiation is a prominent type of radiation that transfers heat.

Infrared radiation is electromagnetic radiation at a wavelength between 700 nm and 1 mm.[128] Lower-temperature infrared emitters (long and medium wavelengths) are typically used to heat and dry non-metallic materials because they generally absorb radiation at longer wavelengths. In contrast, short wavelength emitters are used for heating suitable materials to higher temperatures at high intensities.[125] Infrared heating is one of the most widely used electric heating techniques in all branches of industry.[125] The radiant efficiency (energy output as radiation to the energy input of the heater) lies between 50% and 86%, depending on the emitter type.[127] The limitations of infrared energy are waste heat dissipation and insufficient penetration.[128]

Microwave heating presents another possible electric heating technology.[129] Here, the electromagnetic energy is converted to thermal energy through the alternating direction of the electromagnetic field. The excited molecules with a dipole movement are set to motion, and ionic species migrate, causing friction and thus generating heat.[130–132] Different materials have distinctive capabilities to dissipate this microwave energy to heat. Arpia *et al.*, for example, classify woody biomass as a poor microwave absorber, whereas biochar from biomass is considered a good absorber.[133] The conversion efficiency of electricity to microwave ranges from 50% (2450 MHz) to 85% (915 MHz).[132]

Advantages of microwave heating include the ability to heat solid or liquid media without direct contact from distance, similar to infrared heating, but unlike resistance heating.[134] Furthermore, the heating is selective, causes smaller temperature gradients in the material, and has a high heating rate.[134] As a result, larger particles can be processed, avoiding the need for particle size reduction.[135] Future challenges are tests and scale-up of continuously running processes. However, microwave heating can lead to the formation of "micro plasmas," which appear as hot-spots or sparks, leading to much higher temperatures in the surrounding regions than the mean temperature of the material.[130] We excluded the microwave

assisted-synthesis from Section 4.1.3 due to the limited relevance for the eBtX process (information in ESI†).

Besides electric resistance heating or microwave heating, induction is another option to supply energy in the form of heat to the process. Based on alternating magnetic fields, materials that are ferromagnetic, conductive, or both at the same time can be heated.[136] In conductive materials, the magnetic field causes an electric current (Eddy current) to dissipate heat *via* Joule heating.[136] For ferromagnetic materials, heat energy is released during the change of orientation of magnetic dipoles (hysteresis loss).[136] The advantages of induction heating are efficiencies of above 90%, fast heating, and controlled heat input.[137] Inductively-heated synthesis is excluded from the paper but presented in the ESI.†

4.1.1 Electrically-heated pretreatment. To supply the pretreatment processes with medium- to high-temperature heat, electric heating can be applied.[138] However, a standalone BtX plant usually has a heat surplus from hot syngas cooling after gasification and exothermic synthesis processes. Therefore, internal heat integration can typically cover the heating demand for preheating and most pretreatment processes. Using electricity for heating is questionable for low-temperature processes like biomass drying, torrefaction and HTC. However, the options for electrically-heated biomass drying are presented here for completeness.

Conventional dryers use steam or hot air as an agent for heat transport. These media can easily be heated by resistance heating, making it possible to use conventional dryer setups. The advantage of infrared, microwave, and induction drying is the direct heat transfer to the bulk material. The same applies to the use of induction, infrared and microwave heating for torrefaction or HTC, including several additional advantages over conventional methods, such as higher heating rates, lower temperature gradients, and the ability to process larger particle sizes. However, it remains unclear whether the energy efficiency of such heating is superior to that of conventional processes. Due to the low-temperature level and the small amounts of energy required for drying, torrefaction, or HTC compared to the overall process, details on microwave-assisted HTC and torrefaction, and infrared, microwave-assisted and induction drying are presented in the ESI.† The following section focuses solely on electrified pyrolysis.

Microwave-assisted pyrolysis is the most researched process in microwave-heated thermochemical processes[133] and shows the most drastic but positive change in product yield and properties compared to conventional pyrolysis.[133,139] The biomass can be treated with or without microwave absorbers for enhanced absorption.[140] The technology is not tested in pilot plant size, but the first concepts for scale-up are developed.[141]

The higher heating rates of microwave heating results in higher release rates of volatile components while secondary decomposition of volatiles is also promoted. This leads to higher gas yields during biomass pyrolysis. At the same time, the yield of liquid products decreases during microwave-assisted pyrolysis compared to conventional pyrolysis.[133,142] The liquid product has a higher heating value, lower oxygen content, and higher carbon content.[133] The properties of the biochar can also be improved. It is more uniform and has a higher surface area, for example.[133] Compared to conventional pyrolysis, microwave-assisted pyrolysis is expected to have lower processing times and higher energy efficiency.[130] The impact of microwave-assisted pyrolysis on the gasification properties of char has been tested. The reactivity of the biochar is increased compared to conventional pyrolysis.[143,144] However, other researchers found the opposite relation.[145] Due to the complex relationships in microwave-assisted pyrolysis, the influence of (micro) plasma cannot be excluded. Therefore, it can be assumed that using microwaves is not a pure heating of the pyrolysis step.

Inductively-heated pyrolysis is especially suitable as technology for intermediate to fast pyrolysis due to the high heating rates.[146] Several studies compare induction heated pyrolysis to conventionally heated pyrolysis for sewage sludge,[147] solid recovered fuel,[146] and sawdust.[148] For example, higher BET surface area of the char,[147,148] higher energy yield,[147] or altered gas composition[146,147] were reported compared to conventionally heated pyrolysis. Further studies report experimental results from inductively-heated pyrolysis.[149–151] Electrical resistance heating is used in screw reactors (Auger reactor) for pyrolysis, a common practice for these reactor types.[152] However, the process is of lower importance in this context.

4.1.2 Electrically-heated gasification. The application of electrical heating to gasification primarily aims at reaching near allothermal gasification resulting in a reduced gasification agent demand. Introducing heat to the gasifier maximizes the potential concentration and mass flow of H_2 and CO within the raw syngas leading to higher product yields. Diverse technology options, such as resistance, microwave, or induction heating can provide electrical heating either upstream or directly within the gasifier. Fig. 8 shows different options and technologies of electrically-heated gasification depending on the gasifier type and point of electrical heating. Alternatively, concentrated solar power or other high-temperature sources could be utilized,[82] which are not in the scope of this review.

One possible option is to use an indirect heat supply to increase the temperature of any stream entering the gasification reactor, such as the feedstock itself, the employed fluidization agent or high-temperature steam. Microwave and electric resistance heating might be viable options here. Inductive heating is only applicable to heat suitable bed material in FB gasifiers. Among other electrically enhanced BtX process concepts, Butera *et al.* modeled a process using the so-called two-stage electrically-heated gasifier, where the pyrolysis gas entering an updraft fixed bed char gasifier is electrically preheated to 950 °C.[63] Their results show that up to 88 MW_{el} can be incorporated for a 100 MW_{th} biomass input.[63]

Electric resistance heating is applied for pilot scale gasifiers due to simplicity and feasibility for small-scale plants as heating source.[153,154] Mayerhofer *et al.* used electrically-heated heat pipes in a pilot-scale BFB gasifier to investigate tar formation under different operating parameters.[155] However,

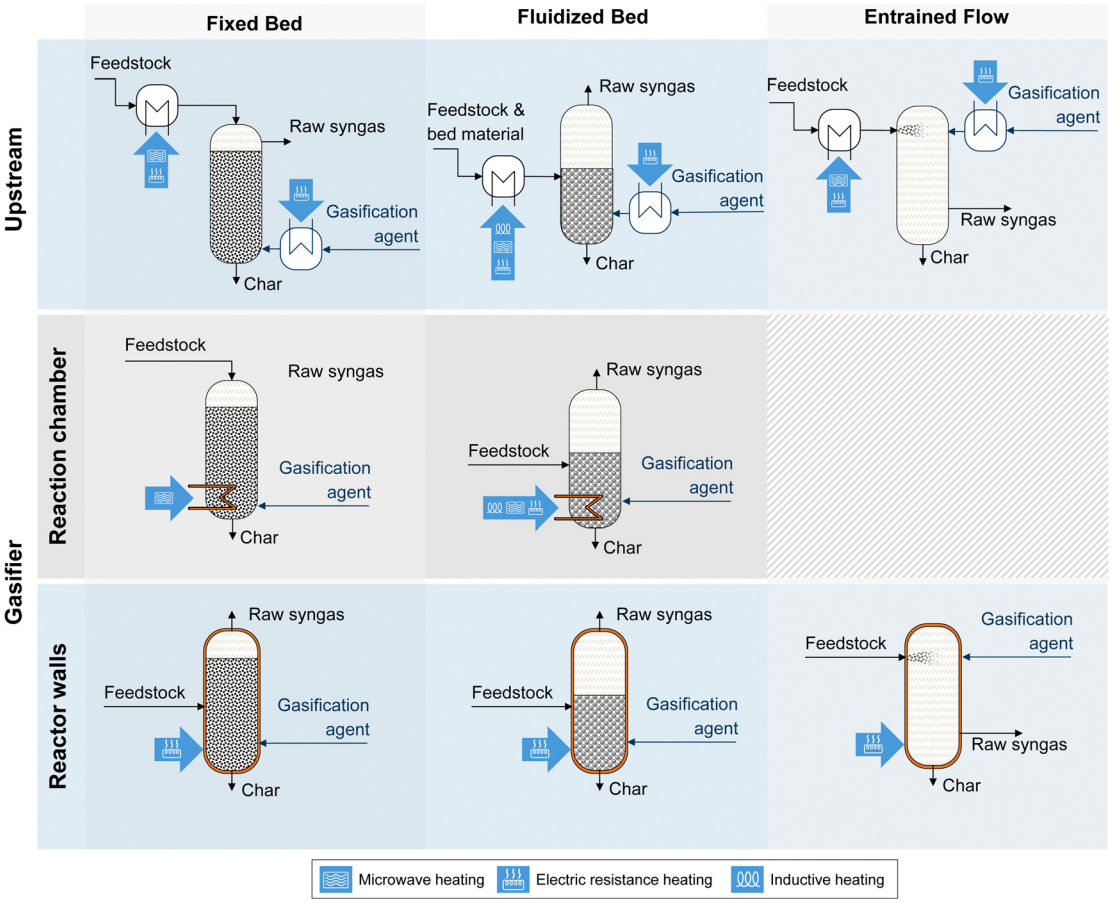

Fig. 8 Simplified schematics of different options and technologies to electrically heat gasification depending on gasifier reactor type and point of electrical heating. For fixed bed gasification a downdraft gasifier setup is shown exemplarily. Carrier gas, and auxiliaries are not included for simplicity.

the energetic performance of the process was not investigated. Lenis-Rodas *et al.* studied the steam-blown gasification of high moisture content biomass in a three-dimensional model with heated gasifier walls.[156,157] They found that a higher heat flux at the syngas outlet benefits efficiency and H_2 concentration in the product gas.[156] Reaching the ash melting temperature on the surface of such heaters must be avoided.[158]

As discussed in Section 3.1.3, Putta *et al.* determined from their process simulation that direct electricity addition to the gasifier as heat combined with H_2 addition is more advantageous than only adding H_2.[111] They varied the share of electrical energy added to the gasifier and water electrolysis. For a biomass input of 130 MW_{th} to the gasifier, the optimal amount of heat to the gasifier *via* electrical heating was approximately 50 MW_{th}, equivalent to about 37–39% of the biomass energy input.[111] Song *et al.* performed an analysis of an electrically-heated fluidized bed biomass gasifier for the production of SNG.[159] The authors state that electrical heat addition is more beneficial in cost and efficiency than adding H_2. With a biomass input of 105 MW_{th}, an electrical heating of 38 MW_{el} is required assuming electric resistance heating with a power-to-heat efficiency of 99%. In this scenario, the energy yield is 68.0%.[159] Song *et al.* also conducted an exergy analysis on the process ending before SNG synthesis with the produced syngas.[160] They conclude that electrically-heated gasification consumes less electricity and generates syngas with higher chemical exergy value than water electrolysis-assisted gasification for the same mass flow rate of feedstock. They reason that the exergy loss in water electrolysis is significant, with an exergy efficiency ranging from 54.1% to 79.1%.

Butera *et al.* modeled two concepts for electrically-heated gasification.[63] One is the so-called two-stage electro gasifier with electric heating providing the heat for gasification reactions through resistance elements inside a fluidized bed gasifier.[63,161,162] Up to 11.3 MW_{el} are electrically supplied to the gasification reactor for a 100 MW_{th} biomass input. In a second concept, a BFB gasifier is electrically-heated *via* heat pipes. In the case of using the BFB gasifier, 15.8 MW_{el} are added. However, quantifying these concepts must be cautiously treated as the simulated cases include multiple electricity integration modes along the process chain. It should be noted that the current process modeling studies reviewed above do not consider the technical feasibility of electrical heating. Furthermore, the technical realization has not been shown yet in a relevant scale.

Microwave-assisted gasification operates by converting the energy of microwaves into heat with the bed material or biomass as absorbers. Thus, microwave-assisted gasification

is limited to fixed bed and fluidized bed gasifiers. Since it is a relatively new field, the technology lacks the design of gasifiers, energetic performance assessment, and economic assessment.[11,134] A recent review on microwave-heated gasification emphasizes the benefits of microwave heating compared to conventional gasification.[12] Zhang *et al.* review the CFD-based simulation models for microwave-assisted gasification,[11] and Arpia *et al.* review the concepts and experimental studies on different types of microwave-assisted gasification technologies.[13] Ke *et al.* assessed the energy performance of an air-blown biomass gasifier under microwave irradiation.[163] Xie *et al.* developed a concept for a dual fluidized bed gasifier heated with microwave radiation.[164]

Induction-heated gasification gained little attention. Wu *et al.* found an improved H_2 yield in catalyzed steam gasification of biomass for an induction heated system.[165] Further improvements were possible by the addition of metallic particles to the reactor.

4.1.3 Electrically-heated syngas conditioning. The electrification of high-temperature reforming processes to produce syngas, condition syngas or reforming is developed. Very view publications focus specifically on the reforming of hydrocarbons in syngas. Usually, electric resistance heating of the reactor is used to supply heat to the reaction chamber. Possible applications include catalyzed reactions like steam methane reforming, MeOH cracking, rWGS or dehydrogenation.[166] Gas outlet temperatures can vary between 900 °C and 1300 °C.[166] Especially the electrically-heated steam methane reforming gained interest in cutting CO_2 emissions.[167–169] Commercial offers also exist for the electrically-heated rWGS process.[170]

Direct electric resistance heating of the reactor chamber allows allothermal operation cutting the need for heat generation *via* combustion (POX). Melin *et al.* performed a process simulation for ethanol production based on biomass gasification and H_2 addition.[91] One investigated scenario included an electrically-heated reformer with a power-to-heat efficiency of 100%. Results show that the eBtX efficiency is increased with the electrically-heated reformer from 53.6% to 57.3% compared to an allothermal reformer with O_2 as a combustion agent. The electrical power input for 5.36 MW_{th} of biomass was 0.96 MW_{el}. The levelized cost of ethanol was slightly lower for the electrically-heated reformer than for the allothermal reformer.

Butera *et al.* used a SOEL as an electrically-heated catalytic reactor with high-frequency alternating current (AC) and no air flow on the O_2 side to reform hydrocarbons and tars.[63,162] Up to 8.5 MW_{el} could be electrically supplied to the AC reformer for a 100 MW_{th} biomass input. In addition, the employed pre-reformer could also be electrically-heated to allow most of the reforming to occur in the pre-reformer when the solid oxide cell is in SOEL mode. This solution was, however, discarded due to the complexity of the reformer design. Instead, Butera *et al.* used electrical heating of the raw syngas after a bubbling fluidized bed gasifier before entering a tar reformer.[63] Their results show that up to 4.5 MW_{el} can be added to the tar reformer for a 100 MW_{th} biomass input.[63] However, the impact of both concepts cannot be assessed independently because the simulated cases include multiple electrification options along the process chain.

Microwave-assisted reforming uses microwaves to reach sufficient temperatures for the reforming reactions.[142] Microwave heating is beneficial in volumetric heating, enabling faster heating and thus accelerating and enhancing chemical reactions through efficient heat transfer.[171] However, applying microwaves as a direct heat source for reforming reactors is challenging since gases are usually bad absorbers of microwave radiation.[172] Yet, microwave-assisted reforming was found to be a very attractive tar reforming technique in the presence of an absorber material.[173] Li *et al.* state that microwave-assisted reforming shows high removal efficiencies of 97% for real tar components and 100% for model tar components.[172] All evaluations are based on lab-scale experiments and are in the research and development stage without industrial validation.[172]

Induction-heated systems for reforming processes are developed in the context of steam methane reforming,[174–176] dry methane reforming,[174,175] or POX[177] for natural gas or biogas. Catalyst development focuses on high educt conversion and efficient heat dissipation at the same time. Even though the processes are developed for other raw materials, the process concepts can be transferred to syngas reforming. For that, a tailored catalyst for syngas reforming has to be developed. For high-temperature endothermic catalytic processes, induction heating reduces energy losses and equipment cost.[178]

4.2 Plasma-assisted processes

Plasma is widely used in process engineering and presents a promising way to directly electrify the BtX process route (eBtX).[179] Plasma is the fourth state of matter apart from solid, liquid, and gas phase and consists of free electrons, ions, and neutral particles.[14] In general, plasma can be formed by supplying sufficient electrical energy to a plasma gas leading to dissociation of the gas molecules. A sustained electrical arc has to be created between two conductors. In a powerful electric field, the gas between the conductors is ionized and electric current can pass between the conductors.[180] At about 2000 °C, gas molecules dissociate to the atomic state.[180] They become ionized when the temperature is increased to 3000 °C.[180] The degree of ionization of a plasma is controlled by the temperature, which determines the fraction of atoms that have lost or gained electrons. Heat is generated due to the Joule effect, similar to electric resistance heating, across the system and further ionizes gas molecules, thus forming plasma.[180]

Plasma can be categorized as thermal plasma (hot or equilibrium plasma) and non-thermal plasma (cold or non-equilibrium plasma). This classification depends on the thermal equilibrium of the species. When the species are in thermal equilibrium, *i.e.*, electrons and ions are at equal temperatures called thermal plasma.[14,180] Electrically generated thermal plasma can reach temperatures of 20 000 K and above.[14,180] Compared to non-thermal plasma, thermal plasma has a higher degree of ionization and is characterized by a higher energy density and a higher concentration of charged

particles.[180] This enables more mobility and elastic collision and ensures thermal equilibrium between species.[180] Thermal plasma reactors can be classified into four plasma generator types: direct current (DC) plasma reactor (transferred arc reactor and non-transferred arc reactor), AC plasma reactor, radio frequency (RF) plasma reactor, and microwave-assisted plasma reactor.[14,15,181] The efficiency of the power supply device is typically between 40 and 70% for RF and microwave plasma, and between 60 and 90% for thermal DC plasma torches.[15] Thermal AC plasma torches are more efficient, with an efficiency of 90–94% (electricity to thermal plasma energy).[182]

Thermal plasma has a variety of uses in industry, including coating techniques, surface modification, materials processing, and chemical synthesis.[213] In practice, the operating and maintenance costs of the plasma generators and reactors are the decisive factor in determining whether the systems can be operated economically.[183] However, the investment costs of incinerator plants with plasma torches are typically 30–50% lower than conventional incinerators of the same capacity.[183]

Non-thermal plasma has a degree of ionization less than 10^{-4}.[215] Applications of non-thermal plasmas are, for example, low-temperature chemistry, treatment of heat-sensitive materials, and biological tissues. Sources of non-thermal plasmas can, for example, be different types of glow discharges, low-pressure RF discharges, and corona discharges.[216]

The four major options for integrating plasma into BtX processes (see Fig. 7) are described in detail. The different plasma chemistry and reactions induced by non-thermal plasma are driven mainly by electron impact, limiting its use in practice for solid conversion process steps. In addition, it is challenging to uphold the non-thermal plasma, especially when heterogeneous substances are involved. Consequently, the reactor technologies involving solids are of low technological maturity and non-thermal plasmas are of little relevance for the pyrolysis or gasification step.[184,185] Thermal plasma uses the Joule heating effect for high gas temperatures and highly reactive atomic and ionic species to decompose solid organic molecules.[186,187] In addition, fusion occurs for all inorganic components forming inert and stable vitrified slag.[180] The boundaries between pyrolysis and gasification in the presence of plasmas are often blurred because, on the one hand, plasma-assisted gasification usually requires much less gasification medium than conventional gasification and, on the other hand, plasma pyrolysis is operated at significantly higher temperatures than the conventional one. As described in Section 4.2.1, carbonaceous solids react at high temperatures to produce gas and solid products without O_2 in thermal plasma pyrolysis.[15] Plasma-assisted gasification, on the other hand, includes the partial oxidation of the solid species resulting in a high proportion of gaseous products and ash but only small quantities of char (see Section 4.2.2).[15] The second part of this section presents the usage of plasma for gas phase reactions, primarily for syngas reforming (Section 4.2.3) and catalytic synthesis (Section 4.2.4).

4.2.1 Plasma-assisted pyrolysis. High temperatures and the absence of an oxidization agent in combination with an inert plasma gas such as Ar or N_2 characterize thermal plasma pyrolysis. When carbonaceous particles are injected into a thermal plasma, they are heated very rapidly by the plasma and the volatile matter is released and cracked.[15] A cleaner pyrolysis gas can be obtained using plasma-assisted pyrolysis since high-energy species, such as electrons, ions, atoms, and free radicals in plasma, can enhance tar decomposition.[188] The main gaseous products (H_2, CO_2, and CO) can be formed from solid fuel devolatilization followed by secondary reactions in the gas phase and char gasification, making thermal plasma pyrolysis a combination of solid heating and gas phase plasma reforming.[189] Thermal plasma pyrolysis is generally operated without any other energy input than plasma.

Thermal plasma pyrolysis has been of primary interest for organic waste disposal.[15] Research and small-scale development effort are continuing and some commercial plasma waste disposal facilities are operational.[15] Several studies on stand-alone plasma-assisted pyrolysis of biomass were conducted on lab-scale level in batch mode. Integration of plasma pyrolysis into the BtX process chain and modeling or process simulation studies are still pending.

Tang and Huang argue that the high temperature in thermal plasmas (usually 3000–10 000 K) might lead to high thermal losses in the pyrolysis reactor.[188] Instead, they propose using RF plasma operating at moderate energy density and gas temperatures, which could ensure biomass pyrolysis with high gas yields, high-quality char, and little tar formation. The RF plasma heating method employs a high-frequency AC at high voltage, producing a self-heated plasma.[183] In 2005, the research group started investigating RF plasma pyrolysis to treat fir saw dust.[188,190,191] The experiments were in a fixed bed downdraft reactor inside a vacuum reactor using N_2 as carrier and plasma gas.[188] They showed a high gas yield of up to 66 wt.% of the biomass feed, implying that plasma pyrolysis is more of an alternative to gasification than a pretreatment method.

Tu *et al.* also investigated an RF plasma reactor studying the effects of major system parameters on the performance of the rice straw pyrolysis using a fixed bed downdraft batch reactor using N_2 as carrier gas.[183,192] Subsequently, they investigated the pyrolysis of rice straw using a thermal plasma torch as a heat source.[193,194] The thermal plasma pyrolysis was performed in a batch mode using a pilot-scale plasma torch system in an N_2 atmosphere. They showed that solid residues were converted into non-leachable vitrified slag while the high amount of produced pyrolysis gas consists mainly of CO and H_2. Furthermore, increased moisture in the initial biomass results in higher mass yields of H_2 and CO_2.

In 2013, Tang *et al.* used a spouted bed reactor employing a thermal DC plasma to pyrolyze rice hull.[195] The reactor design allowed a uniform bed temperature distribution and stability to decrease the convective and radiant heat losses efficiently. They used N_2 for spouting and plasma gas. However, the setup can generally work as a gasifier when replacing N_2 with a gasifying agent. Lin *et al.* conducted pyrolysis experiments on algae in an atmospheric pressure drop-tube microwave plasma reactor

using N_2 as plasma gas.[189] They showed that the H_2 gas productivity from biomass can be increased with increasing microwave power.[189]

4.2.2 Plasma-assisted gasification. Plasma-assisted gasification uses a plasma torch as an additional external energy source to assist the feedstock gasification into syngas and to convert the inorganic fraction into solid particulates or vitrified slag. Plasma-assisted gasification can allow an allothermal operation to a certain extent using electrically induced plasma as energy input.[196–198] In addition to the plasma-enhanced deconstruction of the solid fraction, rapid gasification of the homogeneous phase and further gasification of char particles occurs in plasma-assisted gasification.[15,179,199,200] Thus, using non-thermal plasma could be beneficial for the gas phase reactions, though it is rarely used in practice due to its incompatibility with solid materials, as described above.

Many factors affect plasma gasification performance, including plasma power, reactor temperature, flow rate of plasma gas, type of plasma gas, residence time in the gasifier, and the feedstock's physical and chemical characteristics.[14,201] Good reviews on plasma pyrolysis and plasma-assisted gasification exist.[14–17] Plasma-assisted gasification allows simple heat input control by adjusting the electrical power.[197,202] It also offers greater flexibility in feedstock selection, cleaner raw syngas, and reduced equipment size.[197,203] The major disadvantage of plasma-assisted gasification is the high design complexity and cost, limiting commercialization.[197,204]

In literature, plasma-assisted gasification concepts are divided into single-stage and two-stage processes according to where the plasma is applied. Fig. 9 shows the single-stage and two-stage integration concepts into the gasification reactor for fixed bed, fluidized bed, and entrained flow gasifiers.

In single-stage plasma-assisted gasification, the feedstock is directly in contact with thermal plasma within the gasifier.[196] High amounts of energy can be incorporated into the gasifier.[196,205] Single-stage plasma systems are increasingly used for thermal waste treatment, as they completely break down the waste into tar-free syngas.[196,202] Large-scale plasma

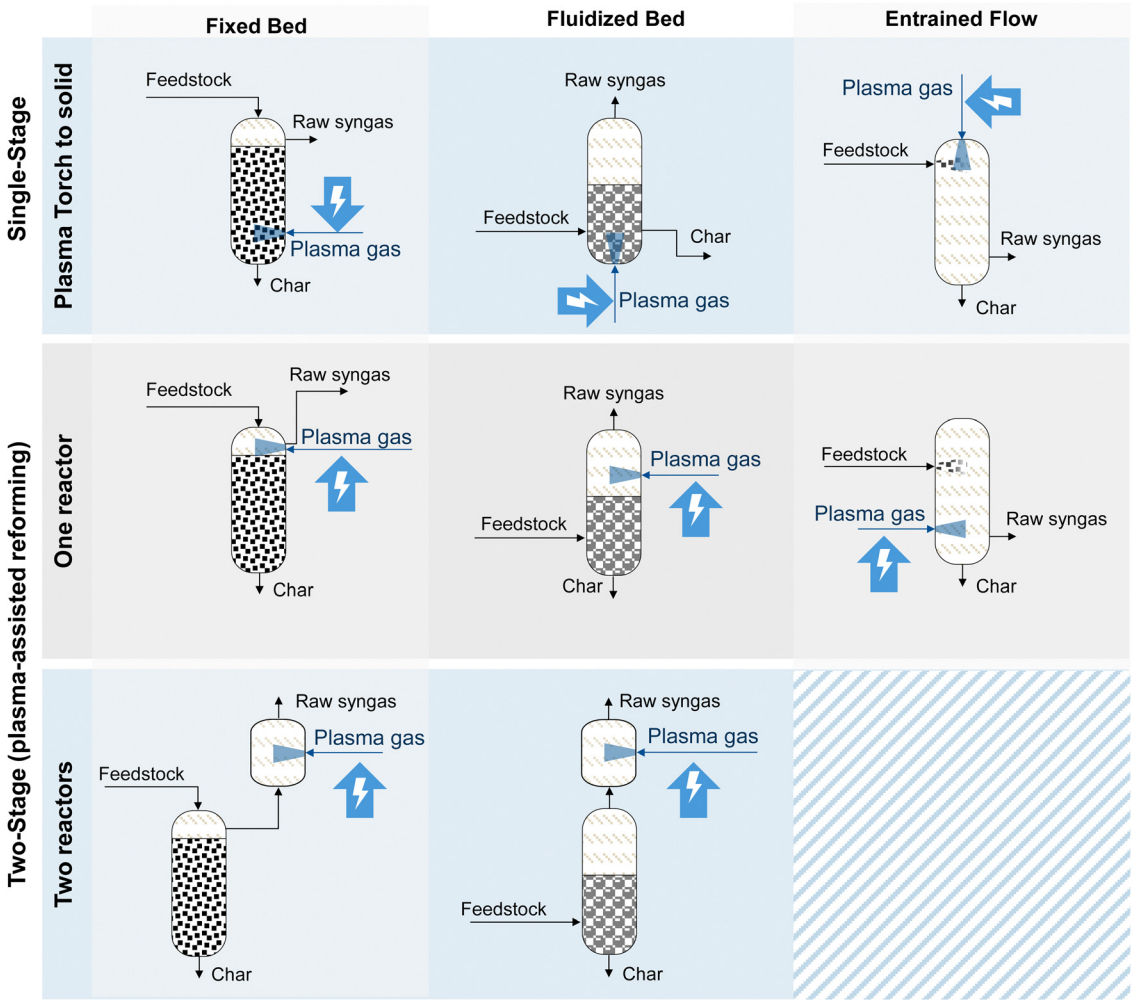

Fig. 9 Simplified schematics of different plasma torch setups for single-stage and two-stage plasma assisted-gasification depending on gasifier reactor type. For fixed bed gasification a downdraft gasifier setup is shown exemplarily. Gasification agent, carrier gas, and auxiliaries are not included for displaying reasons.

Table 6 Literature overview for experimental plasma-assisted gasification using thermal plasma with DC arc-discharge in a fixed bed downdraft gasifier to produce syngas from biomass

Ref.	Raw material input	Plasma gas	ER in MW_{el} per MW_{th}
Zhao *et al.* (2001)[240]	Wood (30–60 kW_{th}), rice husk (10–40 kW_{th})	Ar/H_2	0.68–1.35, 1.01–4.05
Balgaranova (2003)[237]	Sewage sludge[a]	Steam	Not specified
Hrabovsky *et al.* (2006)[222]	Wood (30–210 kW_{th})	Steam/Ar	0.88–3.47
Hlina *et al.* (2006)[221]	Wood (20–230 kW_{th})	Steam/Ar	1.06–6.9
Byun *et al.* (2011)[238]	Paper mill waste (190 kW_{th})	O_2	0.53
Pinaev *et al.* (2011)[239]	Bioorganic silt deposits[a]	Air	not specified
Hlina *et al.* (2014)[223]	Sawdust (160 kW_{th}), wood pellets (145 kW_{th})	Steam/Ar	0.66, 0.66
Diaz *et al.* (2015)[224]	Hard wood shaving, peach pits, almond hulls, grape pomace, coffee ground (18–24 kW_{th})	Steam	0.57–2.82 (0.85–4.27[b])
Wang *et al.* (2015)[227]	Wood (45 kW_{th})	Air or N_2	0.42–1.00
Tamošiūnas *et al.*[c] (2016)[232]	Wood (17 kW_{th})	Steam	2.94
Hrabovsky *et al.* (2017)[198]	Wood saw dust (110–260 kW_{th}), wood pellets (135–270 kW_{th})	Steam/Ar	0.52–1.27, 0.52–1.04
Tamošiūnas *et al.*[c] (2017)[197]	Charcoal (40 kW_{th})	Steam	1.25
Muvhiiwa *et al.* (2020)[229]	Wood pellets (5–10 kW_{th})	$O_2 + N_2$	1.16, 2.17
Aikas *et al.* (2023)[230]	Wood pellets (105 kW_{th})	Air	0.48
Tamošiūnas *et al.*[c] (2023)[231]	Wood pellets (100 kW_{th})	Steam + air	0.5

[a] Thermal biomass input not specified. [b] If steam generation through glow discharge plasma is considered. [c] Using an entrained flow gasifier.

gasification for waste is available on industrial scale.[206] The technology is also proposed for gasifying sewage sludge to produce clean syngas.[233]

Two-stage gasification systems use a conventional gasifier with plasma being used in a downstream processing step. Here, the presence of radicals, atoms, and ions in the plasma medium can significantly improve the reaction kinetics of tar cracking or methane reforming. In that way, integrating electricity as plasma improves the reforming step.[197,198,207] In this step, the syngas can also be further enriched with H_2 through the rWGS reaction (reaction (6)).[202,208] In this review, the single-stage setup is referred to as plasma-assisted gasification. In contrast, the two-stage setup, where plasma gas is typically used within the syngas phase, is referred to as plasma-assisted reforming, which is discussed in Section 4.2.3.

An'shakov *et al.* conducted experiments on organic wastes using a two-stage process with plasma usage in both reactors.[209] A first plasma torch is used in the gasifier, while an electric-arc plasma torch in the second reactor maintains the temperature at 1300–1500 °C.[209,210] Vishwajeet *et al.* conducted experiments using a two-stage gasification system coupling a prototype-entrained flow plasma-assisted gasification reactor with ex-situ plasma vitrification.[211] They showed that although the use of plasma positively affects the quality of the raw syngas, the dilution by plasma gases such as N_2 leads to a low calorific value of the dry syngas.

Several studies on plasma-assisted gasification of biomass were conducted on lab scale level in a batch mode[212–216] and are thus of little relevance for integrating into BtX processes. Also, among the four main plasma types, the number of studies on AC, RF, and microwave plasma is limited to solid feedstock gasification. Rutberg *et al.* and Surov *et al.* used an AC three-phase high-voltage plasma to gasify charcoal and wood in a fixed bed gasifier.[217,218] Yoon and Lee performed plasma-assisted gasification of two kinds of coal and one kind of charcoal using a microwave torch.[236] Sturm *et al.* also conducted lab-scale experiments on integrating thermal microwave plasma into a fixed bed of cellulose for syngas production.[219] Delikonstantisa *et al.* investigated air/N_2 gasification of a byproduct stream from an industrial fermenter in a tubular microwave plasma reactor.[220]

However, the most used reactor for plasma-assisted gasification of biomass is the DC plasma reactor due to its power capacity of up to several megawatts.[197] While this makes the DC arc plasma applicable to industrial-scale operation, it still faces the challenge of electrode contamination and erosion.[197] Table 6 provides an overview of experimental studies on plasma-assisted gasification in mostly fixed-bed downdraft reactors using thermal plasma with DC arc-discharge to produce syngas from a solid biogenic feedstock. Several authors investigate biomass gasification using wood,[198,199,221–231] oak charcoal,[197,232–236] or biogenic wastes.[237–239] Employed plasma gases include air, H_2, steam, Ar, and N_2 with plasma torches ranging from 15 kW_{el}[224,229,237] to 150 kW_{el}.[222,239]

Regarding modeling and process simulations, Table 7 provides an overview of process modeling studies on plasma-assisted gasification using thermal plasma to produce syngas from a solid biogenic feedstock. If reported at all, the ER shows a wide variance from 0.06 to 1.5 MW_{el} per MW_{th}. One major shortcoming of the presented studies is that the processes end with syngas and do not consider any synthesis. The plasma gases used, especially N_2 or Argon, are also inert gases in the synthesis. These gases must either be separated from the gas stream or higher purge streams in the synthesis are needed. Therefore, the integration with a PBtX process chain using these plasma gases is questionable.

Okati *et al.* use a quasi-equilibrium model, whereas all other studies rely on equilibrium models (Gibbs energy minimization). For equilibrium models, plasma input to the gasifier cannot explicitly be modeled, meaning that there is no technological difference between the different types of heat input (plasma, microwave, resistance heating, ...). However, several

Table 7 Literature overview for plasma-assisted gasification modeling using thermal plasma to produce syngas from biomass

Ref.	Raw material input	Plasma gas	ER MW_{el} per MW_{th}
Mountouris *et al.* (2006/2008)[241,242]	Sewage sludge (9 MW_{th})	Air/steam	0.15
Janajreh *et al.* (2013)[199]	Algae, treated wood, untreated wood, pine, needles, plywood (15–16 kW_{th})	Air + steam	0.3–0.5
Metveev *et al.* (2014/2016)[246,247]	Sewage sludge (1 MW_{th})	Air	0.06[a]
Favas *et al.* (2017)[243]	Forest residues, Coffee husk, Vines pruning (27–33 kW_{th})	Air + steam	1.2–1.5
Ismail *et al.* (2019)[245]	Forest residues (33 kW_{th})	Air + steam	1.2
Kuo *et al.* (2020)[248]	Raw + torrefied pine wood chips, rice straw, forest residues, grape marc, and macroalgae[b]	air, steam, and CO_2	not specified
Kuo *et al.* (2021)[249]	Raw and torrefied microalgae biomass[b]	Steam	0.72–1.17
Okati *et al.* (2023)[244]	Pine sawdust[b]	Air	Not specified

[a] Not included in Fig. 15. See ESI. [b] Thermal biomass input not specified.

researchers validated their models against experimental data.[224,225,241–244] Okati *et al.* and Favas *et al.* evaluated the impact of parameters like temperature, steam-to-feedstock ratio, or equivalence ratio on the syngas quality.[243,244]

Seiler *et al.* discuss the results of mass and energy balance calculations for electrified BtX processes, including one pathway for a plasma-assisted, allothermal EFG to increase FT product yield.[55] The study is excluded from Table 7 as little information and data are shared. Furthermore, the pathway still requires H_2 addition before synthesis representing a hybrid directly and indirectly electrified process. Besides zero-dimensional process simulations based on thermodynamic equilibrium calculations, Ismail *et al.* developed a two-dimensional numerical CFD model for simulating the plasma-assisted gasification of forest residues with air and steam.[245] Conducting a parametric analysis on biomass gasification, they showed that higher ERs have a negative effect on the formation of syngas and its LHV, but a positive impact on the carbon conversion efficiency because the oxidation reaction is more pronounced.

4.2.3 Plasma-assisted reforming. As described in Section 4.2.2, multiple authors investigated two-stage gasification processes, with a conventional gasification stage, typically employing a fixed bed downdraft reactor, and a second plasma-assisted reforming step tailoring the syngas composition and purity to the specific needs while vitrifying the solid residue.[196] Compared to single-stage plasma-assisted gasification, this downstream processing step can be retro-fitted at existing gasification plants. Post-gasification plasma treatment decomposes tars and hydrocarbons in the raw syngas. Since reforming reactions typically require high temperatures to take place, plasma reforming, especially non-thermal plasma, might be a way to increase energy efficiency by lowering the operating temperatures.[248]

Due to the pervasive literature on plasma reforming of hydrocarbon-containing gases, a comprehensive review is not provided. Instead, selected examples from literature focusing on syngas reforming are given. The processes are differentiated between thermal and non-thermal plasma, followed by a section addressing plasma catalytic reforming. In the end, we provide an overview of relevant modeling and process simulation studies.

Using thermal plasma, Nair *et al.* showed that at 400 °C, the naphthalene content can be reduced by 50%.[250] They used a pulsed corona plasma system up to 500 °C. In 2012, Eliott *et al.* conducted experiments for microwave plasma tar destruction using surrogate raw syngas from biomass gasification.[251] Striugas *et al.* used thermal air plasma to reform syngas obtained from the co-gasification of sludge and wood chips finding that the main effect of the plasma was to decompose hydrocarbons.[252] Wnukowski and Jamróz also investigated microwave plasma reforming of simulated biomass syngas resulting in increased H_2 and CO concentration and lower hydrocarbon and CO_2 concentration in the syngas.[253,254] In 2019, Mei *et al.* conducted experiments on naphthalene and toluene using thermal plasma reforming, showing that OH radicals enhanced the oxidation and, thus, deconstruction of naphthalene and toluene.[255] Wang *et al.* investigated thermal plasma reforming of naphthalene. OH radicals generated by steam addition are an additional route for the stepwise oxidation of naphthalene and its fragments to CO, CO_2, and water resulting in naphthalene conversion rates up to 85%.[251] Zhou *et al.* and Sun *et al.* used toluene as a model component in a microwave-induced metal discharge reformer.[256,257] Sun *et al.* reached a toluene conversion above 90%.[257] Zhou *et al.* reached lower conversion efficiencies (about 50%).[256] The best toluene conversion was found for iron as catalyst metal.[256] The comparison of thermal cracking at 500 °C and microwave-induced metal discharge showed a faster response than the latter.[256] The conversion rate for metal discharge was 52.6% and 18% for the thermal cracking case, respectively.

Advantages of using non-thermal plasmas for reforming over thermal ones include that they can perform well at low power consumption, thus minimizing energy costs.[258] Several studies deal with the experimental investigation of non-thermal plasma reforming, using tar surrogates (mostly toluene and naphthalene) and pulsed corona discharges or gliding arc plasma showing that the operating temperature can be decreased to about 200–400 °C for high tar conversion.[257,259–266] The addition of steam generates many hydroxyl groups resulting in an oxidation atmosphere for naphthalene leading to a maximum conversion efficiency of 85%.[264]

Furthermore, regarding tar removal, such a hybrid use of catalytic and non-thermal plasma can maximize conversion.[258]

As described in Section 2, catalytic reforming uses a catalyst to enhance the reforming reactions. Synergistic effects have been reported for plasma-assisted catalytic reforming. Therefore, hybrid plasma catalysis could be a breakthrough in syngas reforming methods.[267,268] The following sections deal with plasma-assisted catalytic reforming processes.

2003, Chun *et al.* developed a gliding arc plasma reformer for tar reduction in pyrolysis gas.[269] Using benzene as a tar surrogate, they reached a decomposition efficiency of about 83%. In 2013, Tao *et al.* showed that plasma-assisted catalytic steam reforming performs better than thermal, plasma-assisted, and catalytic reforming for biomass tars using toluene as a model compound.[270] In 2017, Wang *et al.* used a catalyst to enhance the plasma destruction of toluene and found a synergistic effect between the catalyst and plasma-assisted reforming.[271] Zhu *et al.* investigated the non-thermal plasma-catalytic reforming of biogas for syngas production using a rotating gliding arc plasma.[272] Using plasma-catalysis, a high conversion of CH_4 and a moderate selectivity of syngas could be shown.[272] Kong *et al.* studied plasma catalytic tar reforming, showing that a Ni/γ-Al_2O_3 catalyst could improve the destruction efficiency of toluene, naphthalene, and phenanthrene to up to 95%, 89%, and 84%, respectively.[273] In 2019 and 2021, Blanquet *et al.* investigated a two-stage pyrolysis/gasification process using plasma-assisted catalytic reforming.[274,275] They found that the H_2 yield could increase, and the tar content could decrease through plasma-assisted catalytic reforming. Craven *et al.* conducted lab-scale experiments on non-thermal plasma-assisted catalytic reforming of cellulosic biomass-derived syngas from a fixed bed gasifier, indicating that the non-thermal plasma allows for higher tar conversion in the reformer and, thus, a higher quality syngas.[276] In 2022, Wang *et al.* investigated a two-stage process combining pyrolysis and plasma reforming using a dielectric-barrier discharge (DBD) reactor.[277] They found that the plasma-catalytic synergy was dominant in the reforming stage at 250 °C, whereas the catalyst played a dominant role in the plasma-catalytic reforming at temperatures around 550 °C. Ashok and Kawi investigated perovskite-derived materials for plasma-assisted catalytic biomass tar reforming.[278] They showed a toluene conversion of 98% using an integrated catalytic DBD plasma process.

There are many publications on plasma reforming models yet a lack of process models integrating plasma-assisted reforming into BtX processes. Consequently, only publications focusing on eBtX process modeling are considered in this review. Bernada *et al.* modeled a two-stage waste gasification unit employing a traveling bed waste gasifier and plasma tar reformer.[279] Materazzi *et al.* simulatively investigated the thermodynamic advantages of a two-step plasma-assisted process over the conventional one-step gasification.[196] Their process employs a conventional fluidized bed gasifier for refuse-derived fuel and a subsequent tar plasma reformer. They argued that staging the oxidant injection in two separate reactors could improve the system's efficiency, reducing plasma power consumption. They showed that the two-stage gasification system improves carbon efficiency and gas yield. The authors further developed a possible mechanism for plasma-stimulated tar conversion[280] and experimentally examined the fate of residues in the two-stage process.[281] In 2014, Marias *et al.* modeled and commissioned a high-temperature reactor for thermal plasma-assisted reforming of tar-containing syngas from an RDF/biomass gasification reactor.[282] Later they showed that a conversion of at least 95% of the incoming tars can be achieved under certain conditions.[283]

4.2.4 Plasma-assisted catalytic synthesis. Plasma-assisted catalytic synthesis combines a catalytic material with non-thermal plasma to enhance performance for gas processing applications such as removing pollutants and producing chemicals.[284] When producing higher-value chemicals and fuels, non-thermal plasma systems offer the advantage of operating the process at room temperature and pressure, while conventional synthesis requires higher temperature and higher pressure (>20 bar).[285] In addition, non-thermal plasma systems are characterized by their flexible reactor design, compatible with fluctuating renewable energies.[286] Non-thermal plasma can enhance chemical reactions due to the high density of free, high-energy electrons and their ability to generate ions by ionizing molecules, atoms, and radicals.[172] The combination of heterogeneous catalyst and reactive plasma gas can provide alternative reaction pathways with lowered energy barriers that could improve yield, selectivity, increase in reaction rates, and thus the overall efficiency of the process.[284] There are two mechanisms by which plasma catalysis works:[284]

1. placing a catalyst either directly in plasma or downstream from it changes the operation of the discharge physically or chemically,

2. using plasma to activate a catalyst which changes the behavior of the catalytic process beneficially.

Yet, few studies on plasma-assisted synthesis are available for converting gasification-derived syngas into fuels or chemicals following the BtX pathway. However, processes for the hydrogenation of CO_2 are developed as they can overcome the stability of CO_2 without the need for high temperatures or high pressures.[285,287–292] So far, only DBD (with and without packing), gliding arc, microwave and RF plasmas, and surface discharge have been investigated.[293] The only plausible configuration for microwave and gliding-arc systems is with the catalyst located after the plasma.[294] Therefore, DBDs are almost exclusively used for plasma catalysis.[294]

When reacting H_2 with CO_2 in a plasma-assisted process, CO_2 methanation and the rWGS reaction predominate.[285] Some authors investigated the methanation of CO and CO_2 using non-thermal DBD setups showing that high CO and CO_2 conversion and CH_4 selectivity could be reached at much lower temperatures than in conventional methanation due to a plasma-catalytic synergistic effect.[295–298] Arita and Iizuka improved the energy efficiency of such plasma-catalytic SNG production from CO_2 and H_2 in a low-pressure square-pulse cross-field discharge by applying a magnetic field to the reactor.[299] Furthermore, Xu *et al.* investigated simultaneous toluene removal and gasification-derived syngas methanation using the combination of packed-bed DBD and catalyst.[300] They

Table 8 Literature overview for process simulation studies of in-line integration of co-electrolysis into BtX processes (eBtX) including the used gasification technologies. KPI values derived from the data in the respective literature

			ER	PY	η_C	EY
Ref.	Main product	Gasification[a]	MW_{el} per MW_{th}	$kg_{product\ per}$ $kg_{biomass,dry}$	%	%
Pozzo *et al.* (2015)[313]	DME	TSG	0.81	0.86 kg_{DME} per $kg_{biomass,dry}$	92% (DME + MeOH) 91% (DME only)	75% (DME only)
Monaco *et al.* (2018)[312]	DME SNG FT	TSG (3)	0.76 1.05 0.57	0.86 kg_{DME} per $kg_{biomass,dry}$ 0.59 kg_{SNG} per $kg_{biomass,dry}$ 0.46 kg_{FT} per $kg_{biomass,dry}$	90% 89% 80%	78% 80% 71%
Clausen *et al.* (2019)[314]	SNG	TSG[b]	1.14	0.65 kg_{SNG} per $kg_{biomass,dry}$	99%	82%
Clausen *et al.* (2019)[315]	SNG	TSG[c] (2)[d]	0.71 0.65	0.51 kg_{SNG} per $kg_{biomass,dry}$ 0.42 kg_{SNG} per $kg_{biomass,dry}$	54% 44%	81% 65%
Butera *et al.*[e] (2019)[161]	MeOH	TSEG	0.45	1.02 kg_{MeOH} per $kg_{biomass,dry}$	76%	77%
Butera *et al.*[e] (2020)[162]	MeOH	TSEG	0.68	1.19 kg_{MeOH} per $kg_{biomass,dry}$	89%	77%
Butera *et al.*[e] (2020)[63]	MeOH	TSEG	0.67	1.19 kg_{MeOH} per $kg_{biomass,dry}$	89%	77%
		TSEHG	0.74	1.20 kg_{MeOH} per $kg_{biomass,dry}$	90%	75%
		e-BFB	0.72	1.10 kg_{MeOH} per $kg_{biomass,dry}$	82%	70%
Steinrücken *et al.* (2023)[124]	FT	EFG	0.32	0.36 kg_{FT} per $kg_{biomass,dry}$	61%	57%
			0.57	0.44 kg_{FT} per $kg_{biomass,dry}$	74%	58%
			0.68	0.47 kg_{FT} per $kg_{biomass,dry}$	79%	58%

[a] TSG: Two-Stage gasifier (by DTU); TSEG: two-stage electro-gasifier, gasifier is electrically-heated with heating elements in the bed; TSEHG: two-stage electrically-heated gasifier, gas to gasifier is electrically preheated, e-BFB: bubbling fluidized bed gasifier heated *via* heat pipes; EFG: Entrained flow gasification. [b] New TSG design using two updraft fixed beds, one for pyrolysis and one for char gasification. [c] New TSG design using updraft fixed pyrolysis and fluid bed char gasification. [d] Case 1: biogas plant integrated, case 2: pre-processed manure as feedstock. [e] In addition to co-electrolysis, electricity is used to heat gasifier. EY includes SOEL and el. heating requirements.

showed that using plasma catalysis treatment, high-efficiency simultaneous toluene removal (>97%) and syngas methanation with a CO conversion rate of about 88% and CH_4 selectivity of 97% can be achieved at 400 °C. CO_2 hydrogenation towards oxygenates such as MeOH can proceed at mild process conditions and with high selectivity.[285,301–303]

Mukhriza and Oktarina suggest that non-thermal plasma allows FT reactions to take place at lower operation temperatures than conventional FT synthesis due to a synergistic effect between plasma and catalyst that enhances the catalytic activity and prolongs catalyst lifetime as well as leading to better heat removal.[304] With rapid reactions promoted by plasma species and reduced volume and maintenance required by the plasma-catalytic technology, plasma-assisted FT synthesis could provide an alternative to the conventional FT process.[305] Non-thermal plasma-catalytic FT synthesis at ambient conditions can promote the synthesis of C_2–C_5 hydrocarbons but also suppress the undesired CH_4 formation.[306–308] It was shown that higher operating pressures are beneficial for high selectivity to lighter hydrocarbons.[306] It is possible to control the FT activity and selectivity inside the plasma-catalytic process by optimizing operating pressure.[306] Despite the difficulties of ignition and sustaining a stable electric discharge at pressures higher than 1 MPa,[309] high operating pressure combined with active plasma species has been further investigated to produce hydrocarbons through FT synthesis. The formation of C_1 to C_3 species increases with pressure when converting syngas *via* non-thermal plasma-catalysis.[305,309–311]

4.3 In-line integration of co-electrolysis

The in-line co-electrolysis of the cleaned syngas after gasification was already introduced in Section 3.2 (Fig. 6). The cleaned syngas composition from the gasifier determines the composition of the product syngas.[119]

The available studies shown in Table 8 consider the production of SNG, MeOH, DME, and FT products. With the Polytechnic University of Turin, the Technical University of Denmark, and the Technical University of Munich (TUM), only three research groups are working on this topic of which all, but TUM use the gasifiers developed by DTU. ER ranges from 0.32 to 1.14 MW_{el} per MW_{th}. Carbon efficiencies range from 44 to 99%. Due to the extensive literature, a comprehensive description of all studies is omitted here and provided in the ESI.†

Monaco *et al.* investigated co-electrolysis integration into the BtX pathway, among other process options, to produce DME, SNG, or FT products.[312] The gasification section is based on the work of Pozzo *et al.*, who also investigated the coupling of a woody biomass gasifier with a co-electrolysis unit to produce DME or MeOH.[313] Clausen *et al.* further investigated a co-electrolysis-based system, using pressurized SOEL coupled with gasification and thermochemical SNG production.[314] In a similar approach, Clausen *et al.* investigated the coupling of a two-stage gasification reactor gasifying wet manure as challenging feedstock to syngas and co-electrolysis.[315] Butera *et al.* investigated a system combining a pyrolysis step with in-line co-electrolysis followed by gasification to produce MeOH.[161] This so-called two-stage electro-gasifier, as introduced in Section 4.1.2, is electrically-heated with heating elements in the bed, contributing to 20% of the overall electricity requirement of the plant, which makes a comparison with other process options challenging.[161] Butera *et al.* further developed this concept by allowing more flexible power generation and fuel production.[162] In an alternative process concept the SOEL is operated in co-electrolysis mode on a tar-free syngas from tar reforming after gasification.[63]

Using the same 0D model as introduced in Section 3.2, Steinrücken *et al.* simulated multiple in-line co-electrolysis options placing the SOEL after a ZnO guard bed but before CO_2 removal.[124] They show that process efficiency and energy yield can be significantly increased for identical product yield and carbon efficiency compared to the processes using H_2 addition and the conventional BtX and PtX reference models. Their results indicated, that in-line co-electrolysis is limited to carbon efficiencies of up to 80% while no such limitation seems to exist for parallel co-electrolysis integration.[124]

Wang *et al.* investigated a polygeneration process to flexibly produce power or chemicals, including multiple co-electrolysis modes[107] The research is focused on the optimal conceptual plant design employing multi-time heat and mass integration platform and multiple objective functions and is thus excluded in Table 8. Recalde *et al.* investigated a process coupling supercritical water gasification with a SOEL (680 °C, 20 bar) in co-electrolysis mode.[316] However, the investigated process stops at syngas production, which is not further upgraded and combines an unreasonable electrification ratio between electricity (123 kW_{el} for SOEL) and biomass (10.6 kW_{th}). Therefore, the study is excluded in Table 8.

5. Technological feasibility and maturity of electrification options

Not all introduced direct and indirect electrification options for BtX processes are technologically feasible and applicable to BtX processes. In Section 5.1, the electrification options are therefore discussed regarding their feasibility and applicability. Part of the discussion is to explore whether different technologies which are technologically feasible and positive on the overall process performance, are reasonable from a system level perspective. The section pre-selects process options and technologies that should be considered for the electrification of BtX processes. While some electrification options might be theoretically possible and technologically feasible, they are further limited by their technological maturity and impact on the other equipment involved when integrated into P-/eBtX. Section 5.2 assesses the maturity of the technologies.

5.1 Technological feasibility

The feasibility of an electrification option not only depends on that technology's maturity. Just because, for example, direct electrical heating of the walls of an entrained flow gasifier is technically possible, does not mean that this is a reasonable use of electrical power for the individual technology or the overall chain, let alone better than other options such as *e.g.*, the use of thermal plasma. To assess whether an electrification option is technologically feasible, the process options eBtX and PBtX are differentiated along the process chain into pretreatment (Section 5.1.1), gasification (Section 5.1.2), syngas conditioning (Section 5.1.3), and catalytic synthesis (Section 5.1.4). Feasibility comprises of the fact that a technology qualifies technically and energetically as electrification option and that it reasonably contributes to overall process improvements. It is assessed in comparison to other electrified processes of the same category.

5.1.1 Pretreatment. Electrification of pretreatment technologies relies on direct electrification like resistive heating, induction, infrared, microwave, or plasma. The application of direct electrification is governed by technical limitations, power-to-heat efficiency (resistance > induction > plasma > microwaves), and heat transfer limitations. Generally, the ER for pretreatment processes is low compared to other options. Table 9 summarizes the identified options for electrification where indirect electrification through a heat transfer media and preheating of process streams are excluded.

Induction-, infrared-, and microwave-heating for low-temperature pretreatment processes may offer several advantages over conventional methods, including higher heating rates, reduced processing time, lower temperature gradients, and the ability to handle larger particle sizes. However, it remains uncertain whether the efficiency of such heating is superior to that of conventional methods. In addition, the electrification of pretreatment processes is questionable for low and medium-temperature heat applications since internal heat integration can meet the heat demand for pretreatment processes. Especially the electrification of drying, HTC, and torrefaction is not recommended.

However, electrification can supply heat at the required temperature level for higher-temperature pretreatment processes. Especially for pyrolysis, which might not be covered through heat integration, electrification avoids fired heating with natural or pyrolysis gas, for example. Since microwave-heating has the lowest power-to-heat efficiency, the other heating options are more suitable.

5.1.2 Gasification. Besides options for indirect electrification through H_2 addition to the gasifier, resistance-, microwave-, or inductive heating as well as thermal plasma can be used for direct electrification of gasification. Table 10 provides an overview of the named technologies and evaluates their impact on the overall process and feasibility.

All presented technologies but hydrogasification aim at providing the necessary energy for the endothermic gasification reactions. Instead of generating heat through partial oxidation, as in autothermal mode, the operation of the gasifier can be either partially or fully brought to allothermal operation with electrification. Allothermal operation leads to a higher cold gas efficiency, lower O_2 demand, higher heating value of the syngas, and higher concentration of H_2 and CO in the raw syngas. Furthermore, the improved syngas yield towards H_2 and CO reduces the need for WGS. However, the amount of heat that can be added to the gasifier is limited.

H_2 addition to gasification presents a straightforward approach to either operate the gasifier in a mode approaching allothermal operation or to use H_2 as gasification agent for the hydrogasification reaction. However, hydrogasification requires an additional heat source such as direct electric heating and should only be used if the goal is to produce a methane-rich product gas. Furthermore, the carbon conversion in the gasifier

Table 9 Qualitative assessment of technologically viable electrification options in the pretreatment step

Process (section in this review)	Characteristics and impact on overall process	Feasibility for P-/eBtX[a]
Infrared, microwave-assisted & Inductively-heated drying (4.1.1)	– Possibly improved fuel properties for gasification – Heat supply at low to medium temperatures	–[c]
Microwave-assisted torrefaction and HTC (4.1.1)	– Negligible impact on overall process performance – Fast heating rates compared to conventional alternatives allow for more dynamic operation	
– Pyrolysis		
Resistance-heated (4.1.1)	– Fast heating rates compared to conventional alternatives allow for more dynamic operation	+
Microwave-assisted (4.1.1)	– Likely improved fuel properties for gasification	o[d]
Inductively-heated (4.1.1)	– Heat supply at high temperatures	+
Plasma-assisted[b] (4.2.1)	Impact on overall process performance unclear	+

[a] – Not feasible; o feasible but with technological limitations, + feasible and recommended. [b] Using thermal plasma. [c] Not feasible for electrification due to the abundance of low-temperature heat within BtX processes. [d] Feasible for electrification of BtX process but not recommended due to low power-to-heat efficiency.

Table 10 Qualitative assessment of technologically viable electrification options in the gasification step including entrained flow gasification (EFG), bubbling fluidized bed (BFB), circulating fluidized bed (CFB), as well as fixed bed (FB) gasification

Process (section in this review)	Characteristics and impact on overall process	Feasibility for P-/eBtX[a]		
		EFG	BFB, CFB	FB
Hydrogasification (3.1.1)	– Increased methane formation – Slow reaction kinetics (requires high temperatures, low carbon conversion)	–[b]	o[c]	o[c]
H_2 to gasifier (3.1.1)	– Towards allothermal operation: higher syngas quality – Lower CO_2 but higher H_2O content – Faster kinetics	+	+	+
Electrically-heated gasification (4.1.2)				
Resistance-heated gasification	– Towards allothermal operation: higher syngas quality	–[d]	+	+
Microwave-assisted gasification	– Lower gasification agent demand	–[ef]	o[f]	o[f]
Inductively heated gasification		–[e]	+	+
Plasma-assisted gasification[g] (4.2.2)	– Towards allothermal operation: higher syngas quality – Faster kinetics and optionally plasma reforming of gas phase – Lower gasification agent demand	+	+	+

[a] – not feasible; o feasible but with technological limitations, + feasible and recommended. [b] Not applicable to EFG due to thermodynamic limitations of the hydrogasification reaction. [c] Only recommended for SNG production and in combination with external heat supply. [d] Only electrically-heated walls are technologically possible, but not feasible for most operating points in EFG. [e] Requires appropriate absorbers. [f] Feasible for electrification of BtX process but not recommended due to low power-to-heat efficiency in comparison to other available technologies. [g] Single-stage gasification using thermal plasma.

is limited by the slow reaction kinetics. H_2 combustion in the gasifier offers an in-situ heat release but with lower efficiency compared to most of the direct electrification technologies.

In electrically-heated gasification, electric resistance heating can be used to supply heat to the gasifier taking advantage of the high power-to-heat efficiency of electric resistance heating. One major concern is the efficient heat transfer from the heat source to the gasification reactions. Reaching sufficiently high temperatures is a question of material and thus cost. In fixed bed and fluidized bed gasifiers, electrically-heated pipes can add heat to the solid or fluidized bed. The heat transfer using heating elements in fluidized beds is already investigated,[317] but for the application in reactors for thermochemical energy storage.[318] The bed material can also be heated outside the reaction zone in circulating fluidized bed gasifiers. Heat transfer just from the reactor wall to the reaction zones is difficult in fixed and fluidized beds. EFG requires very high-temperature heat addition due to the high temperatures in the reaction zone. Resistance heating elements in the flame of the gasifier seem unreasonable. Heat transfer from the walls seem the only option. However, heated walls on the inside of the gasifier are questionable. For brick-lined or membrane walls, the additional energy input would counteract their original purpose of protecting the wall material. Therefore, resistance heating cannot be used in EFG.

Another option is using induction or microwaves to supply heat for near allothermal gasification. This process only applies to fixed or fluidized bed gasifiers with the requisite of good absorption properties of the solid particles for the respective technology. Despite technological feasibility, microwave-heating suffers from low efficiency making its usefulness questionable.

Plasma-assisted gasification offers several advantages, including applicability to all gasifier types, precise control through adjustable electrical power and flexibility in the choice of feed material. This enables greater flexibility in selecting feedstocks resulting in cleaner syngas with reduced tar concentrations. Experimental studies have demonstrated the technical feasibility of plasma gasification, highlighting its potential for practical implementation. However, it is essential to note that some researchers rely on plasma gases like N_2 and Ar, which dilute the syngas and do not align well with the objectives of the electrified BtX (eBtX) process chain. Therefore, careful consideration should be given to selecting appropriate plasma gases to ensure compatibility with the overall eBtX process.

5.1.3 Syngas conditioning. The electrification of syngas conditioning, can be differentiated between indirect electrification (H_2 in quenching after EFG, H_2 addition to reforming, H_2 addition to rWGS, parallel co-electrolysis) and direct electrification (electrically-heated reforming, plasma reforming, in-line co-electrolysis), and the integration of (co-electrolysis) as shown in Table 11.

In general, adding H_2 to syngas conditioning processes presents a straightforward approach for increasing syngas heating value and SN for synthesis. H_2 addition to the quench allows to quickly lower hot syngas temperature in a combined gas and chemical quench approach. However, downstream equipment has be sized according to the larger gas flow and lower concentration of impurities in the gas stream.

For fixed and fluidized bed gasifiers the most important step in syngas conditioning is syngas reforming. Conventional reformers use high temperatures to reduce tar content and increase the CO and H_2 yield. Adding H_2 to reforming allows H_2O_2 combustion and enhances tar reduction through H_2 usage in the reforming reactions. Similarly, electrified reforming enables higher CO and H_2 output since no combustion reactions occur, as in POX or ATR. The ER for reforming was reported to be rather small compared to other electrification processes (ER $<$ 0.2 MW_{el} per MW_{th}[61,91,161]). While microwave- and inductively-heated reforming are considered feasible options for eBtX processes, they are only viable with a suitable absorber material, such as a catalyst in catalytic reforming. Resistance heating and induction are more suitable options since microwave heating has the lowest power-to-heat efficiency.

In this context, plasma is a promising option due to its high efficiency and energy density. In plasma gasification, two-stage processes, combining conventional gasification with plasma-assisted reforming allow for tailoring the syngas composition and purity while vitrifying the solid residue. Thermal and non-thermal plasma have been explored for reforming purposes, with different studies demonstrating their effectiveness in tar removal and syngas reforming. Non-thermal plasma has the advantage of lower power consumption and feasibility for a range of syngas compositions. Additionally, the combination of plasma and catalytic reforming has shown promising synergistic effects, making it a possible breakthrough for syngas reforming. To what degree electricity can be incorporated into a plasma reforming step remains uncertain.

Integrating co-electrolysis into the overall process chain offers a synergistic combination of the BtX and PtX pathways for syngas supply to synthesis. Co-electrolysis is compatible with all common gasifier technologies and has the potential simultaneously replace the WGS and the need for a water electrolysis. For the parallel configuration (Section 3.2), the CO_2 stream separated from the syngas in the AGR unit can be recycled to the process after co-electrolysis. Adjusting the SN by

Table 11 Qualitative assessment of technologically viable electrification options in the syngas conditioning step

Process (section in this review)	Characteristics and impact on overall process	Feasibility for P-/eBtX[a]
H_2 for syngas quenching[b] (3.1.2)	– Possible positive effect on chemical equilibrium for higher quality syngas after gasification – Dilution of syngas before gas cleaning – Larger downstream equipment	+
H_2 reforming[c] (3.1.2)	– Possible positive effects on tar destruction	+
Electrically-heated reforming[c] (4.1.3)		+
Resistance-heated	– Higher quality syngas and lower O_2 demand compared to POX	o[e]
Microwave-assisted[d]	– Possibly higher overall process efficiency	+
Inductively-heated[d]		
Plasma-assisted reforming[c] (4.2.3)	– Higher quality syngas and less O_2 demand compared to POX	
	– Possible benefits from plasma-catalytic effects when using non-thermal plasma	+
Integration of co-electrolysis (3.2, 4.3)	– Allows for efficient SN adjustment for high carbon efficiency and product yield	+[f]
H_2 to rWGS[g] (3.1.2)	– Allows for CO_2 shift and CO_2 utilization before synthesis and SN adjustment for high carbon efficiency	+

[a] –Not feasible; o feasible but with technological limitations, + feasible and recommended. [b] Quenching only required for entrained flow gasification. [c] Reforming only required for fixed bed and fluidized bed gasification. [d] Requires solid induction or microwave absorbers. [e] Feasible for electrification of BtX process but not recommended due to low power-to-heat efficiency in comparison to other available technologies. [f] Parallel integration is preferable to the in-line configuration due to the complexity of the integration and the technical challenges associated with in-line integration. [g] Mainly beneficial for FT synthesis where CO_2 cannot be converted. If rWGS is employed, an electrically-heated rWGS reactor (Section 4.1.3) is recommended.

varying the CO_2 feed is another advantage of this configuration. Integrating co-electrolysis in-line (Section 4.3) poses certain challenges are associated with this configuration, such as a lower partial pressure of reactants, leading to decreased efficiency and higher investment and operating costs due to the need for all the syngas to pass through the electrolysis process. Additionally, impurities in the syngas can result in catalyst poisoning. Therefore, the parallel configuration is recommended for a first-of-its-kind system (see Section 6.2).

H_2 addition to the rWGS step is especially applicable for the FT route since CO is required in FT synthesis as CO_2 typically cannot be converted. To increase carbon utilization additional H_2 addition before rWGS is required. For this case, a rWGS reactor must shift CO_2 and H_2 to CO and H_2O before synthesis (reaction (6)). The electrification of this endothermic rWGS reaction, which needs high temperatures, presents a promising eBtX approach. Using H_2 from water electrolysis and providing the necessary heat input for the rWGS process through electrical heating results in a hybrid PBtX and eBtX process.

5.1.4 Catalytic synthesis. The exothermicity of all syngas conversion reactions (as shown in eqn (7)–(9)) renders the addition of heat through electrification unnecessary and potentially counterproductive. A technically feasible and straightforward approach involves the addition of H_2 before synthesis, which has demonstrated positive effects on carbon efficiency and product yield in various process simulations (Section 6.1). Consequently, this option is strongly recommended for electrifying BtX processes.

For plasma-assisted synthesis, early research results indicate vague advantages of this technology. Non-thermal plasma shows the potential of operating the synthesis at milder process conditions. Lower operating pressure offers the possibility to lower the operating pressure of the upstream process (gasification and syngas conditioning), possibly leading to economic savings. Additionally, plasma-assisted synthesis can influence selectivity, which is an exciting feature for improved yields in FT towards desired products (Table 12).

5.2 Technological maturity, limitations and research needs

Among the feasible electrified process options, the technical maturity significantly influences its near future implementation. While some of the technical limitations are intrinsic to the technologies under consideration, others are due to the current early stage of development for this technology. Furthermore, the integration of each electrification option with BtX process must also be considered. While a technology might be commercially available, its seamless integration into the BtX process chain could present substantial challenges or hurdles. On the contrary, an immature technology may be easily integrated into the process once it reaches an appropriate level of technological maturity.

Table 13 shows the technological maturity of the electrification options recommended in Section 5.1 expressed as technology readiness level (TRL) of the technology itself. Additionally, the impact of the electrified process option on the downstream equipment compared to a conventional BtX process is shown. The effect on upstream equipment is not included in Table 13 since only plasma-assisted gasification impacts upstream equipment, which can be rather substantial. The TRL, following the definition by the European Union,[319] refers to the maturity of the respective technology (gasifier, quench, rWGS, synthesis reactor), instead of the overall P-/eBtX processes.

Generally, direct electrification has a lower TRL than the indirect electrification technologies. However, the maturity of any indirect PBtX process depends on both the H_2 production technology and the process technology where H_2 is added. TRL of water electrolysis for H_2 production depends on the type of electrolyzer (AEL: TRL = 9, PEMEL: TRL = 9, SOEL: TRL = 6–7). Considering the high maturity of AEL and PEMEL, the supply of green H_2 can be assessed as commercialized technology. It is also expected that the development of SOEL will continue so that no inherent technical limitations are imposed on the technology. The main research needs here are in materials research for long-term stability, in pressurized operation for better integration into the BtX process chain, in maintaining high efficiency without the use of air as a purge gas, and in scaling. As SOEL is very promising for integrating heat from high-temperature process units such as the gasification, this heat integration itself represents a technical challenge, but one that should be manageable from an engineering perspective.

The challenge for PBtL processes is thus typically related to H_2 addition to the process and the related impact on downstream equipment. The most promising and straight forward route is the H_2 addition before the synthesis. In the case of FT synthesis, the H_2 addition might be placed before a rWGS unit to convert CO_2 to CO. Most direct electrification routes *via* H_2 addition have not been validated in a relevant environment and scale. However, the implementation should be technically feasible without much effort.

Table 12 Qualitative assessment of technologically viable electrification options in the synthesis step

Process (section in this review)	Characteristics and impact on overall process	Feasibility for P-/eBtX[a]
– H_2 to synthesis (3.1.3)	Allows for SN adjustment to reach high carbon efficiency and product yield Allows new reactor concepts (staged synthesis)	+
– Plasma-assisted synthesis[b] (4.2.4)	Possibly milder process conditions might lead to cost reduction along the whole process chain Possibly higher product selectivity	+

[a] – Not feasible; o feasible but with technological limitations, + feasible and recommended. [b] Employing non-thermal plasma.

Table 13 Assessment of technological maturity and impact on downstream equipment of recommended electrification options

	Electrified process (section in this review)	TRL	Change in downstream equipment specification[a]
Pre-treatment	Microwave-assisted pyrolysis (4.1.1)	5–6	– No
	Inductively-heated pyrolysis (4.1.1)	5–6	– No
	Plasma-assisted pyrolysis[b] (4.2.1)	5–6	– No
Gasification	Hydrogasification[c] (3.1.1)	4–5	– Other equipment needed
	H_2 to gasifier (3.1.1)	6–7[i]	– Marginal
	Resistively-heated gasification[d] (4.1.2)	5–6	– Yes
	Microwave-assisted gasification (4.1.2)	5–6	– Yes
	Inductively-heated gasification (4.1.2)	4–5	– Yes
	Plasma-assisted gasification[e] (4.2.2)	5–6	– Yes
Syngas conditioning	H_2 for syngas quenching[f] (3.1.2)	8–9[i]	– Yes
	Resistively-heated reforming[g] (4.1.3)	7–8[i]	– Marginal
	Inductively-heated reforming[g] (4.1.3)	4–5	– Marginal
	Plasma-assisted reforming[g] (4.2.3)	5–6	– Marginal
	H_2 to rWGS[h] (3.1.2)	8–9[i]	– Yes
	Integration of co-electrolysis in-line (3.2) parallel (4.3)	3 4–5	– Yes Yes
Synthesis	H_2 to synthesis (3.1.3)	8–9[i]	– Yes
	Plasma-assisted synthesis[h] (4.2.4)	≤ 3	– Yes

[a] For example: equipment size, material, utilities. [b] Using thermal plasma. [c] Only for SNG production and in combination with external heat supply *i.e.* electrically-heated or plasma-assisted gasification. [d] Not recommended for entrained flow gasifiers. Probably requires additional heat supply for fixed bed and fluidized bed gasifiers. [e] Here: single-stage using thermal plasma. [f] Quenching only required for entrained flow gasification. [g] Reforming only required for fixed bed and fluidized bed gasification. [h] Mainly beneficial for FT synthesis where CO2 cannot be converted. If rWGS is employed, an electrically-heated rWGS reactor (Section 4.1.3, TRL = 8) is recommended. [i] Not demonstrated yet, but technical hurdles are minimal.

Similar to water electrolysis, SOEL for co-electrolysis is expected to continue its development until it is ready for the market, so that there are no intrinsic technical limits to the technology. Parallel co-electrolysis integration is compatible with various gasifier technologies and can simultaneously replace the WGS and the need for water electrolysis. In addition to the technical research needs already mentioned, the contractability of in-line co-electrolysis with real syngas should be mentioned here in particular. Not only is pressurized operation much more sensible and important than in the parallel configuration. There is also a great need for research into whether and in what quantities impurities in the syngas influence the SOEL. To what extend the in-line co-electrolysis with syngas from gasification can be operated remains to be proven.

The maturity of directly electrified processes is generally lower and demonstration in relevant scale is lacking for most of the processes. Resistively- and inductively-heated reforming is developed for other reforming processes. But the technologies can be easily adapted to the syngas applications. Generally, the heating technologies are well understood but must be tailored for the utilization in a P-/eBtX process. It should be repeatably mentioned however, that especially microwave heating suffers from an intrinsic limitation in power-to-heat efficiency: electrical resistance heating ($\sim$100%)[138] > induction heating (>90%)[137] > plasma torch (40–94%)[201] > Microwave heating (20–60%).[320] One key research need involves the development and optimization of reactor designs that enhance the efficiency of these heating technologies specifically in the context of biomass conversion and gasification processes. Understanding and mitigating potential issues related to heat transfer, scalability, and reactor material compatibility are critical areas of investigation. Moreover, exploring methods to integrate these heating technologies seamlessly into existing and evolving P-/eBtX process configurations is essential. Investigating the influence of various biomass feedstocks on the performance and efficiency of these heating technologies is key.

While thermal plasma technology, particularly in the context of plasma gasification, is theoretically mature and lacks intrinsic engineering barriers, its effective application to biomass solid conversion presents notable challenges requiring focused engineering research. A critical challenge is the adaptation of thermal plasma to utilize CO_2 and H_2O as plasma gases instead of inert gases, that are commonly employed in small-scale experimental studies due to its simplicity. Demonstrating the feasibility of using CO_2 and steam, especially considering the latter's corrosive nature, represents a key engineering hurdle. Genuine plasma torch design and matching control techniques will be instrumental in overcoming this challenge and optimizing the efficiency of thermal plasma in biomass conversion processes. Additionally, addressing issues related to erosion and the continuous replacement of electrodes is crucial for the feasibility of such technologies. Learning from experiences in waste-to-X plasma facilities can provide valuable insights, but specific adaptations for biomass feedstocks are necessary. Comprehensive studies focusing on the unique aspects of plasma gasification in the context of electrified BtX processes will contribute to develop this technology for sustainable and efficient large-scale applications.

In contrast, the maturity of non-thermal plasma applications for example for synthesis must be assessed very low due to the early research stage. While non-thermal plasmas are promising for gas applications such as reforming and synthesis due

to their catalytic nature, there are significant TRL challenges, with the chief concern being the substantial hurdle of operating under very low pressures. Whether this is a fundamental limitation or an obstacle that can be overcome with further research and a better understanding of the basic physical principles requires further in-depth investigation. Engineering research needs to focus on the development of genuine solutions, particularly in achieving pressure levels that are compatible with other process steps along the BtX process chain.

6. Meta-analysis of electrification options

This section evaluates PBtX and eBtX processes using a meta-analytic approach, exclusively relying on data from process simulations. In Section 6.1, the H_2 addition to synthesis is quantitatively analyzed and established as a reference process. In Section 6.2, the integration of co-electrolysis is evaluated and compared to the PBtX reference processes from Section 6.1. In Section 6.3, eBtX processes are investigated and subjected to a comprehensive comparison. Due to the relatively limited depth of available data, this assessment and comparison adopt a predominantly qualitative approach. Thea data and additional graphs are provided in the ESI.†

6.1 Analysis of H_2 addition to synthesis

H_2-addition is technologically trivial to implement and uses only technologies that are already highly mature today (for H_2 from low-temperature electrolysis, see Section 5.2). Many researchers have broadly investigated these processes from an overall system perspective. The extensive process data basis enables a quantitative assessment of the KPIs, thus positioning PBtX processes as a reference for comparing and evaluating alternative electrification options.

This section provides a quantitative analysis of PBtX processes with H_2 addition, focusing on cases where H_2 is introduced directly before the synthesis or preceding the rWGS step, excluding possibilities of H_2 addition to gasification, quench, or reforming. The exclusion is justified as H_2 addition to these processes is rarely explored at process level and for available process simulations the evaluation due to mixing with other electrified process does not allow to isolate the impact of the H_2 addition. Given the extensive research on H_2 addition, they serve as valuable references for other electrification options.

The data presented here is taken from Tables 2–4 and is grouped by electrolysis technologies and products. The comparison is made based on the KPIs defined in eqn (1)–(4), including carbon efficiency η_C and product yield PY (Section 6.1.1) as well as the PBtX energy yield (EY_{PBtX}) (Section 6.1.2).

6.1.1 Effect of H2 addition on carbon efficiency and product yield. Fig. 10 illustrates how the degree of electrification, denoted by an elevated ER, positively correlates with carbon efficiency and product yield. Carbon efficiency and product yield share a linear relationship (see eqn (2)). This trend of increasing carbon efficiency and product yield is evident across all products.

Fig. 10(a) illustrates the carbon efficiency over ER, including $\overline{\eta_{C,BtX}}$ as BtX reference processes (see Table 14). In Fig. 10(b), a

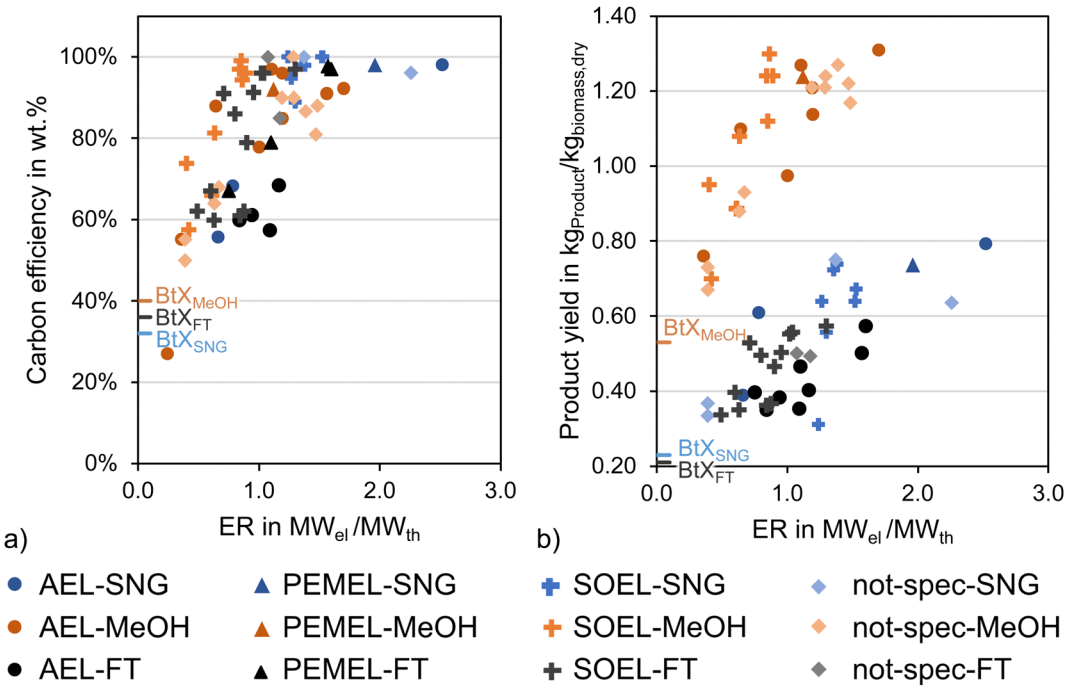

Fig. 10 Dependency of (a) carbon efficiency and (b) product yield PY on electrification ratio ER for PBtX processes using H_2 addition to synthesis steps (and rWGS) based on literature review. Different colors are used to differentiate the production of synthetic natural gas (SNG), Methanol (MeOH) or Fischer–Tropsch (FT) products. Different symbols represent the types of water electrolysis including alkaline (AEL), proton exchange membrane (PEMEL), or solid oxide electrolysis (SOEL). For data basis see Tables S2–S4 and ESI.†

Table 14 Product yields and carbon efficiencies of BtX processes as reference and results from mathematical derivations for meta-analytical evaluation of PBtX processes

KPI	Unit	SNG	MeOH	FT	Ref.
$\overline{\eta_{C,BtX}}$	%	32%	40%	36%	68
$\eta_{C,BtX\rightarrow PBtX}(ER=0)^a$	%	31%	34%	30%	—
$\overline{PY_{BtX}}$	$kg_{product}\ kg_{biomass,dry}^{-1}$	0.25	0.59	0.23	68
$PY_{BtX\rightarrow PBtX}(ER=0)$	$kg_{product}\ kg_{biomass,dry}^{-1}$	0.21	0.53	0.17	—

[a] LHV of biomass of 18 MJ per kg_{dry} and carbon content of biomass of 50 $wt\%_{dry}$ used for calculations.

comparison of the achievable product yields is presented, with corresponding BtX process product yields $\overline{PY_{BtX}}$(see Table 14). It is evident, that the production of SNG *via* PBtX requires a higher degree of electrification (ER = 0.4–2.5 $MW_{el}\ MW_{th}^{-1}$) compared to FT products or MeOH (ER = 0.35–1.8 $MW_{el}\ MW_{th}^{-1}$). This is mainly due to the higher SN required for methanation, as discussed in Section 2. The higher achievable product yields for MeOH are attributed to its higher molecular weight per carbon atom due to the oxygen content. The observed graph indicates a potential linear relationship between ER and PY, although definitive conclusions cannot be drawn at this stage.

Processes employing SOEL typically attain higher carbon efficiency and product yield at the same ER compared to low-temperature electrolysis, such as PEMEL and AEL, due to the higher electrolysis efficiency of SOEL impacting the ER. Nevertheless, carbon efficiencies of above 90% are also achieved with PEMEL or AEL for all products. Due to variations in modeling methodology, such as conversion efficiencies, particularly for electrolysis efficiency, differences in biomass composition, and overall process design, these trends in Fig. 10 must be treated cautiously.

Based on the assumption that EY_{BtX} and ER are subject to a linear relationship ($\overline{EY_{PtX,LT}}$, $\overline{EY_{PtX,HT}}$ as slope, $\overline{EY_{BtX}}$ as y-axis intercept, see eqn (14) in Section 6.1.2), the definitions in eqn (3) for PY and η_C can be used to derive at a dependency expression of product yield and carbon efficiency on ER:

$$PY_{BtX\rightarrow PBtX} = \frac{\dot{m}_{product}}{\dot{m}_{biomass,dry}} = f(ER) = \frac{LHV_{biomass}}{LHV_{product}} \cdot \left(\overline{EY_{BtX}} + \overline{EY_{PtX,LT/HT}} * ER\right) \quad (12)$$

$$\eta_{C,BtX\rightarrow PBtX} = \frac{\dot{m}_{C,product}}{\dot{m}_{C,biomass}} = PY \cdot \frac{w_{C,product}}{w_{C,biomass,dry}} = f(ER) = \frac{LHV_{biomass}}{LHV_{product}} \frac{w_{C,product}}{w_{C,biomass,dry}} \times \left(\overline{EY_{BtX}} + \overline{EY_{PtX,LT/HT}} * ER\right) \quad (13)$$

Table 15 provides $\overline{EY_{BtX}}$ and $\overline{EY_{PtX,LT/HT}}$ for reference BtX and PtX processes. The resulting graphs for $PY_{BtX\rightarrow PBtX}$ and $\eta_{C,BtX\rightarrow PBtX}$ are included in the ESI,† for all products. Using eqn (12) and (13), product yield and carbon efficiency for pure BtX processes (ER = 0) can be extrapolated. The results are compared with values from literature in Table 14. Whether the fact that the resulting values for carbon efficiency and product yield tend to be too lower than the literature data is a consequence of synergetic effects in PBtX processes or merely a result of the heterogeneity of the variable used for our calculations cannot be conclusively answered at this point. To gain further insights, more research is needed, such as a systematic, simulative process route comparison based on the same biogenic feedstocks.

6.1.2 Effect of H_2-addition on energy yield. This section analyses the impact of the degree of electrification on the energy yield (EY), which offers energetic comparability between different products than the product yield discussed in the section before. In the following, eqn (14)–(16) are derived mathematically to quantify the influence of ER on the EY of PBtX processes.

Fig. 11 illustrates the influence of ER on both BtX energy yield EY_{BtX} and PtX energy yield EY_{PtX} as defined in eqn (3). Table 15 provides the reference energy yield of BtX and PtX processes, which serve as a basis for the subsequent calculations. The literature-based energy yields of pure PtX processes are distinguished according to low-temperature (LT: PEM, AEL) and high-temperature (HT: SOEL) electrolysis ($\overline{EY_{PtX,LT}}$, $\overline{EY_{PtX,HT}}$). The energy yields depend on assumptions but especially the values for BtX can differ depending on chosen parameters like, for example, biomass composition, plant layout, or gasifier type.

The product-specific meta-analysis in Fig. 11 shows an increase in EY_{BtX} with an increasing ER. EY_{BtX} can exceed 100% due to its definition excluding electricity input. The enhancement in product yield and carbon efficiency resulting from H_2 addition (see Section 6.1.1) is directly proportional to the chemical energy stored in the product. The energy yield EY_{PtX} of PBtX processes are generally higher than the energy

Table 15 Energy yields of BtX and PtX processes as reference for meta-analytical evaluation of PBtX processes

KPI	Unit	SNG	MeOH	FT	Ref.
$\overline{EY_{BtX}}$	$MW_{product}\ MW_{biomass}^{-1}$	0.57	0.59	0.40	68
$\overline{EY_{PtX,LT}}$	$MW_{product}\ MW_{electrolysis}^{-1}$	0.52	0.55	0.45	321
$\overline{EY_{PtX,HT}}$	$MW_{product}\ MW_{electrolysis}^{-1}$	0.84	0.75	0.59	322 and 323
$\overline{EY_{PtX,co\text{-}electrolysis}}$	$MW_{product}\ MW_{electrolysis}^{-1}$	0.84	0.79	0.65	322 and 323

yield of PtX, due to the biomass feedstock's intrinsically carried energy input for PBtX processes. Fig. 11 shows the general decrease in EY_{PtX} with an increasing ER.

One can assume that EY_{BtX} and ER are subject to a linear relationship. If there is no synergitic effects in PBtX processes the energy yield for the respective LT or HT PtX reference process ($\overline{EY_{PtX,LT}}$, $\overline{EY_{PtX,HT}}$) represents the slope, while the mean energy yield of the product specific BtX processes $\overline{EY_{BtX}}$ serves as the intercept:

$$EY_{BtX\rightarrow PBtX} = \frac{\dot{m}_{product} LHV_{product}}{\dot{m}_{biomass} LHV_{biomass}} = f(ER) = \overline{EY_{BtX}} + \overline{EY_{PtX,LT/HT}} * ER \quad (14)$$

Expressing the EY_{PtX} as a function of ER, based on the findings for $EY_{BtX\rightarrow PBtX}$ in eqn (14) and (15) can be derived by substituting $EY_{BtX\rightarrow PBtX}$ as in eqn (14) for $EY_{PtX\rightarrow PBtX}$ as shown in Fig. 11:

$$EY_{PtX\rightarrow PBtX} = \frac{\dot{m}_{product} LHV_{product}}{\dot{E}_{electrolysis}} = f(ER) = \frac{EY_{BtX\rightarrow PBtX}}{ER} = \overline{EY_{PtX,LT/HT}} + \frac{\overline{EY_{BtX}}}{ER} \quad (15)$$

Based on this definition for the energy yield, adding H_2 generally leads to energetic improvements with increasing ER compared to the PtX process. Fig. 11 shows the derived equations as dotted lines. However, the validity of the equation is limited to a specific range of ER values. For electrification ratios approaching zero, the energy yield $EY_{PtX\rightarrow PBtX}$ will approach infinity, which is merely a mathematical property arising from the increasing share of energy derived from biomass. Conversely, for large ER values, $EY_{PtX\rightarrow PBtX}$ will approach the asymptotic value of $\overline{EY_{PtX,LT/HT}}$ as predicted by the equation. Yet, achieving extremely high ER values is not technically feasible due to the limited availability of carbon from biomass, and further electrification will not lead to an increased product yield.

Fig. 12 shows the PBtX energy yield EY_{PBtX} for each product as defined in eqn (3) depending on ER. A relationship for EY_{PBtX} can be derived based on the definition of ER and $EY_{BtX\rightarrow PBtX}$ and $EY_{PtX\rightarrow PBtX}$ as shown in eqn (16). The derived equation suggests that at very low ER values, EY_{PBtX} approaches $\overline{EY_{BtX}}$. This is a reasonable observation since no electrification leads to a BtX process. Conversely, for high ER values, EY_{PBtX} approaches $\overline{EY_{PtX,LT/HT}}$, aligning with the expected behavior since a high degree of electrification approximates a purely power-based process design. However, it is crucial to acknowledge that very high ER values are not practically attainable due to carbon limitations.

$$EY_{PBtX} = \frac{\dot{m}_{product} LHV_{product}}{\dot{m}_{biomass} LHV_{biomass} + \dot{E}_{electr.}} = f(ER) = \frac{\dot{m}_{product} LHV_{product}}{\dot{m}_{biomass} LHV_{biomass}(1+ER)} = \frac{EY_{BtX\rightarrow PBtX}}{1+ER} = \frac{\overline{EY_{BtX}} + \overline{EY_{PtX,LT/HT}} \cdot ER}{1+ER} \quad (16)$$

Categorizing the energy yield of PBtX processes by product type unveils that FT consistently exhibits the lowest energy yield, while MeOH and SNG show higher values. EY_{PBtX} values demonstrate variability, ranging from 52% to 78% for SNG, 51% to 74% for MeOH and 46% to 70% for FT. Remarkably, substantial variations occur even for the same product and equal ER values. For instance, in the case of MeOH at an ER of approximately 0.4, EY_{PBtX} differs between 56% and 74%. Consequently, only general trends and overarching observations can be inferred.

As Fig. 12 shows, the energy yield EY_{PBtX} for SNG and MeOH slightly decreases with ER for low-temperature electrolysis. This implies that in these cases, no efficiency gains can be expected with additional electricity input, *i.e.* more H_2 addition. However, energy yield increases with ER for high-temperature electrolysis for all products and for FT products with low-temperature electrolysis.

Based on this *meta*-analysis of the literature-derived data and the resulting mathematical derivations supported by Fig. 11 and 12, it can be concluded that PBtX processes are conceptualized as a superposition of BtX and PtX processes. Depending on the degree of electrification, they exhibit characteristics closer to BtX or PtX processes, thus combining the advantages and disadvantages of the respective processes. It should be stated that the literature values do not fully align with the data presented in Fig. 11 and 12 due to variations in assumptions, such as biomass composition, conversion efficiencies, and process operations, across different studies. Finally, the derived equations might not comprehensively capture all effects of H_2 addition to BtX processes. Whether and to what extent synergies can be exploited in PBtX cannot be conclusively determined based on the meta-analysis. However, it is reasonable to assume that PBtX processes have an advantage over PtX and BtX due to heat and material integration, as well as the omission of CO_2 capture, which is needed in PtX processes. For FT products, this apparent synergetic effect becomes quite profound. This is most likely because of the significantly decreased demand of CO_2 conversion to CO as CO from biomass gasification can be more efficiently produced compared to carbon capture and CO_2-to-CO conversion.

6.2 Comparison of H_2 addition and co-electrolysis integration

Compared to PBtX processes, eBtX options are less frequently investigated on a process or system level. Only for processes using co-electrolysis either in parallel (PBtX) or in in-line configuration (eBtX) a more significant number of process simulation studies exist to assess the impact of electrification on the overall process performance.

Fig. 13 shows the influence of ER on carbon efficiency for parallel (PBtX) and in-line (eBtX) integration of co-electrolysis producing SNG, MeOH or FT products. The graphs also include data points for indirect electrification *via* H_2 addition to synthesis (and rWGS). It is evident that both parallel and in-line co-electrolysis follow the general trend of PBtX processes and that, in principle, a higher ER results in a higher carbon efficiency and thus also a higher product yield. Furthermore, the integration of co-electrolysis slightly outperforms classical PBtX processes using water electrolysis for all products. In general, water electrolysis *via* SOEL performs similarly well, while low-temperature technologies need higher ERs to achieve the same carbon efficiencies. Depending on the product, specific

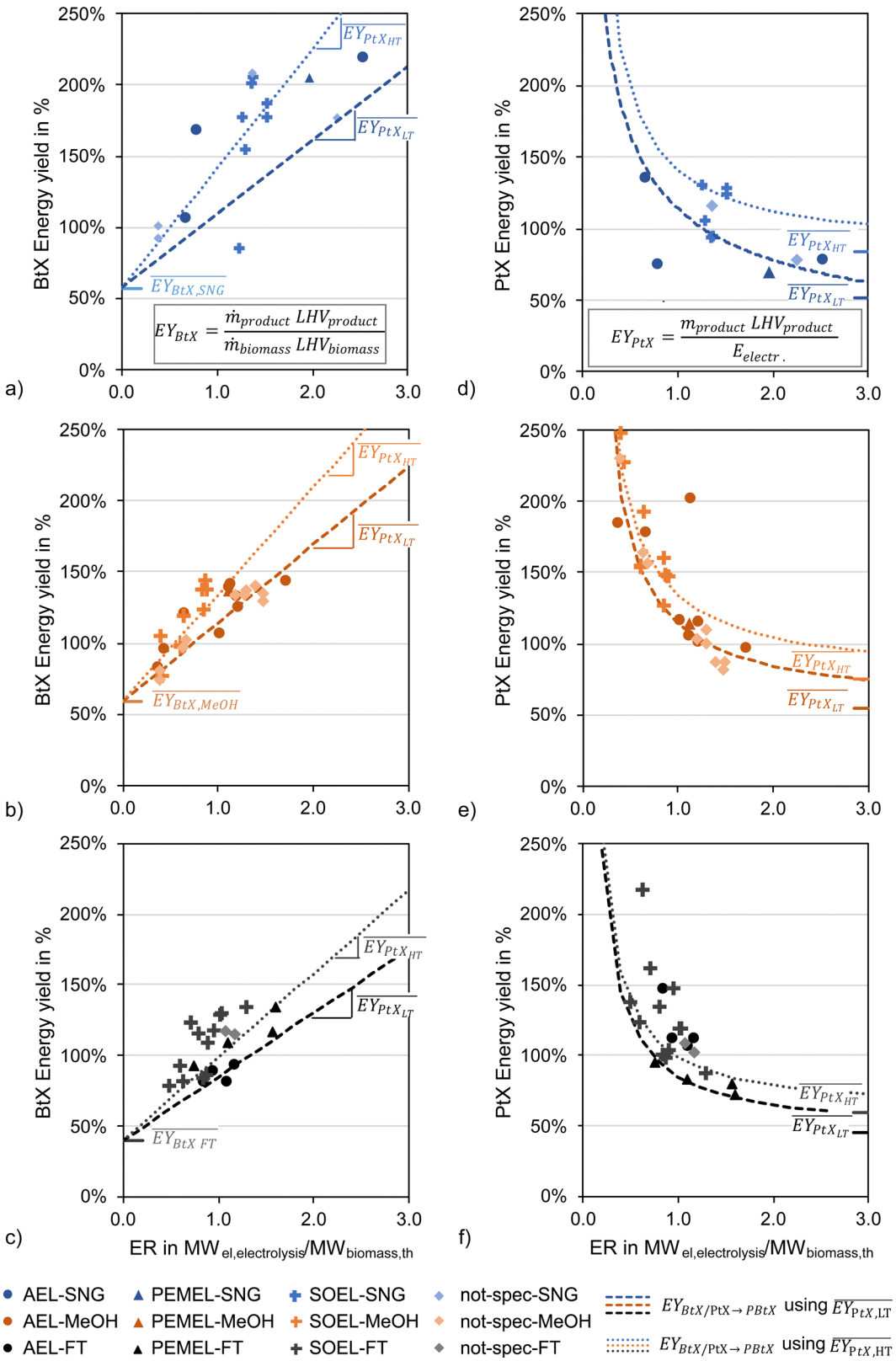

Fig. 11 Dependency of (a)–(c) BtX energy yield and (d) and (e) PtX energy PY on electrification ratio, ER, for PBtX processes using H_2 addition to synthesis (and rWGS) based on literature review. The graphs are separated into the production of (a) and (d) synthetic natural gas (SNG), (b) and (e) Methanol (MeOH) or (c) and (f) Fischer–Tropsch (FT) products. Data includes the derived equations for $EY_{BtX \rightarrow PBtX}$ (eqn (14)) and $EY_{PtX \rightarrow PBtX}$ (eqn (15)) using high-temperature (HT) or low-temperature (LT) PtX reference processes. Different symbols represent the types of electrolysers including alkaline (AEL), proton exchange membrane (PEMEL), or solid oxide electrolysis (SOEL). For data basis see Tables S2–S4 and ESI.†

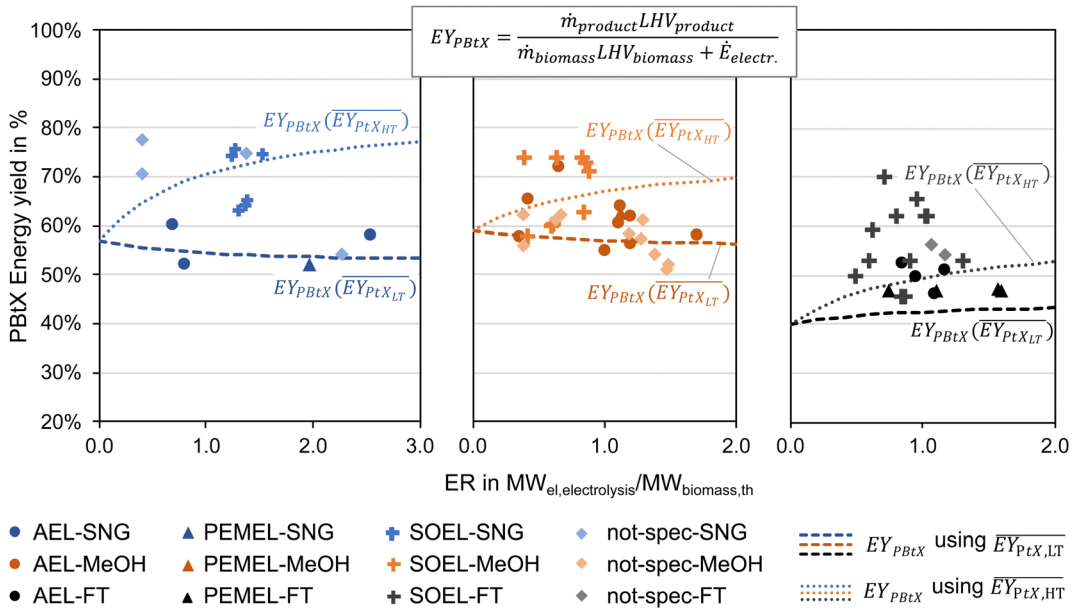

Fig. 12 Dependency of PBtX energy yield EY_{PBtX} on electrification ratio, ER, for PBtX processes using H_2 addition to synthesis (and rWGS) based on literature review. The graphs are separated into the production of synthetic natural gas (SNG), Methanol (MeOH) or Fischer–Tropsch (FT) products. Data includes the derived equations for EY_{PBtX} (eqn (16)) using high-temperature (HT) or low-temperature (LT) PtX reference processes. Different symbols represent the types of electrolysers including alkaline (AEL), proton exchange membrane (PEMEL), or solid oxide electrolysis (SOEL). For data basis see Tables S2–S4 and ESI.†

minimum values of ER are required to achieve 90% carbon efficiency. While this value is around 0.7 for MeOH and FT, an ER of approximately 1.0 is required for SNG production.

Assuming the linear relationship of EY_{BtX} and ER also for co-electrolysis integration, the mean energy yield for the respective PtX process ($\overline{EY_{PtX,co\text{-}el.}}$, Table) acts as the slope and eqn (14)–(15) can also be used for co-electrolysis P-/eBtX processes. The ESI,† includes the data basis for this analysis and a representation of the derived graphs for $PY_{BtX\rightarrow PBtX}$, $\eta_{C,BtX\rightarrow PBtX}$, $EY_{BtX\rightarrow PBtX}$, and $EY_{PtX\rightarrow PBtX}$ based on high-temperature co-electrolysis PtX reference processes.

Fig. 14 compares parallel (PBtX) and in-line (eBtX) integration of co-electrolysis with the indirect electrification of BtX processes *via* H_2 addition to synthesis (and rWGS) (PBtX) in terms of PBtX energy yield EY_{PBtX}. Since values for $\overline{EY_{PtX,co\text{-}el.}}$ are quite similar to $\overline{EY_{PtX,HT}}$ for all products (Table), the energy yield for integrating co-electrolysis or using SOEL for H_2 addition is similar. In these scenarios, the general trend shows an increase in EY_{PBtX} with increasing ER values where EY_{PBtX} exhibits a range spanning from approximately 63% to 82% for SNG, 61% to 77% for MeOH and 50% to 71% for FT with far lass variation than in the PBtX cases. These EY_{PBtX} values for co-electrolysis substantially exceed the curve depicted from eqn (16), indicating the potential for synergies, even more so than in the cases of pure H_2 addition. Nevertheless, it should be emphasized that further research is required for definitive confirmation of these findings.

6.3 Conclusions for novel electrification options

As mentioned above, in comparison to H_2 addition to synthesis, alternative electrification options have received less attention, leading to limited data availability and reliability. In the context of direct electrification technologies, one promising eBtX option involves directly supplying electricity to the gasifier. However, available process simulation studies on electrically-heated gasification and plasma gasification are scarce. Also, H_2 addition to gasification for hydrogasification, while promising, is not investigated extensively.

Due to the limited number of process simulation studies on electrically-heated gasifiers, hydrogasification, and plasma gasification (solely considering syngas production), only a qualitative comparison and an ER range can be provided without quantifying the impact on other KPIs. Fig. 15 shows the range of ER for the various technologies in the reviewed studies with ER values from Tables 2–8.

Fig. 15 shows that hydrogasification seems competitive with classical H_2 addition before the synthesis in terms of ER. While an assessment of other KPIs (η_C, PY or EY) is theoretically possible, the restricted dataset from a limited range of researchers reduces validity.

Regarding direct electrification options for eBtX processes, inherent technical limitations restrict the extent of electricity integration into the process. As such, the maximum investigated ER of electrically-heated gasification is limited. While no further conclusions on the implications for η_C and PY are possible at this point, a high power-to-heat efficiency might be advantageous in terms of energy yield. Plasma-assisted gasification (based mostly on small-scale experimental data), however, appears to enable ERs in a reasonable range. Since no studies exist investigating the entire eBtX process using plasma-assisted gasification, the impact of ER on η_C, PY or EY cannot be assessed.

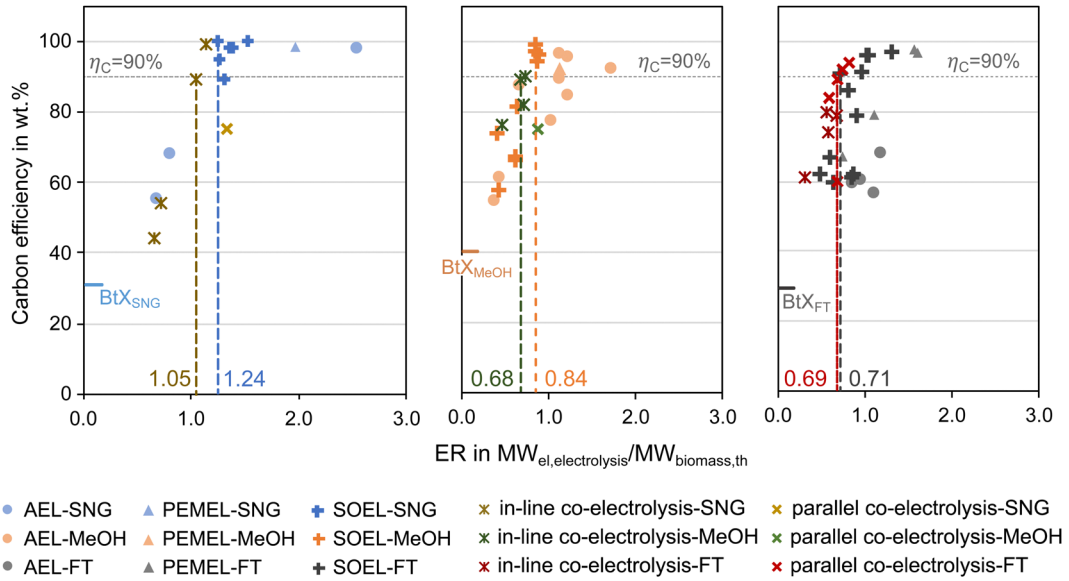

Fig. 13 Dependency of carbon efficiency η_C on electrification ratio, ER, for PBtX processes using H_2 addition to synthesis (and rWGS), and parallel (PBtX) and in-line (eBtX) integration of co-electrolysis based on literature review. The graphs are separated into the production of synthetic natural gas (SNG), Methanol (MeOH) or Fischer–Tropsch (FT) products. H_2 addition from water electrolysis include the use of alkaline (AEL), proton exchange membrane (PEMEL), or solid oxide electrolysis (SOEL). Studies that do not specify the used electrolysis technology are neglected. Dotted lines represent the required minimum ER to achieve 90% carbon efficiency. For data basis see Tables S2–S5 and S8 and ESI.†

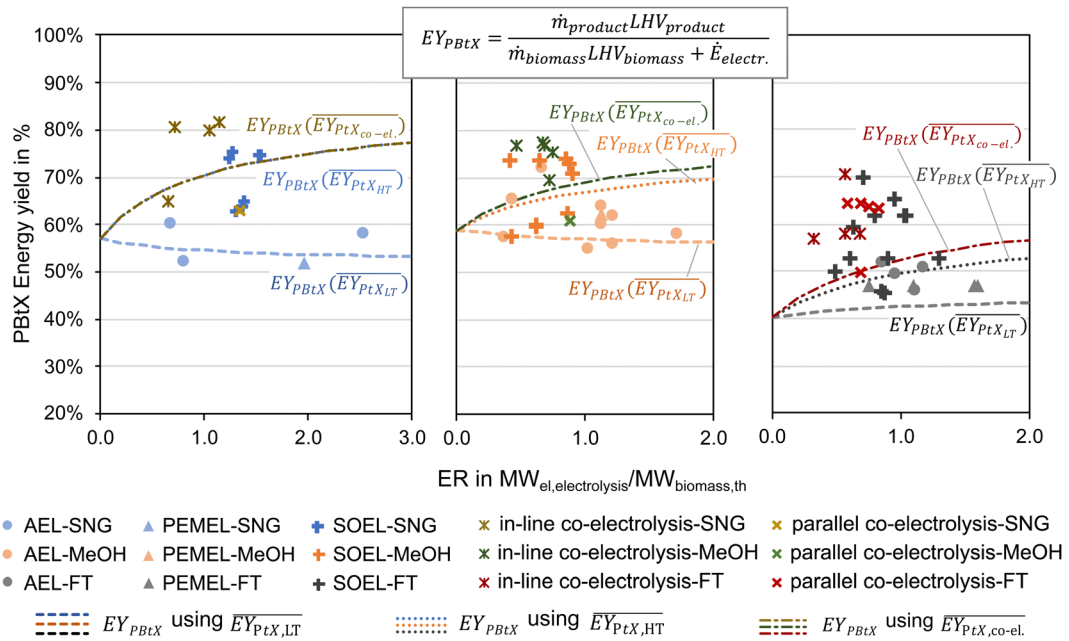

Fig. 14 Dependency of PBtX energy yield EY_{PBtX} on electrification ratio, ER, for PBtX processes using H_2 addition to synthesis ((and rWGS)), and parallel (PBtX) and in-line (eBtX) integration of co-electrolysis based on literature review. The graphs were separated into the production of synthetic natural gas (SNG), Methanol (MeOH) or Fischer–Tropsch (FT) products. Data includes the derived equation for EY_{PBtX} (eqn (16)) using high-temperature (HT), low-temperature (LT) or co-electrolysis (co-el.) PtX reference processes. Different symbols represent the types of water electrolysers including alkaline (AEL), proton exchange membrane (PEMEL), or solid oxide electrolysis (SOEL). Studies that do not specify the used water electrolysis technology are neglected for simplicity. For data basis see Tables S2–S5 and S8 and ESI.†

For the reference P-/eBtX processes *via* H_2 addition to synthesis and co-electrolysis integration achieving 90% carbon efficiency requires an ER of about 0.7 for MeOH and FT, and 1.0 for SNG production (Sections 6.1 and 6.2). As shown in Fig. 15, with ER range spanning from 0.15 to 1.48 for plasma gasification and 0.13–1.45 for hydrogasification, the two options theoretically possess the potential for total process enhancement comparable to the reference scenarios. No such conclusion can

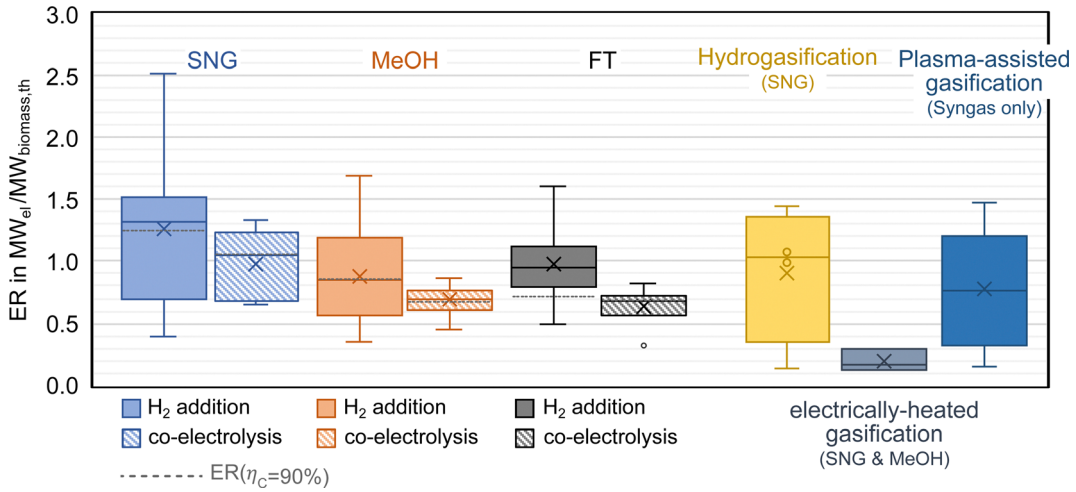

Fig. 15 Comparison of electrification ratios for different electrification options, including PBtX processes using H_2 addition to synthesis (and rWGS), parallel (PBtX) and in-line (eBtX) integration of co-electrolysis to produce synthetic natural gas (SNG), Methanol (MeOH) or Fischer–Tropsch (FT) products, hydrogasification to produce SNG, electrically-heated gasification to produce SNG or MeOH and plasma-assisted gasification to produce syngas. For data basis see Tables S2–S5, S7 and S8 and ESI.†

be drawn for the electrically-heated gasifier processes. Whether any of these technologies allows to achieve $\eta_C \geq 90\%$ with ER values in the order of the reference values, or whether a combination of technologies will be needed, remains to be proven.

Should any of the alternative P-/eBtX processes manage to achieve $\eta_C \geq 90\%$ with ER values below the above-mentioned reference values, it would be regarded as promising. The potential impact of more directly electrified processes on the KPIs is of considerable interest, given the high-power conversion efficiency of direct electrification. However, based on the currently available data, it is not possible to determine which processes are the most promising regarding material or energy efficiency.

A hybrid approach that combines direct and indirect electrification holds potential as a feasible strategy for overcome observed limitations in product yield and carbon efficiency of eBtX technologies by indirect electrification. Furthermore, hybrid approaches benefit from the potentially higher conversion efficiencies of direct electrification technologies. It is reasonable to assume that combinations of electrification technologies will be employed and that such P-/eBtX processes have an advantage over PtX and BtX. However, it remains to be demonstrated whether and to what extent electrified processes can exploit synergistic effects, with this demonstration being crucial for a comprehensive assessment of process feasibility, supported by the validation and demonstration by rigorous experimental studies.

7. System level aspects and perspectives on electrification

In addition to the technological key performance indicators of P-/eBtX processes, higher system aspects, specifically sustainability and economic criteria must also be considered for a holistic evaluation of any process chain. Section 7.1 examines the supply and associated GHG emissions of biomass and electricity/H_2, as well as water and land use and the impact of plant location and site selection. Furthermore, economic factors for P-/eBtX plants are discussed. Section 7.2 covers the flexibilization and dynamic operation based on a fluctuating electricity input.

7.1 Impact of plant location and site selection

Securing a reliable supply of feedstock is a vital prerequisite for the practical operation of P-/eBtX processes. Thus, biomass, renewable electricity, water, or green H_2 from off-site sources are the resources that need to be sustainably sourced to achieve the goal of low environmental impact products. These criteria are not only mutually interdependent with sometimes conflicting interests, as shown in Fig. 16, but also subject to many external factors. The overall objective of P-/eBtX processes is to maximize carbon efficiency while minimizing total costs and life-cycle GHG emissions across the entire P-/eBtX supply chain. Given this complexity, a rigorous optimization approach using multi-criteria decision analysis is neither generally feasible nor possible within the scope of this study. However, this section presents the key decision variables to identify suitable plant locations for P-/eBtX processes.

7.1.1 Feedstock supply and infrastructure. When deciding on the location of new P-/eBtX plants powered by a combination of biomass feedstock and renewable electricity, logistical aspects related to the upstream and downstream equipment of the plants in the entire value chain must be considered. The profitability of such plants depends on their geographic location in relation to feedstock locations and product delivery destinations.[324] Whether biomass or power supply is the limiting factor for site selection ultimately depends on the location and process configuration.

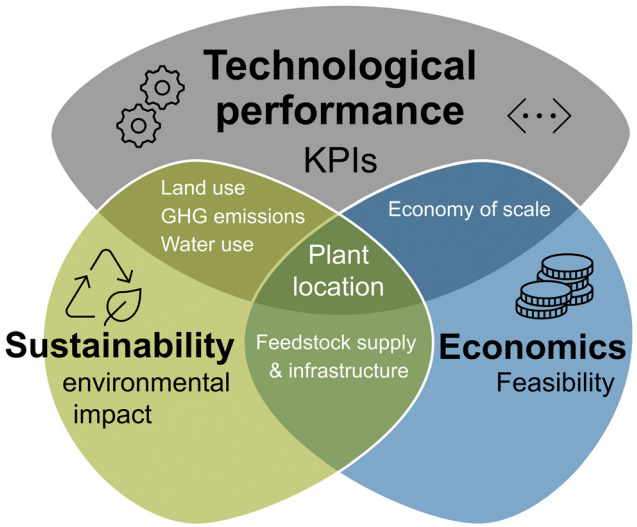

Fig. 16 Key criteria and conflicting interests when evaluating optimal P-/eBtX plant locations from a system perspective.

Biomass availability strongly depends on the region, has a comparatively low energy density, and is challenging to store to compensate for seasonal fluctuations. It can either be sourced locally, regionally or transported to the plant from a greater distance. In addition, decentralized and centralized pretreatment concepts exist. For P-/eBtX processes, the availability of electricity or H_2 poses an additional prerequisite. However, PBtX and eBtX processes have different supply constraints. For eBtX plants, the availability of sufficient green electricity must be guaranteed at any given time. The electric energy must thus be available nearby or delivered *via* the high-voltage transmission grid, potentially with sufficient electricity storage capacity to compensate the intermittency. For PBtX plants, the required green H_2 can be either produced on-site using renewables thus resulting in similar requirements as eBtX or be produced off-site and transported to the plant's location. Also, a combination of off-site and on-site H_2 production is possible.

In addition to the basic availability of feedstock, transportation infrastructure at a potential plant site also plays a critical role. Generally, the infrastructure for transporting raw materials and products must be established for a functioning supply chain. The infrastructure must be able to deal with the required mass and energy flows, including road, rail, or ship transportation for biomass, H_2 transportation *via e.g.* pipeline, or transmission lines for electricity supply. The presence of already existing infrastructure is closely linked to the decision as to whether it should be a greenfield or brownfield plant. In addition to existing transport infrastructure, the latter offers the enormous advantage of being integrated into existing industrial processes and, for example, obtaining process heat or feeding it profitably into an existing district heating network.

Long-distance transportation of woody biomass has been done for larger biomass-fired power plants or pulp mills for example *via* rail or ship. However, locally-sourced biomass offers advantages regarding transport needs and, thus, economics and sustainability,[325] especially for bulky biomass such as agricultural waste and forest residues. Therefore, limiting the transport distances to less than 100 km is advised, which means road transport *via* truck to the plant.[326] The same applies to the transport of the final product. Depending on the type of product, a road, port or pipeline infrastructure is necessary. Road transport distances of up to 200 km for liquid products can be considered reasonable.[327]

For on-site H_2 production or eBtX plants, the plant is constrained by the availability and supply of green electricity *via* an on-site renewable power source or a sufficient grid supply. In addition to the local availability of electricity, the availability of electricity over time is a decisive factor. With fluctuating renewables, dynamic operation or storage solutions are indispensable. Here, decentralized off-site H_2 production has a decisive advantage (see Section 7.2).

However, also plants using off-site H_2 production is associated with many process penalties. For example, the waste heat generated during the syngas train can usually be used in the electrolysis process allowing for SOEL to be used at high efficiency. If this is not the case, as with off-site production, the heat cannot usually be used to supply heat to other processes at greenfield plants and might has to be cooled back at high cost. As a rule, the electricity generation and its transport must be offset against the levelized costs of H_2 production, including H_2 transportation cost, to decide whether an off-site H_2 production is feasible. In addition, there is a shortage of O_2 as a byproduct of water electrolysis, which makes either on-site O_2 production or O_2 supply necessary. Here also, a partly on-site H_2 production *via* water electrolysis to cover the O_2 demand can provide a mitigating solution.

In a future hydrogen economy, PBtX processes with off-site H_2 production hold a potential advantage over on-site H_2 generation and eBtX processes due to the better storability (see Section 7.2) and transportability of H_2 compared to electricity. H_2 can be transported *via* pipelines or other means to reach remote processing facilities, efficiently utilizing renewable energy sources in different geographical areas. PBtX facilities may be in regions with abundant biomass resources but distant from the point of renewable energy generation. Furthermore, retrofitting a BtX plant once the H_2 infrastructure is implemented needs to be considered already today during construction.

In the context of siting P-/eBtX plants based on a combination of biomass feedstock and renewable electricity, there are multiple decisions to be made that cover several critical aspects. Seasonal fluctuations in biomass availability, coupled with dependence on diverse transportation modes, pose challenges in assessing the economic and sustainable implications of transport distance limitations. The decision between greenfield and brownfield plants significantly impacts existing industrial processes and integration into district heating networks. The reliability of green electricity, alternative storage options and grid supply depends on factors such as on-site or off-site integration and the choice between storing and transporting H_2 and electricity. Evaluating trade-offs in on-site and

off-site hydrogen production, encompassing waste heat utilization, transportation costs, and O_2 supply, is essential. Exploring the benefits of P-/eBtX processes in infrastructure planning, especially in a future hydrogen economy, requires frameworks that consider retrofit needs and the efficient use of renewable energy in different geographical areas. Addressing these gaps will improve understanding of the factors that influence siting decisions for P-/eBtX plants and contribute to increased efficiency, sustainability, and economic viability of these processes. Methodologies like GIS-based multi-criteria decision analysis, cross-industry collaboration from agriculture to transportation and the involvement of key players from the oil and gas industry, politics, and society. Land use and greenhouse gas emissions.

While a holistic and integrated life cycle sustainability assessment could encompass sustainability aspects for specific locations, this review focuses on the basic framework and the environmental and sustainability key factors that ultimately determine environmentally optimal plant locations. Thus, this work encompasses considerations such as land use for biomass sourcing and the provision of renewable electricity, which in turn enable the realization of economically feasible plant scales in accordance with the economy of scale principle. GHG emissions associated with the sourcing and transportation of feedstock materials must also be considered. At this point, it should be emphasized that all the processes considered are based on the premise that only biomass residues, which are not in competition with other uses, are to be used. Another environmental and sustainability criterion is the use and supply of water.

The electrification of BtX processes opens the possibility of increasing carbon efficiency and product yield. With this trait, the process can produce more fuels or chemicals from the same amount of biomass. The availability of sustainable biomass is a limiting factor for electrified BtX besides the availability of renewable electricity and/or H_2 supply. As for the US, Agrawal *et al.* state that the PBtX route with H_2 addition to the synthesis step can cover the US fuel demand based on the domestically available biomass.[56] For the BtX route, only 25–31% of the fuel demand can be covered. They also argue that the land area required for the PBtX process, which involved biomass cultivation and hydrogen production from solar energy, could be reduced by 61% to 72% compared to BtX processes, depending on the examined case.

The maximum amount of MeOH that can theoretically be produced in Europe *via* BtX or P-/eBtX was evaluated based on our own calculations. The calculations and references are given in the ESI.† Based on the sustainable biomass potential in Europe of 156.8 $Mt_{biomass,dry}$ per a,[328] the conventional BtX path can produce 83.1 Mt_{MeOH}, which corresponds to 78.5% of the global MeOH demand in 2022 (105.8 Mt_{MeOH} per a[329]). For a P/eBtX approach boosting carbon efficiency to 90%, a production amount of 188 Mt_{MeOH} per a is technically viable. The product yield for the P-/eBtX processes increases by 2.3-fold compared to the BtX route.

A simplified calculation to produce 100 MW_{LHV} methanol demonstrates these effects of electrification. While the methanol output of the plant is kept constant, the biomass input is matched to meet the demand. Using a circular-shaped biomass supply area around the plant with an equally distributed biomass density, the impact of electrification on biomass demand is shown in Fig. 17. The roads for transportation are not considered and the biomass is delivered to the plant in the center in a straight line from the pickup point. All calculations use the linear relationship between η_C and ER as defined in eqn (13). All additional assumptions and results are provided in the ESI.†

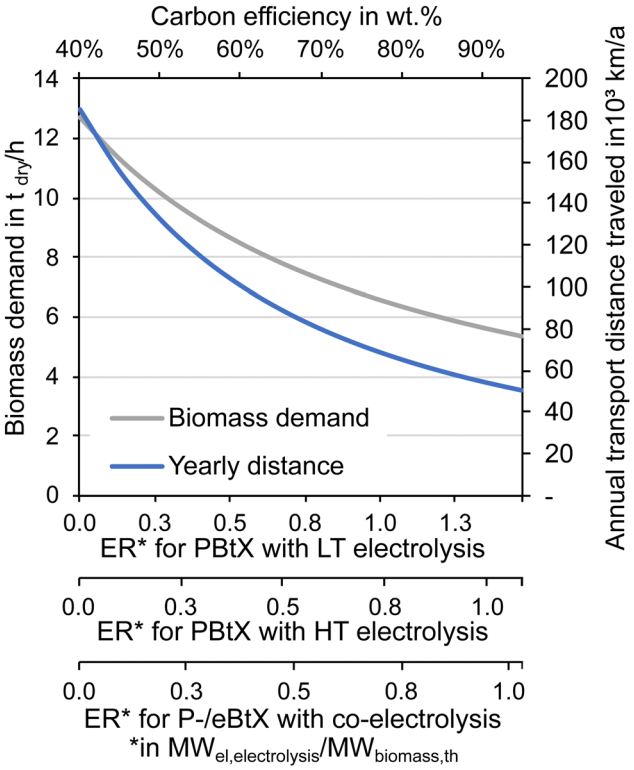

Fig. 17 Influence of carbon efficiency (degree of electrification) on biomass demand for a PBtX plant with constant methanol production of 100 MW_{LHV} (calculations and other graphs in ESI†).

Fig. 17 illustrates the relationship between degree of electrification and required land area. Based on this simplified approach, the required radius for supplying biomass to the plant is decreased from 29 km (η_C = 40%) to 19 km (η_C = 90%). This results in a 70% reduction in annual transportation distance and corresponding transportation costs. While, the impact of transportation cost is small compared to other cost components of PBtX processes, the land use is crucial. Using electrification of BtX to boost carbon efficiency, land requirement can be reduced by 56% from 2591 km^2 (η_C = 40%) to 1152 km^2 (η_C = 95%).

Furthermore, GHG emissions from biomass transportation can also be reduced by up to 73%. While the reductions in transportation may be negligible compared to the emission reduction potential of the electricity used (see below), other emissions that affect the local environment, such as noise or NOx, are also reduced in addition to GHG emissions.

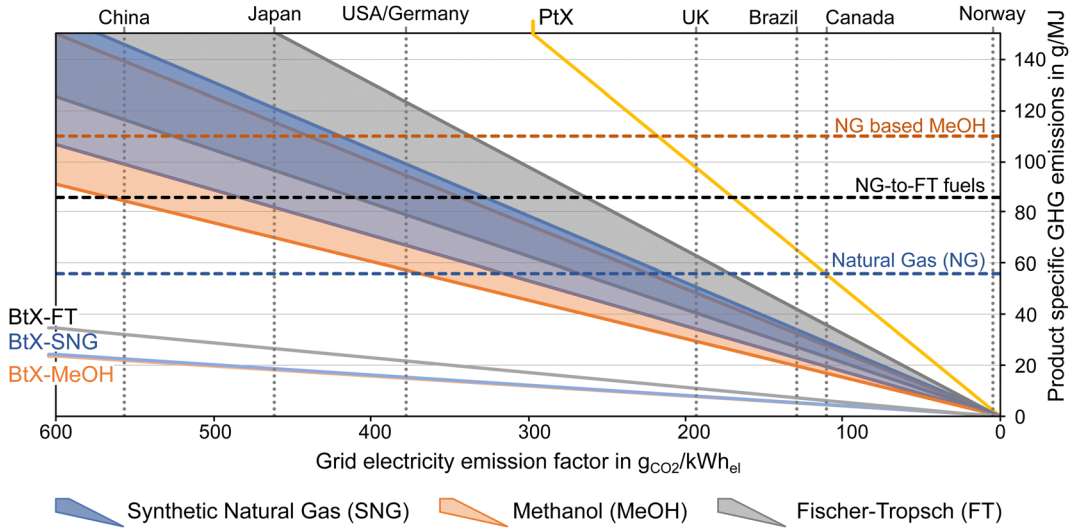

Fig. 18 Product-specific GHG emissions for P-/eBtX processes for 90% carbon efficiency depending on grid electricity factor[334] compared to Biomass-to-X (BtX), Power-to-X (PtX) and fossil alternatives. Reference values and calculations in the ESI.†

As mentioned above, the GHG emissions of the P-/eBtX product will be mainly influenced by the type of electricity used. The P-/eBtX product's emissions are between those of a PtX product, with the highest carbon footprint, and a BtX product, with the lowest emissions. Since the electrical intensity of the process is damped by using biomass as another feedstock, P-/eBtX processes are more viable for reaching GHG reduction targets even for electricity with a higher emission factor.

Fig. 18 illustrates the impact of the carbon intensity of the electricity on the specific GHG emissions of P-/eBtX products in comparison with the same products from pure BtX and PtX. All assumptions and data sources are provided in the ESI.† For P-/eBtX processes, a range for the required ER of 1.1–1.3 for SNG and 0.7–1.2 for MeOH and FT were assumed to achieve a 90% carbon efficiency based on the meta-analysis in Section 6. The shown graphs are solely based on indirect process emissions due to the use of grid electricity. As reference, the horizontal lines indicate the emissions of conventional natural gas,[330] natural gas-derived MeOH[331] and FT products derived from Gas-to-Liquid.[332]

As the graphs show, the BtX processes have a very low electricity demand, which is responsible for indirect emissions when grid electricity is used. Since biomass residues are assumed to be carbon-neutral, they perform significantly better than the P-/eBtX, PtX and fossil alternatives. The PtX reference process has the largest carbon footprint, where the very conservative assumption was made that only hydrogen is produced using PEMEL. The resulting ranges for the P-/eBtX processes laying between BtX and PtX clearly highlight the hybrid nature. Accordingly, SNG processes become preferable to the fossil equivalent at an emission factor of 240–310 g CO_2 per kW per h_{el}. For MeOH emission reduction can be assumed starting from an emission factor below 730–440 g CO_2 per kW per h_{el}. In the case of FT products, this is the case at 260–410 g_{CO_2} per kW per h_{el}. The lower the carbon-intensity of electricity, the lower the product specific GHG emission and the smaller the absolute difference between products. Thus, PBtX processes are only viable if low-carbon intensive electricity is available while performing better in terms of emissions than PtX processes.

The current EU regulations, particularly the RED II Directive and subsequent proposals like RED3, set ambitious sustainability and GHG emissions reduction criteria for biofuels and renewable fuels of non-biological origin (RFNBO). Based on today's RED II,[333] biofuels need to reach an emission reduction of 65%. For fuels of non-biological origin a reduction target of 70% applies. Electrified BtX processes can contribute to reaching this goal for biofuels. The emissions from transportation, and extraction and cultivation of raw materials which are part of the CO_2 balance defined in RED II are allocated on an increased amount of product for the same biomass input (see Fig. 10 and 17). However, emissions for processing by electricity utilization will increase. Consequently, products of electrified BtX routes will most likely reach higher emission factors than BtX products as discussed in Fig. 18. It is important to mention, that as of today, the question of how synfuels, derived partly from electrolytic renewable hydrogen and partly from biological sources as in the discussed e-/PBtX processes, fit into the current EU framework remains unanswered. An e-/PBtX friendly regulatory framework could facilitate the role out of the technology with its obvious advantages presented in this review.

When it comes to on-site water electrolysis, which requires a continuous supply of feed water, selecting a water source is crucial. As an infrastructural criterion, the proximity to the nearest water source is key, with coastal sites relying on seawater and inland sites on freshwater. An essential sustainability aspect involves assessing the water risk within the site's region. Consequently, for inland locations, the water source region

should exhibit a low level of water stress. In the case of coastal sites, marine protected areas must be excluded to prevent negative environmental consequences associated with desalination plant discharges.[335]

7.1.2 Economics. A product cost comparison as done for technical parameters, is not included in this review since differing assumptions and boundary conditions do not allow for comparable results. A general cost assessment involving data from process simulations shows that the prices of products from electrified BtX processes are between BtX and PtX processes.[71,336] This review highlights the changes in the contribution of capital expenditure as well as feedstock and utility cost, which accounts for the majority of the final product cost.

For BtX, PtX and P-/eBtX processes, feedstock costs represent the primary cost component, which is of course very location dependent. Furthermore, feedstock cost and plant capacity scale linearly, while investment costs show economy of scale for larger plants.[327] For BtX processes, biomass feedstock costs account for about 40% of the net production costs.[71] Electricity expenses for PtX processes generally make up around 70% of the total cost.[71] For PBtL processes, biomass feedstock costs now account for about 25% of total expenditures, and electricity costs account for about 30–40%.[71]

Whether and to what extent dynamic operation, *e.g.* based on the electricity price, can have a profitable effect on the production cost needs to be assessed. Section 7.2 discusses technical and economic challenges of dynamic operation in more detail.

For P-/eBtX processes, the cost of electricity or H_2 has the most significant impact on the price of the final product. This crucial supply of electricity or H_2 is closely related to a plant's location. Locations with high electricity prices will not be preferred for eBtX plants and PBtX plants with on-site H_2 generation. For this location, importing H_2 for a PBtX might be more viable. To fully assess the economics of electrified processes, the investment costs are not to be neglected. For some electrified technologies like water electrolysis the influence on capital expenditures of the whole PBtX plant can be significant. For other technologies, the impact might be less significant or equalizes due to savings for smaller equipment size. For PBtX processes, water electrolysis is responsible for the main share of operating and investment cost. Typically, 90% of the electricity requirement and 40% of the capital cost are related to water electrolysis.[337]

An existing H_2 infrastructure with a market for H_2 changes the way of thinking about economic and technical considerations for a PBtX plant. In a future hydrogen economy, international markets for H_2 allow for a cost-effective and steady supply of green H_2. With long-term contracts, the H_2 price can be fixed, lowering the financial risk. Furthermore, the technical risk of operating a huge water electrolysis is erased.

A comprehensive comparison of production costs, similar to the technical parameters, is considered difficult due to the different assumptions and boundary conditions in the various studies but is necessary to assess the feasibility of such processes. Since raw material cost will always be one, if not the most important cost driver for BtX, PtX and P-/eBtX processes, the location of the plant is of crucial importance. Site-specific economic analyses are therefore required to realistically estimate the costs for electricity and biomass supply. Since electrified technologies, especially electrolysis technologies, have a significant impact on investment costs, detailed and up-to-date cost estimates are essential, especially for emerging technologies. Dynamic operation, especially in response to fluctuating electricity prices, makes the economic assessment even more complex. One desirable option is the steady-state operation in the syngas train by storing intermittent H_2. However, the economic viability of this approach requires careful consideration, given the challenges associated with H_2 storage (see also Section 7.2). The role of an existing H_2 infrastructure, especially in the context of a future hydrogen economy, changes these economic considerations, potentially mitigating financial risks. This development must be constantly monitored and reassessed. Flexibilization and dynamic operation of electrified processes.

A key challenge of the energy transition is the volatility of renewable electricity generation. One major favorable aspect of electrifying BtX processes is the potential for flexible electricity usage. Such an operational strategy has the potential to be economically self-sustaining in a suitable electricity market. Profit can be attained through energy price arbitrage or ancillary grid services.

Most presented technologies and concepts technically allow dynamic electrical power usage. For example, a dynamic load change is possible in seconds for running water electrolysis (PEMEL and AEL).[45] There are, however, several challenges related to dynamic operation. Primarily, the time response of the entire P-/eBtX facility must be evaluated holistically. Moreover, dynamic operation tends to increase investment costs due to the need for oversized equipment or plant components solely activated during specific operational modes. Apart from this necessity for several instances of oversizing and backup equipment provisions, process integration emerges as a significant drawback in electricity market-driven power integration. Integrating highly interdependent processes necessitates complex control strategies, which already poses challenges and becomes even more intricate when integrating fluctuating renewable sources. This complexity is particularly crucial when it comes to heat integration.

Furthermore, the operation of the core BtX syngas train typically aims at reaching high full-load hours as plant components are running at their optimal design point reaching high efficiencies and durability. This desirable steady-state operation results in profit maximization which contradicts any dynamic operation. Another disadvantage of flexible electricity integration is the decrease in overall efficiency and product yield when complete carbon conversion cannot be achieved and carbon is lost in the form of CO_2. Since this is an inherent process limitation of any of P-/eBtX process, dynamic operation is not conducive if maximum carbon turnover and product yields are the goal.

However, several principles apply to flexibilization to make it as profitable as possible. The flexible operation influences the equipment downstream of the point of flexibilization. Impacts range from changes in thermodynamic properties like pressure or temperature to chemical properties like gas composition or impurities. To ensure the most efficient and undisturbed operation, the flexibilization should be placed as far down the process chain as possible. It should have the smallest impact on changes of properties of syngas or pretreated material. If possible, backup buffering using storage tanks would be also a viable option to mitigate downstream impact.

Especially, pretreatment process can be operated flexibly if pretreated material can be buffered, and the pretreatment capacity is oversized. Decentralized pretreatment sites, decoupling pretreatment and main syngas train could allow for subprocesses to be run economically at the energy price. However, it must be taken into account that the amount of electricity that can be integrated in the pretreatment step is generally comparatively small.

For gasification, syngas condition and synthesis, no buffering is viable and any dynamic operation will impact downstream equipment. For example, in gasifiers, the mode of operation would change between allothermal and autothermal mode if heat is supplied *via* electrification. This would cause a change in syngas composition, making backup equipment in the syngas conditioning train, like WGS and CO_2 removal, indispensable to operate the synthesis.

In conclusion, the flexibilization of electrified BtX processes is not trivial from a technical and economic point. The trade-off between flexible and steady-state operating must be considered carefully. The recommendation for flexibilization are the placement of electrified process steps as far down of the process chain as possible and the electrification of process steps which have a low impact on the downstream process (see Table 13). To limit the impact of flexibilization, using a narrow range of flexibilization might be more viable than using the full range of flexibilization since the process is then operating more closely to an optimal economic and technical design point. While many of the technologies presented technically enable dynamic electricity use, several challenges need to be overcome. For each technology, it is necessary to evaluate the dynamic behavior as well as the partial load capability. In addition, a holistic evaluation of the time behavior of entire P/eBtX processes is still pending.

As H_2 hold better storability (see Section 7.1.1) than electricity, H_2 can be produced during periods of excess renewable energy generation and stored for later use in PBtX processes. Stored H_2 can be utilized to provide a stable and reliable energy source for the conversion of biomass feedstock, decoupling the volatile hydrogen production from the steady-state operation of the syngas conversion process. Intermediate H_2 storage within PBtX processes offer resilience. They allow for the synchronization of H_2 availability with the operational needs of the conversion process, reducing the risk of process disruptions due to intermittent renewable energy generation. Additionally, the plant would most likely run at maximum capacity to increase product output with no room for flexibilization. The role of an existing H_2 infrastructure, especially in the context of a future hydrogen economy, could provide a stable supply of green H_2. However, the challenges associated with H_2 storage, including technical challenges, additional costs and safety considerations, highlight the importance of flexible BtX operation as a key area for future research.

8. Conclusion

In conclusion, this paper has comprehensively examined the potential of electrifying Biomass-to-X (BtX) processes to enhance the conventional pathways. By integrating electricity, BtX processes can overcome their inherent limitations in carbon efficiency. These electrified BtX processes hold the promise of contributing significantly to the decarbonization and transition away from fossil fuels in major industries.

Two primary pathways for electrifying BtX processes have been explored: indirect electrification (PBtX) and direct electrification (eBtX). In the case of PBtX, the addition of H_2 at different points along the process chain has been a key focus. Since H_2 production from water electrolysis is a mature technology, the technological readiness of indirect electrification only depends on the point of H_2 addition. Additionally, O_2 from water electrolysis can be used for gasification and syngas conditioning. While adding H_2 to the water gas shift reactor and synthesis has been extensively investigated, other routes such as H_2 addition to the gasifier or syngas conditioning show promise but require further validation.

For direct electrification (eBtX), technologies are all in the early research stage and need more development to assess their impact on the BtX process reliably. The sole supply of heat energy at low and medium heat *via* direct electrification is less viable as enough heat is usually available. However, the supply of high-temperature heat, especially in the gasifier or the syngas conditioning, seems promising. Additionally, the target-oriented addition of heat to the biomass, gas, or catalyst is beneficial compared to using a heat exchanger to heat surfaces. For pyrolysis, gasification and reforming (all endothermic processes), high temperature heat can be supplied to the process by induction, microwaves, plasma, or electrical heating. Additionally, plasma technology stands out as an intriguing option for introducing energy into the gasifier and syngas conditioning stages. Plasma-based processes have the advantage of simultaneous heat input and reforming properties of plasma. Initial process simulations of electrically-heated processes have indicated efficiency and economic benefits. The concept of co-electrolysis also emerges as a promising approach for enhancing BtX processes.

In terms of technological feasibility and maturity, the power-to-heat efficiency and the way heat is transferred play a crucial role in deciding if adding heat to a process is feasible. Among the technologies discussed in this paper, not all are equally suitable for electrifying a BtX process. When it comes to maturity, indirect electrification through H_2 addition shows

higher readiness compared to technologies like co-electrolysis (both parallel and in-line integration) and direct electrification. On the other hand, technologies like co-electrolysis and direct electrification are still in earlier stages of development. Among the co-electrolysis options, parallel integration seems to be more technologically feasible than in-line integration due to its simpler implementation.

Overcoming component-level engineering challenges is crucial for the success of electrified BtX processes. Specific technology options demand focused research, such as material stability and pressurized operation SOEL, and optimizing reactor designs for heating technologies like resistive and inductive heating. The adaptation of thermal plasma for biomass conversion requires innovations in plasma torch design and addressing issues of erosion and electrode replacement. Non-thermal plasma applications for synthesis necessitate in-depth research on operating under low pressures. Further, the development and optimization of control techniques considering biomass feedstock variations, are critical for seamless integration into existing and evolving electrified BtX process configurations.

Evaluation of electrification effectiveness is focused on key performance indicators, such as carbon efficiency, product yield, and energy yield to measure its impact on process performance. It is important to recognize that variations in the reported performance data are attributed to different modeling approaches and assumptions, such as biomass composition, conversion efficiencies, and process configurations. The adoption of electrification leads to improvements in carbon efficiency and product yield. Achieving a carbon efficiency of 90% requires an electrification ratio of around 0.7 $MW_{el}\ MW_{biomass}^{-1}$ for MeOH and FT, and about 1.0 $MW_{el}\ MW_{biomass}^{-1}$ for SNG production. Whether electrification options like plasma gasification, hydrogasification, or electrically heated conversion technologies can match these electrification ratios remains to be demonstrated. Achieving values below these benchmarks is considered highly promising.

The energy yield for H_2 addition depends on the type of electrolysis technology employed. High-temperature electrolysis demonstrates better efficiency, resulting in higher energy yields. Moreover, the integration of co-electrolysis slightly outperforms classical PBtX processes using water electrolysis. Co-electrolysis is superior in terms of product yield, carbon efficiency, and energy yield for all products. Whether and to what extent such PBtX processes exploit synergies cannot be conclusively determined based on the meta-analysis. However, it is reasonable to assume that PBtX processes have an advantage over PtX and BtX due to heat and material integration, as well as the omission of CO_2 capture, which is common in pure PtX processes. Especially interesting and beneficial are hybrid processes constituting of a combination of direct and indirect electrification.

In evaluating the electrification of BtX processes, a holistic perspective shows the multiple implications that go beyond technical performance. System-level considerations encompass sustainability, economics, and operational flexibility. Plant location emerges as a key determinant, impacting feedstock supply, infrastructure, and transportation logistics. Sustainability factors such as land use, greenhouse gas emissions, and water usage underscore the significance of resource availability in allowing low-impact, high-efficiency P-/eBtX processes. Economic viability of such processes is tightly linked to the cost of resources, particularly electricity or H_2. The potential of a future hydrogen economy to stabilize costs and supply of H_2 adds a new dimension to process economics. Meanwhile, the idea of flexible electricity usage in electrified BtX processes requires careful case-to-case evaluation, balancing the benefits of energy price arbitrage and grid services with the complexities of dynamic operation.

From this system perspective, a robust framework is required for infrastructure planning and decision-making. Addressing contradictions in energy policies, especially regarding synfuels from electrolytic renewable hydrogen and biological sources, necessitates research to ensure compliance with regulations and sustainability certification, considering life cycle assessment (LCA). Conducting comprehensive cost assessments, accounting for location-specific factors and updating estimates for emerging technologies, is crucial. Overcoming challenges in dynamic operation, evaluating partial load capability, and conducting holistic evaluations of time behavior for entire P/eBtX processes are imperative. Further research is needed on intermediate H_2 storage resilience, synchronizing H_2 availability, and understanding the role of existing H_2 infrastructure in a future hydrogen economy.

Further research needs to address the experimental investigation on pilot plant scale especially for direct electrification technologies. Furthermore, these technologies need to be evaluated from a process level. Processes developed for other purposes need to be tailored to the application in electrified BtX processes. The plant location and further aspects of scale up needs to be addressed.

Author contributions

Daniel Klüh and Marcel Dossow contributed equally to the paper and share the first authorship. Conceptualization: Dossow, Klüh; Funding acquisition: Spliethoff; Investigation: Dossow, Klüh; Methodology: Dossow, Klüh; Project administration: Dossow, Klüh, Fendt; Supervision: Umeki, Spliethoff, Fendt; Visualization: Dossow, Klüh; Writing – original draft: Dossow, Klüh; Writing – review & editing: Dossow, Klüh, Umeki, Fendt, Gaderer.

Abbreviations

AC	Alternating current
AEL	Alkaline electrolysis
AGR	Acid gas removal
ATR	Autothermal reforming
BFB	Bubbling fluidized bed
BtX	Biomass-to-X

CFB	Circulating fluidized bed
DBD	Dielectric-barrier discharge
DC	Direct current
DME	Dimethyl ether
DTU	Technical university of denmark
eBtX	Electrified biomass-to-X
EFG	Entrained flow gasification
ER	Electrification ratio
EY	Energy yield
FB	Fixed bed
FT	Fischer–Tropsch
GHG	Greenhouse gas
HT	High-temperature
HTC	Hydrothermal carbonization
KPI	Key performance indicator
LHV	Lower heating value
LT	Low-temperature
MeOH	Methanol
PBtX	Power-and-biomass-to-X
PEMEL	Proton exchange membrane electrolysis
POX	Partial oxidation reforming
PtX	Power-to-X
PY	Product yield
RF	Radio frequency
SI	Supplementary information
SN	Stoichiometric number
SNG	Synthetic natural gas
SOEL	Solid oxide electrolysis
TRL	Technology readiness level
TUM	Technical university of munich
WGS	Water–gas shift

Conflicts of interest

The authors declare no conflict of interest.

Acknowledgements

We gratefully acknowledge funding of the projects ''Verena'' (03EE5044B) sponsored by the German Federal Ministry of Economic Affairs and Climate Action, and ''REDEFINE H2E'' (01DD21005) sponsored by the German Federal Ministry of Education and Research. In addition, the authors acknowledge the cooperation within the Network TUM.Hydrogen and PtX. The authors would like to thank Dr Andrius Tamošiūnas and Sebastian Bastek for proofreading section ''4.2 Plasma-assisted processes'' and Benjamin Steinrücken for his support on topics related to solid oxide electrolysis.

References

1 BP, bp Statistical Review of World Energy, available at: https://www.bp.com/content/dam/bp/business-sites/en/global/corporate/pdfs/energy-economics/statistical-review/bp-stats-review-2022-full-report.pdf, accessed 23 August 2022.
2 A. Revi, H. de Coninck, M. Babiker, P. Bertoldi, M. Buckeridge, A. Cartwright, W. Dong, J. Ford, S. Fuss, J.-C. Hourcade, D. Ley, R. Mechler, P. Newman, A. Revokatova, S. Schultz, L. Steg, T. Sugiyama, M. Araos, S. Bakker and E. Wollenberg, *Global Warming of 1.5 °C*, 2018, pp. 313–443.
3 K. van Kranenburg, E. Schols, H. Gelevert, R. de Kler, Y. van Delft and M. Weeda, Empowering the chemical industry. Opportunities for electrification, available at: https://www.voltachem.com/images/uploads/voltachem_electrification_whitepaper_2016.pdf, accessed 23 August 2023.
4 D. H. König, M. Freiberg, R.-U. Dietrich and A. Wörner, *Fuel*, 2015, **159**, 289–297.
5 R. Agrawal and N. R. Singh, *AIChE J.*, 2009, **55**, 1898–1905.
6 C. Philibert, *Renewable Energy for Industry – From green energy to green materials and fuels*, 2017.
7 J. Rissman, C. Bataille, E. Masanet, N. Aden, W. R. Morrow, N. Zhou, N. Elliott, R. Dell, N. Heeren, B. Huckestein, J. Cresko, S. A. Miller, J. Roy, P. Fennell, B. Cremmins, T. Koch Blank, D. Hone, E. D. Williams, S. de La Rue Can, B. Sisson, M. Williams, J. Katzenberger, D. Burtraw, G. Sethi, H. Ping, D. Danielson, H. Lu, T. Lorber, J. Dinkel and J. Helseth, *Appl. Energy*, 2020, **266**, 114848.
8 A. Poluzzi, G. Guandalini, F. d'Amore and M. C. Romano, *Curr Sustainable Renewable Energy Rep*, 2021, **8**, 242–252.
9 T. Durka, T. van Gerven and A. Stankiewicz, *Chem. Eng. Technol.*, 2009, **32**, 1301–1312.
10 Y. Zhang, P. Chen, S. Liu, P. Peng, M. Min, Y. Cheng, E. Anderson, N. Zhou, L. Fan, C. Liu, G. Chen, Y. Liu, H. Lei, B. Li and R. Ruan, *Bioresour. Technol.*, 2017, **230**, 143–151.
11 Y. Zhang, C. Ke, W. Fu, Y. Cui, M. A. Rehan and B. Li, *Renewable Energy*, 2020, **154**, 488–496.
12 I. Rosyadi, S. Suyitno, A. X. Ilyas, A. Faishal, A. Budiono and M. Yusuf, *Biofuel Res. J.*, 2022, **9**, 1573–1591.
13 A. A. Arpia, T.-B. Nguyen, W.-H. Chen, C.-D. Dong and Y. S. Ok, *Chemosphere*, 2022, **287**, 132014.
14 A. Sanlisoy and M. O. Carpinlioglu, *Int. J. Hydrogen Energy*, 2017, **42**, 1361–1365.
15 L. Tang, H. Huang, H. Hao and K. Zhao, *J. Electrost.*, 2013, **71**, 839–847.
16 H. Song, G. Yang, P. Xue, Y. Li, J. Zou, S. Wang, H. Yang and H. Chen, *Appl. Energy Combustion Sci.*, 2022, **10**, 100059.
17 V. S. Sikarwar, M. Zhao, P. Clough, J. Yao, X. Zhong, M. Z. Memon, N. Shah, E. J. Anthony and P. S. Fennell, *Energy Environ. Sci.*, 2016, **9**, 2939–2977.
18 P. Bergman, A. Boersma, R. Zwart and J. Kiel, *Torrefaction for Biomass Co-Firing in Existing Coal-Fired Power Stations*, 2005.
19 V. S. Sikarwar, M. Zhao, P. S. Fennell, N. Shah and E. J. Anthony, *Prog. Energy Combust. Sci.*, 2017, 61.
20 J. Shankar Tumuluru, S. Sokhansanj, J. R. Hess, C. T. Wright and R. D. Boardman, *Ind. Biotechnol.*, 2011, **7**, 384–401.
21 F. Jin, *Application of Hydrothermal Reactions to Biomass Conversion*, Springer Berlin Heidelberg, Berlin, Heidelberg, 2014.

22 M. Kaltschmitt, *Energie Aus Biomasse. Grundlagen, Techniken und Verfahren*, Springer Berlin, Heidelberg, Berlin, Heidelberg, 2nd edn, 2009.
23 A. V. Bridgwater, A. J. Toft and J. G. Brammer, *Renewable Sustainable Energy Rev.*, 2002, **6**, 181–246.
24 A. Bridgwater, S. Czernik, J. Diebold, D. Meier, A. Oasmaa, C. Peacocke, J. Piskorz and D. Radlein, *Fast pyrolysis of biomass: a handbook*, 1999.
25 M. Balat, M. Balat, E. Kırtay and H. Balat, *Energy Convers. Manage.*, 2009, **50**, 3158–3168.
26 M. Burgt, *Gasification*, Elsevier Science & Technology, Oxford, 2nd edn, 2008.
27 A. Tremel, D. Becherer, S. Fendt, M. Gaderer and H. Spliethoff, *Energy Convers. Manage.*, 2013, **69**, 95–106.
28 S. Hafner, *Biomass to Chemicals*, Berlin, 2022.
29 L. B. Allegue and J. Hinge, Biogas and bio-syngas upgrading, available at: **https://www.teknologisk.dk/_/media/52679_Report-Biogas%20and%20syngas%20upgrading.pdf**, accessed 13 August 2023.
30 V. Dieterich, A. Buttler, A. Hanel, H. Spliethoff and S. Fendt, *Energy Environ. Sci.*, 2020, **13**, 3207–3252.
31 N. Kaisalo, J. Kihlman, I. Hannula and P. Simell, *Fuel*, 2015, **147**, 208–220.
32 S. Ali, K. Sørensen and M. P. Nielsen, *Renewable Energy*, 2020, **154**, 1025–1034.
33 I. Hannula, *Synthetic fuels and light olefins from biomass residues, carbon dioxide and electricity: Performance and cost analysis*, Dissertation, 2015.
34 J.-M. Lavoie, *Front. Chem.*, 2014, **2**, 81.
35 M. Claeys and E. van Steen, in *Fischer-Tropsch technology*, ed. A. Steynberg and M. Dry, Elsevier, Amsterdam, 2006, vol. 152, pp. 601–680.
36 L. P. R. Pala, Q. Wang, G. Kolb and V. Hessel, *Renewable Energy*, 2017, **101**, 484–492.
37 A. Mena Subiranas, *Combining Fischer-Tropsch Synthesis (FTS) and Hydrocarbon Reactions in one Reactor*, Universitätsverlag Karlsruhe, Karlsruhe, 2009.
38 A. de Klerk, *Energy Environ. Sci.*, 2011, **4**, 1177.
39 J. Ott, V. Gronemann, F. Pontzen, E. Fiedler, G. Grossmann, D. B. Kersebohm, G. Weiss and C. Witte, *Ullmann's Encyclopedia of Industrial Chemistry*, Wiley-VCH Verlag GmbH & Co. KGaA, Weinheim, Germany, 2000, vol. 16, p. 197.
40 F. Fischer and H. Tropsch, *Brennst.-Chem.*, 1923, 193–197.
41 A. N. Stranges, *Fischer-Tropsch Synthesis, Catalyst and Catalysis*, Elsevier, 2007, vol. 163, pp. 1–27.
42 J. van de Loosdrecht, F. G. Botes, I. M. Ciobica, A. Ferreira, P. Gibson, D. J. Moodley, A. M. Saib, J. L. Visagie, C. J. Weststrate and J. W. Niemantsverdriet, in *Comprehensive inorganic chemistry II. From elements to applications*, ed. J. Reedijk, Elsevier, Amsterdam, 2nd edn, 2013, pp. 525–557.
43 J. Kopyscinski, T. J. Schildhauer and S. M. Biollaz, *Fuel*, 2010, **89**, 1763–1783.
44 IRENA, Green Hydrogen Cost Reduction: Scaling up Electrolysers to Meet the 1.5 °C Climate Goal, available at: **https://www.irena.org/-/media/Files/IRENA/Agency/Publication/2020/Dec/IRENA_Green_hydrogen_cost_2020.pdf**, accessed 6 May 2022.
45 A. Buttler and H. Spliethoff, *Renewable Sustainable Energy Rev.*, 2018, **82**, 2440–2454.
46 M. Riedel, M. P. Heddrich and K. A. Friedrich, *Int. J. Hydrogen Energy*, 2019, **44**, 4570–4581.
47 Q. Fang, L. Blum and D. Stolten, *J. Electrochem. Soc.*, 2019, **166**, F1320–F1325.
48 J. E. O'Brien, M. G. McKellar, E. A. Harvego and C. M. Stoots, *Int. J. Hydrogen Energy*, 2010, **35**, 4808–4819.
49 X. Sun, P. V. Hendriksen, A. Hauch, A. K. Clausen, T. Lehtinen and M. Noponen, *ECS Trans.*, 2021, **103**, 1083–1091.
50 N. Oulette, H.-H. Rogner and D. S. Scott, *Int. J. Hydrogen Energy*, 1995, **20**, 873–880.
51 M. Specht, A. Bandi, F. Baumgart, C. N. Murray and J. Gretz, *Greenhouse Gas Control Technologies 4*, Elsevier, 1999, vol. 20, pp. 723–727.
52 T. M. Dabros, M. Z. Stummann, M. Høj, P. A. Jensen, J.-D. Grunwaldt, J. Gabrielsen, P. M. Mortensen and A. D. Jensen, *Prog. Energy Combust. Sci.*, 2018, **68**, 268–309.
53 S. Oh, J. Lee, S. S. Lam, E. E. Kwon, J.-M. Ha, D. C. W. Tsang, Y. S. Ok, W.-H. Chen and Y.-K. Park, *Bioresour. Technol.*, 2021, **342**, 126067.
54 P. Basu, *Biomass Gasification, Pyrolysis and Torrefaction*, Elsevier, 2018, pp. 155–187.
55 J.-M. Seiler, C. Hohwiller, J. Imbach and J.-F. Luciani, *Energy*, 2010, **35**, 3587–3592.
56 R. Agrawal, N. R. Singh, F. H. Ribeiro and W. N. Delgass, *Proc. Natl. Acad. Sci. U. S. A.*, 2007, **104**, 4828–4833.
57 E. Barbuzza, G. Buceti, A. Pozio, M. Santarelli and S. Tosti, *Fuel*, 2019, **242**, 520–531.
58 M. Mozaffarian and R. W. R. Zwart, *Feasibility of biomass/waste-related SNG production technologies*, 2003.
59 L. Shufen and S. Ruizheng, *Fuel*, 1994, **73**, 413–416.
60 F. Mohseni, M. Görling and P. Alvfors, *Proceedings of the World Renewable Energy Congress – Sweden, 8–13 May, 2011*, Linköping University Electronic Press, Linköping, Sweden, 2011, pp. 287–294.
61 L. Røngaard Clausen, *Design of novel DME/methanol synthesis plants based on gasification of biomass*, Dissertation, DTU Mechanical Engineering; DCAMM, Lyngby, 1st edn, 2011, No. S 123.
62 L. R. Clausen, *Energy*, 2015, **85**, 94–104.
63 G. Butera, S. Fendt, S. H. Jensen, J. Ahrenfeldt and L. R. Clausen, *Energy*, 2020, **208**, 118432.
64 M. Houben, H. Delange and A. Vansteenhoven, *Fuel*, 2005, **84**, 817–824.
65 T. A. van der Hoeven, H. C. de Lange and A. A. van Steenhoven, *Fuel*, 2006, **85**, 1101–1110.
66 W. Ahmad, L. Lin and M. Strand, *Energy*, 2022, **239**, 122251.
67 H. Svensson, P. Tunå, C. Hulteberg and J. Brandin, *Fuel*, 2013, **106**, 271–278.
68 A. Hanel, V. Dieterich, S. Bastek, H. Spliethoff and S. Fendt, *Energy Convers. Manage.*, 2022, **274**, 116424.

69 M. Gassner and F. Maréchal, *Energy*, 2008, **33**, 189–198.
70 I. Ridjan, B. Vad Mathiesen and D. Connolly, *SOEC pathways for the production of synthetic fuels. The transport case*, Department of Development and Planning, Aalborg University, 2013.
71 I. Hannula, *Biomass Bioenergy*, 2015, **74**, 26–46.
72 I. Hannula, *Energy*, 2016, **104**, 199–212.
73 P. Trop and D. Goricanec, *Energy*, 2016, **108**, 155–161.
74 L. R. Clausen, *Energy*, 2017, **125**, 327–336.
75 H. Æ. Sigurjonsson and L. R. Clausen, *Appl. Energy*, 2018, **216**, 323–337.
76 R. Anghilante, C. Müller, M. Schmid, D. Colomar, F. Ortloff, R. Spörl, A. Brisse and F. Graf, *Energy Convers. Manage.*, 2019, **183**, 462–473.
77 H. Zhang, L. Wang, J. van Herle, F. Maréchal and U. Desideri, *Appl. Energy*, 2020, **270**, 115113.
78 A. Poluzzi, G. Guandalini and M. C. Romano, *Biomass Bioenergy*, 2020, **142**, 105618.
79 R. Kofler and L. R. Clausen, *Smart Energy*, 2021, **2**, 100015.
80 E. Giglio, G. Vitale, A. Lanzini and M. Santarelli, *Biomass Bioenergy*, 2021, **148**, 106017.
81 D. Mignard and C. Pritchard, *Chem. Eng. Res. Des.*, 2008, **86**, 473–487.
82 E. G. Hertwich and X. Zhang, *Environ. Sci. Technol.*, 2009, **43**, 4207–4212.
83 L. R. Clausen, N. Houbak and B. Elmegaard, *Energy*, 2010, **35**, 2338–2347.
84 H. Firmansyah, Y. Tan and J. Yan, *Energy Proc.*, 2018, **145**, 576–581.
85 H. Zhang, L. Wang, F. Maréchal and U. Desideri, *Development of Integrated High Temperature and Low Temperature Fischer-Tropsch System for High Value Chemicals Coproduction*, 2019, **158**, 4548–4553.
86 G. Butera, R. Ø. Gadsbøll, G. Ravenni, J. Ahrenfeldt, U. B. Henriksen and L. R. Clausen, *Energy*, 2020, **199**, 117405.
87 H. Zhang, L. Wang, M. Pérez-Fortes, J. van Herle, F. Maréchal and U. Desideri, *Appl. Energy*, 2020, **258**, 114071.
88 M. Hennig and M. Haase, *Fuel Process. Technol.*, 2021, **216**, 106776.
89 G. Butera, S. H. Jensen, J. Ahrenfeldt and L. R. Clausen, *Fuel Process. Technol.*, 2021, **215**, 106718.
90 A. Poluzzi, G. Guandalini, S. Guffanti, M. Martinelli, S. Moioli, P. Huttenhuis, G. Rexwinkel, J. Palonen, E. Martelli, G. Groppi and M. C. Romano, *Front. Energy Res.*, 2022, **9**, 1–23.
91 K. Melin, H. Nieminen, D. Klüh, A. Laari, T. Koiranen and M. Gaderer, *Front. Energy Res.*, 2022, **10**, 1–17.
92 N. de Fournas and M. Wei, *Energy Convers. Manage.*, 2022, **257**, 115440.
93 M. Ostadi, L. Bromberg, D. R. Cohn and E. Gençer, *Fuel*, 2023, **334**, 126697.
94 E. Anetjärvi, E. Vakkilainen and K. Melin, *Energy*, 2023, **276**, 127202.
95 R. C. Baliban, J. A. Elia and C. A. Floudas, *Ind. Eng. Chem. Res.*, 2010, **49**, 7343–7370.
96 Q. Bernical, X. Joulia, I. Noirot-Le Borgne, P. Floquet, P. Baurens and G. Boissonnet, *11th international symposium on process systems engineering – PSE2012*, Elsevier, Oxford, 2012, vol. 31, pp. 865–869.
97 Q. Bernical, X. Joulia, I. Noirot-Le Borgne, P. Floquet, P. Baurens and G. Boissonnet, *Ind. Eng. Chem. Res.*, 2013, **52**, 7189–7195.
98 F. G. Albrecht, D. H. König, N. Baucks and R.-U. Dietrich, *Fuel*, 2017, **194**, 511–526.
99 M. Hillestad, M. Ostadi, G. Alamo Serrano, E. Rytter, B. Austbø, J. G. Pharoah and O. S. Burheim, *Fuel*, 2018, **234**, 1431–1451.
100 E. Kurkela, S. Tuomi, M. Kurkela and I. Hiltunen, *Flexible Hybrid Process for Combined Production of Heat, Power and Renewable Feedstock for Refineries*, 2019.
101 F. Habermeyer, E. Kurkela, S. Maier and R.-U. Dietrich, *Front. Energy Res.*, 2021, 684.
102 M. Dossow, V. Dieterich, A. Hanel, H. Spliethoff and S. Fendt, *Renewable Sustainable Energy Rev.*, 2021, 2021.
103 U. Pandey, K. R. Putta, K. R. Rout, E. Rytter, E. A. Blekkan and M. Hillestad, *Front. Energy Res.*, 2022, **10**, 1–14.
104 F. Habermeyer, J. Weyand, S. Maier, E. Kurkela and R.-U. Dietrich, *Biomass Conv. Bioref.*, 2023, DOI: **10.1007/s13399-022-03671-y**.
105 S. Müller, P. Groß, R. Rauch, R. Zweiler, C. Aichernig, M. Fuchs and H. Hofbauer, *Biomass Conv. Bioref.*, 2018, **8**, 275–282.
106 S. Fendt, Experimental investigation of a combined biomass-to-gas / power-to-gas concept for the production of synthetic natural gas (SNG). Dissertation, 2019.
107 L. Wang, Y. Zhang, C. Li, M. Pérez-Fortes, T.-E. Lin, F. Maréchal, J. van Herle and Y. Yang, *Appl. Energy*, 2020, **280**, 115987.
108 S. Larose, R. Labrecque and P. Mangin, *Appl. Sci.*, 2021, **11**, 2672.
109 P. Bareschino, E. Mancusi, C. Tregambi, F. Pepe, M. Urciuolo, P. Brachi and G. Ruoppolo, *Energy*, 2021, **230**, 120863.
110 F. Miccio, A. Picarelli and G. Ruoppolo, *Fuel Process. Technol.*, 2016, **141**, 31–37.
111 K. R. Putta, U. Pandey, L. Gavrilovic, K. R. Rout, E. Rytter, E. A. Blekkan and M. Hillestad, *Front. Energy Res.*, 2022, **9**, 1–14.
112 A. S. Nielsen, M. Ostadi, B. Austbø, M. Hillestad, G. del Alamo and O. Burheim, *Fuel*, 2022, **321**, 123987.
113 S. Mesfun, K. Engvall and A. Toffolo, *Front. Energy Res.*, 2022, 10.
114 R. Küngas, *J. Electrochem. Soc.*, 2020, **167**, 44508.
115 J. Herranz, A. Pătru, E. Fabbri and T. J. Schmidt, *Curr. Opin. Electrochem.*, 2020, **23**, 89–95.
116 Y. Zheng, J. Wang, B. Yu, W. Zhang, J. Chen, J. Qiao and J. Zhang, *Chem. Soc. Rev.*, 2017, **46**, 1427–1463.
117 in *Perry's chemical engineers' handbook*, ed. R. H. Perry and D. W. Green, McGraw-Hill, New York, NY, 1997.
118 S.-W. Kim, H. Kim, K. J. Yoon, J.-H. Lee, B.-K. Kim, W. Choi, J.-H. Lee and J. Hong, *J. Power Sources*, 2015, **280**, 630–639.
119 F. Alenazey, Y. Alyousef, O. Almisned, G. Almutairi, M. Ghouse, D. Montinaro and F. Ghigliazza, *Int. J. Hydrogen Energy*, 2015, **40**, 10274–10280.

120 G. Botta, M. Solimeo, P. Leone and P. V. Aravind, *Fuel Cells*, 2015, **15**, 669–681.
121 W. L. Becker, R. J. Braun, M. Penev and M. Melaina, *Energy*, 2012, **47**, 99–115.
122 L. Wang, M. Rao, S. Diethelm, T.-E. Lin, H. Zhang, A. Hagen, F. Maréchal and J. van Herle, *Appl. Energy*, 2019, **250**, 1432–1445.
123 M. Samavati, A. Martin, M. Santarelli and V. Nemanova, *Energies*, 2018, **11**, 1223.
124 B. Steinrücken, M. Dossow, M. Schmid, M. Hauck, S. Fendt, F. Kerscher and H. Spliethoff, in *36th International Conference on Efficiency, Cost, Optimization, Simulation and Environmental Impact of Energy Systems (ECOS 2023)*, ed. J. R. Smith, ECOS 2023, Las Palmas De Gran Canaria, Spain, 2023, pp. 1170–1181.
125 P. L. Jones, S. Taylor, S. Nakai and J. Jennings, *Electrical Engineer's Reference Book*, Elsevier, 2003, pp. 9-1–9-38.
126 S. Stenström, *Drying Technol.*, 2020, **38**, 825–845.
127 A. S. Mujumdar, *Handbook of Industrial Drying*, CRC Press, 2020.
128 S. Zeng, M. Li, G. Li, W. Lv, X. Liao and L. Wang, *Trends Food Sci. Technol.*, 2022, **121**, 76–92.
129 S. Horikoshi, R. F. Schiffmann, J. Fukushima and N. Serpone, *Microwave Chemical and Materials Processing*, Springer Singapore, Singapore, 2018.
130 X. Zhang, K. Rajagopalan, H. Lei, R. Ruan and B. K. Sharma, *Sustainable Energy Fuels*, 2017, **1**, 1664–1699.
131 P. Rattanadecho and N. Makul, *Drying Technol.*, 2016, **34**, 1–38.
132 K. E. Haque, *Int. J. Miner. Process.*, 1999, **57**, 1–24.
133 A. A. Arpia, W.-H. Chen, S. S. Lam, P. Rousset and M. D. G. de Luna, *Chem. Eng. J.*, 2021, **403**, 126233.
134 I. J. Siddique, A. A. Salema, E. Antunes and R. Vinu, *Renewable Sustainable Energy Rev.*, 2022, **153**, 111767.
135 P. Chen, Q. Xie, Z. Du, F. C. Borges, P. Peng, Y. Cheng, Y. Wan, X. Lin, Y. Liu and R. Ruan, in *Production of Biofuels and Chemicals with Microwave*, ed. Z. Fang, J. R. L. Smith and X. Qi, Springer, Dordrecht, 2015, vol. 3, pp. 83–98.
136 A. Mishra, S. Bag and S. Pal, *Encyclopedia of Renewable and Sustainable Materials*, Elsevier, 2020, pp. 343–357.
137 O. Lucia, P. Maussion, E. J. Dede and J. M. Burdio, *IEEE Trans. Ind. Electron.*, 2014, **61**, 2509–2520.
138 M. Sakr and S. Liu, *Renewable Sustainable Energy Rev.*, 2014, **39**, 262–269.
139 C. Mohabeer, N. Guilhaume, D. Laurenti and Y. Schuurman, *Energies*, 2022, **15**, 3258.
140 F. Mushtaq, R. Mat and F. N. Ani, *Renewable Sustainable Energy Rev.*, 2014, **39**, 555–574.
141 D. Beneroso, T. Monti, E. T. Kostas and J. Robinson, *Chem. Eng. J.*, 2017, **316**, 481–498.
142 F. Guo, Y. Dong, B. Tian, S. Du, S. Liang, N. Zhou, Y. Wang, P. Chen and R. Ruan, *Sustainable Energy Fuels*, 2020, **4**, 5927–5946.
143 C. Wu, V. L. Budarin, M. Wang, V. Sharifi, M. J. Gronnow, Y. Wu, J. Swithenbank, J. H. Clark and P. T. Williams, *Appl. Energy*, 2015, **157**, 533–539.
144 A. M. Parvez, T. Wu, Y. Hong, W. Chen, E. H. Lester, S. Mareta and M. Afzal, *J. Energy Inst.*, 2019, **92**, 730–740.
145 W. Xian-Hua, C. Han-Ping, D. Xue-Jun, Y. Hai-Ping, Z. Shi-Hong and S. Ying-Qiang, *BioRes*, 2009, **4**, 946–959.
146 O. Sosa Sabogal, S. Valin, S. Thiery and S. Salvador, *Chem. Eng. Res. Des.*, 2021, **173**, 206–214.
147 Y. Xue, Y. Zhou, J. Liu, Y. Xiao and T. Wang, *Waste Manage.*, 2021, **120**, 513–521.
148 P. D. Muley, C. Henkel, K. K. Abdollahi and D. Boldor, *Energy Fuels*, 2015, **29**, 7375–7385.
149 L. Wu, H. Ma, J. Mei, Y. Li, Q. Xu and Z. Li, *Int. J. Hydrogen Energy*, 2022, **47**, 5828–5841.
150 P. D. Muley, C. Henkel, K. K. Abdollahi, C. Marculescu and D. Boldor, *Energy Convers. Manage.*, 2016, **117**, 273–280.
151 N. Li, Y. Pan, Z. Yan, Q. Liu, Y. Yan and Z. Liu, *Fuel*, 2023, **336**, 127124.
152 F. Campuzano, R. C. Brown and J. D. Martínez, *Renewable Sustainable Energy Rev.*, 2019, **102**, 372–409.
153 D. Newport, R. Chandran, K. Arcuri, S. Whitney, D. Leo and S. Freitas, *Environ. Prog. Sustainable Energy*, 2012, **31**, 55–58.
154 L. Briesemeister, M. Kremling, S. Fendt and H. Spliethoff, *Chem. Eng. Technol.*, 2017, **40**, 270–277.
155 M. Mayerhofer, P. Mitsakis, X. Meng, W. de Jong, H. Spliethoff and M. Gaderer, *Fuel*, 2012, **99**, 204–209.
156 Y. A. Lenis, G. Maag, C. E. L. de Oliveira, L. Corredor and M. Sanjuan, *J. Energy Resour. Technol.*, 2019, 141.
157 Y. A. Lenis-Rodas, G. Maag, C. E. Lins de Oliveira, L. A. Corredor and M. E. Sanjuan, *Redin*, 2019, 78–82.
158 WO 2011/026629 A2, 2011.
159 G. Song, S. Zhao, X. Wang, X. Cui, H. Wang and J. Xiao, *Case Studies in Thermal Engineering*, 2022.
160 G. Song, H. Qiao, H. Gu and X. Cui, *BioRes*, 2022, **17**, 993–1000.
161 G. Butera, S. H. Jensen, R. O. Gadsboll, J. Ahrenfeldt and L. R. Clausen, *Chem. Eng. Trans.*, 2019, **76**, 1177–1182.
162 G. Butera, S. Højgaard Jensen, R. Østergaard Gadsbøll, J. Ahrenfeldt and L. Røngaard Clausen, *Fuel*, 2020, **271**, 117654.
163 C. Ke, C. Shi, Y. Zhang, M. Guang and B. Li, *Int. J. Hydrogen Energy*, 2022, **204**, 559.
164 Q. Xie, F. C. Borges, Y. Cheng, Y. Wan, Y. Li, X. Lin, Y. Liu, F. Hussain, P. Chen and R. Ruan, *Bioresour. Technol.*, 2014, **156**, 291–296.
165 L. Wu, H. Ma, Z. Yan, Q. Xu and Z. Li, *Energy Convers. Manage.*, 2022, **270**, 116242.
166 WO 2021/110810 A1, 2021.
167 S. T. Wismann, J. S. Engbæk, S. B. Vendelbo, F. B. Bendixen, W. L. Eriksen, K. Aasberg-Petersen, C. Frandsen, I. Chorkendorff and P. M. Mortensen, *Science*, 2019, **364**, 756–759.
168 Haldor Topsoe, eSMR: The future of blue hydrogen, available at: **https://www.topsoe.com/our-resources/knowledge/our-products/equipment/e-smr?hsLang=en**, accessed 18 March 2022.
169 SYPOX, available at: **https://www.sypox.eu/**, accessed 14 August 2023.

170 Haldor Topsoe, eRWGS™: New technology essential for electrofuels production, available at: **https://www.topsoe.com/our-resources/knowledge/our-products/equipment/e-rwgs**, accessed 18 March 2022.
171 P. Lidström, J. Tierney, B. Wathey and J. Westman, *Tetrahedron*, 2001, **57**, 9225–9283.
172 J. Li, J. Tao, B. Yan, L. Jiao, G. Chen and J. Hu, *Renewable Sustainable Energy Rev.*, 2021, **150**, 111510.
173 S. Anis and Z. A. Zainal, *Bioresour. Technol.*, 2014, **151**, 183–190.
174 H. M. Nguyen, C. M. Phan, S. Liu, C. Pham-Huu and L. Nguyen-Dinh, *Chem. Eng. J.*, 2022, **430**, 132934.
175 M. N. Pérez-Camacho, J. Abu-Dahrieh, D. Rooney and K. Sun, *Catal. Today*, 2015, **242**, 129–138.
176 M. R. Almind, S. B. Vendelbo, M. F. Hansen, M. G. Vinum, C. Frandsen, P. M. Mortensen and J. S. Engbæk, *Catal. Today*, 2020, **342**, 13–20.
177 C. Li, B. Kuan, W. J. Lee, N. Burke and J. Patel, *Chem. Eng. Sci.*, 2018, **187**, 189–199.
178 W. Wang, G. Tuci, C. Duong-Viet, Y. Liu, A. Rossin, L. Luconi, J.-M. Nhut, L. Nguyen-Dinh, C. Pham-Huu and G. Giambastiani, *ACS Catal.*, 2019, **9**, 7921–7935.
179 P. Dimitrakellis, E. Delikonstantis, G. D. Stefanidis and D. G. Vlachos, *Green Chem.*, 2022, **24**, 2680–2721.
180 E. Gomez, D. A. Rani, C. R. Cheeseman, D. Deegan, M. Wise and A. R. Boccaccini, *J. Hazard. Mater.*, 2009, **161**, 614–626.
181 M. Tendler, P. Rutberg and G. van Oost, *Plasma Phys. Control. Fusion*, 2005, **47**, A219–A230.
182 P. G. Rutberg, A. N. Bratsev, V. A. Kuznetsov, I. I. Kumkova, V. E. Popov and A. V. Surov, *J. Phys.: Conf. Ser.*, 2012, **406**, 12024.
183 W.-K. Tu, J.-L. Shie, C.-Y. Chang, C.-F. Chang, C.-F. Lin, S.-Y. Yang, J.-T. Kuo, D.-G. Shaw and D.-J. Lee, *Energy Fuels*, 2008, **22**, 24–30.
184 C. Du, J. Wu, D. Ma, Y. Liu, P. Qiu, R. Qiu, S. Liao and D. Gao, *Int. J. Hydrogen Energy*, 2015, **40**, 12634–12649.
185 Y. Pang, T. Hammer, D. Müller and J. Karl, *Processes*, 2019, **7**, 114.
186 B. Lemmens, H. Elslander, I. Vanderreydt, K. Peys, L. Diels, M. Oosterlinck and M. Joos, *Waste Manage.*, 2007, **27**, 1562–1569.
187 A. Fridman and L. A. Kennedy, *Plasma Physics and Engineering*, CRC Press, 2004.
188 L. Tang and H. Huang, *Energy Fuels*, 2005, **19**, 1174–1178.
189 K. C. Lin, Y.-C. Lin and Y.-H. Hsiao, *Energy*, 2014, **64**, 567–574.
190 L. Tang and H. Huang, *Fuel*, 2005, **84**, 2055–2063.
191 L. Tang, H. Wang, H. Hao, Y. Wang and H. Huang, *2010 Asia-Pacific Power and Energy Engineering Conference*, IEEE, 2010, pp. 1–4.
192 W.-K. Tu, J.-L. Shie, C.-Y. Chang, C.-F. Chang, C.-F. Lin, S.-Y. Yang, J. T. Kuo, D.-G. Shaw, Y.-D. You and D.-J. Lee, *Bioresour. Technol.*, 2009, **100**, 2052–2061.
193 J.-L. Shie, F.-J. Tsou and K.-L. Lin, *Bioresour. Technol.*, 2010, **101**, 5571–5577.
194 J.-L. Shie, F.-J. Tsou, K.-L. Lin and C.-Y. Chang, *Bioresour. Technol.*, 2010, **101**, 761–768.
195 L. Tang, H. Huang, X. Yang, H. Hao and K. Zhao, *EPE*, 2013, **05**, 287–290.
196 M. Materazzi, P. Lettieri, L. Mazzei, R. Taylor and C. Chapman, *Fuel*, 2013, **108**, 356–369.
197 A. Tamošiūnas, A. Chouchène, P. Valatkevičius, D. Gimžauskaitė, M. Aikas, R. Uscila, M. Ghorbel and M. Jeguirim, *Energies*, 2017, **10**, 710.
198 M. Hrabovsky, M. Hlina, V. Kopecky, A. Maslani, O. Zivny, P. Krenek, A. Serov and O. Hurba, *Plasma Chem. Plasma Process.*, 2017, **37**, 739–762.
199 I. Janajreh, S. S. Raza and A. S. Valmundsson, *Energy Convers. Manage.*, 2013, **65**, 801–809.
200 M. Minutillo, A. Perna and D. Di Bona, *Energy Convers. Manage.*, 2009, **50**, 2837–2842.
201 P. Rutberg, A. N. Bratsev, V. A. Kuznetsov, V. E. Popov, A. A. Ufimtsev and S. V. Shtengel, *Biomass Bioenergy*, 2011, **35**, 495–504.
202 F. Fabry, C. Rehmet, V. Rohani and L. Fulcheri, *Waste Biomass Valorization*, 2013, **4**, 421–439.
203 L. Mazzoni, M. Almazrouei, C. Ghenai and I. Janajreh, *Energy Proc.*, 2017, **142**, 3480–3485.
204 J. Heberlein and A. B. Murphy, *J. Phys. D: Appl. Phys.*, 2008, **41**, 53001.
205 S. Morrin, P. Lettieri, C. Chapman and L. Mazzei, *Waste Manage.*, 2012, **32**, 676–684.
206 S. Achinas, in *Contemporary Environmental Issues and Challenges in Era of Climate Change*, ed. P. Singh, R. P. Singh and V. Srivastava, Springer Singapore, Singapore, 2020, pp. 261–275.
207 X. Cai, H. Cai, C. Shang and C. Du, *IEEE Trans. Plasma Sci.*, 2021, **49**, 191–213.
208 S. Hamel, H. Hasselbach, S. Weil and W. Krumm, *Energy*, 2007, **32**, 95–107.
209 A. S. An'shakov, P. V. Domarov and E. B. Butakov, *Combust., Explos., Shock Waves*, 2022, **58**, 490–493.
210 A. S. An'shakov, A. V. Cherednichenko, V. A. Serikov and P. V. Domarov, *IOP Conf. Ser.: Mater. Sci. Eng.*, 2019, **560**, 12121.
211 Vishwajeet, H. Pawlak-Kruczek, M. Baranowski, M. Czerep, A. Chorążyczewski, K. Krochmalny, M. Ostrycharczyk, P. Ziółkowski, P. Madejski, T. Mączka, A. Arora, T. Hardy, L. Niedzwiecki, J. Badur and D. Mikielewicz, *Energies*, 2022, **15**, 1948.
212 in *Fuel synthesis for solid oxide fuel cells by plasma spouted bed gasification*, ed. A. Lemoine and J. Jurewicz, Orleans, France, 1st edn, 2001.
213 A. Sanlisoy and M. Ozdinc Carpinlioglu, *Plasma Chem. Plasma Process.*, 2019, **39**, 1211–1225.
214 W. Ma, C. Chu, P. Wang, Z. Guo, S. Lei, L. Zhong and G. Chen, *Adv. Sustainable Syst.*, 2020, **4**, 2000026.
215 A. E. E. Putra, N. Amaliyah, S. Nomura and I. Rahim, *Biomass Conv. Bioref.*, 2022, **12**, 441–446.
216 B. Kabalan, S. Wylie, A. Mason, R. Al-khaddar, A. Al-Shamma'a, C. Lupa, B. Herbert and E. Maddocks, *J. Phys.: Conf. Ser.*, 2011, 307, 12027.

217 A. V. Surov, S. D. Popov, V. E. Popov, D. I. Subbotin, E. O. Serba, V. A. Spodobin, G. Nakonechny and A. V. Pavlov, *Fuel*, 2017, **203**, 1007–1014.
218 P. G. Rutberg, V. A. Kuznetsov, E. O. Serba, S. D. Popov, A. V. Surov, G. V. Nakonechny and A. V. Nikonov, *Appl. Energy*, 2013, **108**, 505–514.
219 G. S. J. Sturm, A. N. Munoz, P. V. Aravind and G. D. Stefanidis, *IEEE Trans. Plasma Sci.*, 2016, **44**, 670–678.
220 E. Delikonstantis, G. Sturm, A. I. Stankiewicz, A. Bosmans, M. Scapinello, C. Dreiser, O. Lade, S. Brand and G. D. Stefanidis, *Chem. Eng. Process.*, 2019, **141**, 107538.
221 M. Hlína, M. Hrabovský, V. Kopecký, M. Konrád, T. Kavka and S. Skoblja, *Czech. J. Phys.*, 2006, **56**, B1179–B1184.
222 M. Hrabovsky, M. Konrad, V. Kopecky, M. Hlina, T. Kavka, O. Chumak, G. van Oost, E. Beeckman and B. Defoort, *High Temp. Mater. Processes*, 2006, **10**, 557–570.
223 M. Hlina, M. Hrabovsky, T. Kavka and M. Konrad, *Waste Manage.*, 2014, **34**, 63–66.
224 G. Diaz, N. Sharma, E. Leal-Quiros and A. Munoz-Hernandez, *Int. J. Hydrogen Energy*, 2015, **40**, 2091–2098.
225 G. Diaz, E. Leal-Quiros, R. A. Smith, J. Elliott and D. Unruh, *J. Phys.: Conf. Ser.*, 2014, **511**, 12081.
226 Z. Zhao, H. Huang, C. Wu, H. Li and Y. Chen, *Eng. Life Sci.*, 2001, **1**, 197.
227 X. Wang, C. Zhang, F. Xie, H. Li and X. Wang, *ICOPE*, 2015, ICOPE-15-C09, 2015.12.
228 R. F. Muvhiiwa, B. Sempuga, D. Hildebrandt and J. van der Walt, *J. Anal. Appl. Pyrolysis*, 2018, **130**, 159–168.
229 R. Muvhiiwa, B. Sempuga and D. Hildebrandt, *Chem. Eng. Sci.*, 2021, **243**, 116793.
230 M. Aikas, D. Gimžauskaitė, A. Tamošiūnas, R. Uscila and V. Snapkauskienė, *Clean Technol. Environ. Policy*, 2023, DOI: 10.1007/s10098-023-02566-4.
231 A. Tamošiūnas, D. Gimžauskaitė, M. Aikas, R. Uscila, V. Snapkauskienė, K. Zakarauskas and M. Praspaliauskas, *Biomass Conv. Bioref.*, 2023, 1–12.
232 A. Tamošiūnas, P. Valatkevičius, V. Valinčius and R. Levinskas, *C. R. Chim.*, 2016, **19**, 433–440.
233 G. Tamošiūnas, U. Aikas and E. Praspaliauskas, *Energies*, 2019, **12**, 2612.
234 V. Grigaitienė, V. Snapkauskienė, P. Valatkevičius, A. Tamošiūnas and V. Valinčius, *Catal. Today*, 2011, **167**, 135–140.
235 A. Tamošiūnas, D. Gimžauskaitė, R. Uscila and M. Aikas, *Appl. Energy*, 2019, **251**, 113306.
236 A. Tamošiūnas, D. Gimžauskaitė, M. Aikas, R. Uscila and K. Zakarauskas, *Int. J. Hydrogen Energy*, 2022, **47**, 12219–12230.
237 J. Balgaranova, *Waste Manage. Res.*, 2003, **21**, 38–41.
238 Y. Byun, M. Cho, J. W. Chung, W. Namkung, H. D. Lee, S. D. Jang, Y.-S. Kim, J.-H. Lee, C.-R. Lee and S.-M. Hwang, *J. Hazard. Mater.*, 2011, **190**, 317–323.
239 A. V. Pinaev, V. A. Faleev and A. E. Urbakh, *Combust., Explos., Shock Waves*, 2011, **47**, 179–184.
240 Z. Zhao, H. Huang, C. Wu, H. Li and Y. Chen, *Eng. Life Sci.*, 2001, **1**, 197.
241 A. Mountouris, E. Voutsas and D. Tassios, *Energy Convers. Manage.*, 2006, **47**, 1723–1737.
242 A. Mountouris, E. Voutsas and D. Tassios, *Energy Convers. Manage.*, 2008, **49**, 2264–2271.
243 J. Favas, E. Monteiro and A. Rouboa, *Int. J. Hydrogen Energy*, 2017, **42**, 10997–11005.
244 A. Okati, M. Reza Khani, B. Shokri, E. Monteiro and A. Rouboa, *Fuel*, 2023, **331**, 125952.
245 T. M. Ismail, E. Monteiro, A. Ramos, M. A. El-Salam and A. Rouboa, *Energy*, 2019, **182**, 1069–1083.
246 I. B. Matveev, S. I. Serbin and N. V. Washchilenko, *IEEE Trans. Plasma Sci.*, 2016, **44**, 3023–3027.
247 I. B. Matveev, S. I. Serbin and N. V. Washchilenko, *IEEE Trans. Plasma Sci.*, 2014, **42**, 3876–3880.
248 P.-C. Kuo, B. Illathukandy, W. Wu and J.-S. Chang, *Bioresour. Technol.*, 2020, **314**, 123740.
249 P.-C. Kuo, B. Illathukandy, W. Wu and J.-S. Chang, *Energy*, 2021, **223**, 120025.
250 S. A. Nair, K. Yan, A. Pemen, G. Winands, F. M. van Gompel, H. van Leuken, E. van Heesch, K. J. Ptasinski and A. Drinkenburg, *J. Electrost.*, 2004, **61**, 117–127.
251 R. M. Eliott, M. F. M. Nogueira, A. S. Silva Sobrinho, B. A. P. Couto, H. S. Maciel and P. T. Lacava, *Energy Fuels*, 2013, **27**, 1174–1181.
252 N. Striūgas, V. Valinčius, N. Pedišius, R. Poškas and K. Zakarauskas, *Waste Manage.*, 2017, **64**, 149–160.
253 P. Jamróz, W. Kordylewski and M. Wnukowski, *Fuel Process. Technol.*, 2018, **169**, 1–14.
254 M. Wnukowski and P. Jamróz, *Fuel Process. Technol.*, 2018, **173**, 229–242.
255 D. Mei, Y. Wang, S. Liu, M. Alliati, H. Yang and X. Tu, *Energy Convers. Manage.*, 2019, **195**, 409–419.
256 Y. Zhou, W. Wang, J. Sun, L. Fu, Z. Song, X. Zhao and Y. Mao, *Energy*, 2017, **126**, 42–52.
257 J. Sun, Q. Wang, W. Wang, Z. Song, X. Zhao, Y. Mao and C. Ma, *Fuel*, 2017, **207**, 121–125.
258 F. Saleem, J. Harris, K. Zhang and A. Harvey, *Chem. Eng. J.*, 2020, **382**, 122761.
259 A. J. M. Pemen, S. A. Nair, K. Yan, E. J. M. van Heesch, K. J. Ptasinski and A. A. H. Drinkenburg, *Plasmas Polym.*, 2003, **8**, 209–224.
260 Y. C. Yang and Y. N. Chun, *Korean J. Chem. Eng.*, 2011, **28**, 539–543.
261 F. Zhu, X. Li, H. Zhang, A. Wu, J. Yan, M. Ni, H. Zhang and A. Buekens, *Fuel*, 2016, **176**, 78–85.
262 S. Liu, D. Mei, L. Wang and X. Tu, *Chem. Eng. J.*, 2017, **307**, 793–802.
263 F. Saleem, K. Zhang and A. Harvey, *Fuel*, 2019, **235**, 1412–1419.
264 Y. Wang, H. Yang and X. Tu, *Energy Convers. Manage.*, 2019, **187**, 593–604.
265 R. Xu, F. Zhu, H. Zhang, P. M. Ruya, X. Kong, L. Li and X. Li, *Energy Fuels*, 2020, **34**, 2045–2054.
266 T. Nunnally, A. Tsangaris, A. Rabinovich, G. Nirenberg, I. Chernets and A. Fridman, *Int. J. Hydrogen Energy*, 2014, **39**, 11976–11989.

267 N. Gao, M. H. Milandile, C. Quan and L. Rundong, *J. Hazard. Mater.*, 2022, **421**, 126764.
268 L. Liu, Z. Zhang, S. Das and S. Kawi, *Appl. Catal., B*, 2019, **250**, 250–272.
269 Y. N. Chun, S. C. Kim and K. Yoshikawa, *Environ. Prog. Sustainable Energy*, 2013, **32**, 837–845.
270 K. Tao, N. Ohta, G. Liu, Y. Yoneyama, T. Wang and N. Tsubaki, *Fuel*, 2013, **104**, 53–57.
271 B. Wang, C. Chi, M. Xu, C. Wang and D. Meng, *Chem. Eng. J.*, 2017, **322**, 679–692.
272 F. Zhu, H. Zhang, X. Yan, J. Yan, M. Ni, X. Li and X. Tu, *Fuel*, 2017, **199**, 430–437.
273 X. Kong, H. Zhang, X. Li, R. Xu, I. Mubeen, L. Li and J. Yan, *Catalysts*, 2019, **9**, 19.
274 E. Blanquet and P. T. Williams, *J. Anal. Appl. Pyrolysis*, 2021, **159**, 105325.
275 E. Blanquet, M. A. Nahil and P. T. Williams, *Catal. Today*, 2019, **337**, 216–224.
276 M. Craven, Y. Wang, H. Yang, C. Wu and X. Tu, *IOPSci-Notes*, 2020, **1**, 24001.
277 W. Wang, Y. Ma, G. Chen, C. Quan, J. Yanik, N. Gao and X. Tu, *Fuel Process. Technol.*, 2022, **234**, 107333.
278 J. Ashok and S. Kawi, *Energy Convers. Manage.*, 2021, **248**, 114802.
279 P. Bernada, F. Marias, A. Deydier, F. Couture and A. Fourcault, *Waste Biomass Valorization*, 2012, **3**, 333–353.
280 M. Materazzi, P. Lettieri, L. Mazzei, R. Taylor and C. Chapman, *Fuel Process. Technol.*, 2014, **128**, 146–157.
281 M. Materazzi, P. Lettieri, L. Mazzei, R. Taylor and C. Chapman, *Fuel*, 2015, **150**, 473–485.
282 F. Marias, R. Demarthon, A. Bloas, J. P. Robert-Arnouil and F. Nebbad, *Waste Biomass Valorization*, 2015, **6**, 97–108.
283 F. Marias, R. Demarthon, A. Bloas and J. P. Robert-Arnouil, *Fuel Process. Technol.*, 2016, **149**, 139–152.
284 J. C. Whitehead, in *Plasma Catalysis*, ed. X. Tu, J. C. Whitehead and T. Nozaki, Springer International Publishing, Cham, 2019, vol. 106, pp. 1–19.
285 B. Ashford, Y. Wang, L. Wang and X. Tu, in *Plasma Catalysis*, ed. X. Tu, J. C. Whitehead and T. Nozaki, Springer International Publishing, Cham, 2019, vol. 106, pp. 271–307.
286 T. Nozaki, S. Kameshima, Z. Sheng, K. Tamura and T. Yamazaki, in *Plasma Catalysis*, ed. X. Tu, J. C. Whitehead and T. Nozaki, Springer International Publishing, Cham, 2019, vol. 106, pp. 231–269.
287 G. Chen, L. Wang, T. Godfroid and R. Snyders, in *Plasma Chemistry and Gas Conversion*, ed. N. Britun and T. Silva, IntechOpen, London, 2018.
288 Y. T. Shah, J. Verma and S. S. Katti, *J. Indian Chem. Soc.*, 2021, **98**, 100152.
289 S. Xu, H. Chen, C. Hardacre and X. Fan, *J. Phys. D: Appl. Phys.*, 2021, **54**, 233001.
290 H. Chen, Y. Mu, S. Xu, S. Xu, C. Hardacre and X. Fan, *Chin. J. Chem. Eng.*, 2020, **28**, 2010–2021.
291 J. Wang, X. Wang, M. S. AlQahtani, S. D. Knecht, S. G. Bilén, W. Chu and C. Song, *Chem. Eng. J.*, 2023, **451**, 138661.
292 X. Tu and J. C. Whitehead, *Int. J. Hydrogen Energy*, 2014, **39**, 9658–9669.
293 A. Bogaerts and R. Snoeckx, in *An Economy Based on Carbon Dioxide and Water*, ed. M. Aresta, I. Karimi and S. Kawi, Springer International Publishing, Cham, 2019, pp. 287–325.
294 A. Bogaerts, X. Tu, J. C. Whitehead, G. Centi, L. Lefferts, O. Guaitella, F. Azzolina-Jury, H.-H. Kim, A. B. Murphy, W. F. Schneider, T. Nozaki, J. C. Hicks, A. Rousseau, F. Thevenet, A. Khacef and M. Carreon, *J. Phys. D: Appl. Phys.*, 2020, **53**, 443001.
295 E. Jwa, S. B. Lee, H. W. Lee and Y. S. Mok, *Fuel Process. Technol.*, 2013, **108**, 89–93.
296 Y. Zeng and X. Tu, *J. Phys. D: Appl. Phys.*, 2017, **50**, 184004.
297 M. Nizio, A. Albarazi, S. Cavadias, J. Amouroux, M. E. Galvez and P. Da Costa, *Int. J. Hydrogen Energy*, 2016, **41**, 11584–11592.
298 M. Nizio, R. Benrabbah, M. Krzak, R. Debek, M. Motak, S. Cavadias, M. E. Gálvez and P. Da Costa, *Catal. Commun.*, 2016, **83**, 14–17.
299 K. Arita and S. Iizuka, *J. Mater. Sci. Chem. Eng.*, 2015, **03**, 69–77.
300 B. Xu, J. Li, J. Xie, Y. Huang, X. Yin and C. Wu, *J. Fuel Chem. Technol.*, 2021, **49**, 967–977.
301 Z. Cui, S. Meng, Y. Yi, A. Jafarzadeh, S. Li, E. C. Neyts, Y. Hao, L. Li, X. Zhang, X. Wang and A. Bogaerts, *ACS Catal.*, 2022, **12**, 1326–1337.
302 S. Liu, L. R. Winter and J. G. Chen, *ACS Catal.*, 2020, **10**, 2855–2871.
303 M. D. Farahani, Y. Zeng and Y. Zheng, *Energy Sci. Eng.*, 2022, **10**, 1572–1583.
304 T. Mukhriza and H. Oktarina, *JSE*, 2021, **6**, 1891–1898.
305 B. B. Govender, S. A. Iwarere and D. Ramjugernath, *Catalysts*, 2021, **11**, 1324.
306 W. S. Al-Harrasi, K. Zhang and G. Akay, *Green Process. Synth.*, 2013, **2**, 479–490.
307 D. Li, V. Rohani, F. Fabry, A. Parakkulam Ramaswamy, M. Sennour and L. Fulcheri, *Appl. Catal., A*, 2019, **588**, 117269.
308 G. Akay, K. Zhang, W. S. S. Al-Harrasi and R. M. Sankaran, *Ind. Eng. Chem. Res.*, 2020, **59**, 12013–12027.
309 S. Iwarere, V. Rohani, D. Ramjugernath, F. Fabry and L. Fulcheri, *Chem. Eng. J.*, 2014, **241**, 1–8.
310 V. Rohani, S. Iwarere, F. Fabry, D. Mourard, E. Izquierdo, D. Ramjugernath and L. Fulcheri, *Plasma Chem. Plasma Process.*, 2011, **31**, 663–679.
311 B. B. Govender, S. A. Iwarere and D. Ramjugernath, *Catalysts*, 2021, **11**, 297.
312 F. Monaco, A. Lanzini and M. Santarelli, *J. Cleaner Product.*, 2018, **170**, 160–173.
313 M. Pozzo, A. Lanzini and M. Santarelli, *Fuel*, 2015, **145**, 39–49.
314 L. R. Clausen, G. Butera and S. H. Jensen, *Energy*, 2019, **172**, 1117–1131.

315 L. R. Clausen, G. Butera and S. H. Jensen, *Energy*, 2019, **188**, 116018.
316 M. Recalde, A. Amladi, V. Venkataraman, T. Woudstra and P. V. Aravind, *Energy Convers. Manage.*, 2022, **270**, 116208.
317 P. Ostermeier, A. Vandersickel, M. Becker, S. Gleis and H. Spliethoff, *Int. J. Comput. Methods Exp. Measure.*, 2017, **6**, 71–85.
318 M. Angerer, M. Becker, S. Härzschel, K. Kröper, S. Gleis, A. Vandersickel and H. Spliethoff, *Energy Rep.*, 2018, **4**, 507–519.
319 European Comission, G. Technology readiness levels (TRL), available at: **https://ec.europa.eu/research/participants/data/ref/h2020/wp/2014_2015/annexes/h2020-wp1415-annex-g-trl_en.pdf**, accessed 14 August 2023.
320 J. Sun, W. Wang and Q. Yue, *Materials*, 2016, **9**, 231.
321 S. Kreidelmeyer, H. Dambeck, A. Kirchner and M. Wünsch, Kosten und Transformationspfade für strombasierte Energieträger, available at: **https://www.bmwk.de/Redaktion/DE/Downloads/Studien/transformationspfade-fuer-strombasierte-energietraeger.pdf?__blob=publicationFile**, accessed 23 August 2023.
322 L. Wang, M. Chen, R. Küngas, T.-E. Lin, S. Diethelm, F. Maréchal and J. van Herle, *Renewable Sustainable Energy Rev.*, 2019, **110**, 174–187.
323 G. Cinti, A. Baldinelli, A. Di Michele and U. Desideri, *Appl. Energy*, 2016, **162**, 308–320.
324 J. A. Elia and C. A. Floudas, *Ann. Rev. Chem. Biomol. Eng.*, 2014, **5**, 147–179.
325 P. A. Willems, *Science*, 2009, **325**, 707–708.
326 I. Dimitriou, H. Goldingay and A. V. Bridgwater, *Renewable Sustainable Energy Rev.*, 2018, **88**, 160–175.
327 O. Onel, A. M. Niziolek, J. A. Elia, R. C. Baliban and C. A. Floudas, *Ind. Eng. Chem. Res.*, 2015, **54**, 359–385.
328 C. Malins, Searle, Stephanie, Baral, Anil, D. Turley and L. Hopwood, Wasted – Europe's untapped resource, available at: **https://theicct.org/sites/default/files/publications/WASTED-final.pdf**, accessed 23 August 2023.
329 Methanol Institute, Methanol Price and Supply/Demand, available at: **https://www.methanol.org/methanol-price-supply-demand/**, accessed 23 August 2023.
330 Umweltbundesamt, Kohlendioxid-Emissionsfaktoren für die deutsche Berichterstattung atmosphärischer Emissionen, available at: **https://www.umweltbundesamt.de/sites/default/files/medien/361/dokumente/co2_ef_liste_2022_brennstoffe_und_industrie_final.xlsx**, accessed 25 August 2023.
331 C. Hamelinck and M. Bunse, Carbon footprint of methanol, available at: **https://www.studiogearup.com/wp-content/uploads/2022/02/2022_sGU-for-MI_Methanol-carbon-footprint-DEF-1.pdf**, accessed 25 August 2023.
332 G. S. Forman, T. E. Hahn and S. D. Jensen, *Environ. Sci. Technol.*, 2011, **45**, 9084–9092.
333 Directive (EU) 2018/2001, 2018.
334 Carbon Footprint-Country specific electricity grid greenhouse gas emission factors, available at: **https://www.carbonfootprint.com/docs/2023_02_emissions_factors_sources_for_2022_electricity_v10.pdf**, accessed 25 August 2023.
335 M. Pfennig, D. Böttger, B. Häckner, D. Geiger, C. Zink, A. Bisevic and L. Jansen, *Appl. Energy*, 2023, **347**, 121289.
336 R.-U. Dietrich, F. G. Albrecht, S. Maier, D. H. König, S. Estelmann, S. Adelung, Z. Bealu and A. Seitz, *Biomass Bioenergy*, 2018, **111**, 165–173.
337 S. A. Isaacs, M. D. Staples, F. Allroggen, D. S. Mallapragada, C. P. Falter and S. R. H. Barrett, *Environ. Sci. Technol.*, 2021, **55**, 8247–8257.